Institutionen för Bygg- och miljöteknik
Avdelningen för Konstruktionsteknik
Lunds Tekniska Högskola
Box 118
221 00 LUND

School of Civil Engineering
Department of Structural Engineering
Lund Institute of Technology
Box 118
S - 221 00 LUND
Sweden

Investigation of stability of glulam roof trusses with large spans

Stabilitet hos underspända limträtakstolar med stora spännvidder

Eva Frühwald

2001

Report TVBK - 5109
ISSN 0349 - 4969
ISRN: LUTVDG/TVBK – 01 / 5109+85p

Diploma Thesis

Supervisors: Sven Thelandersson, Department of Structural Engineering, LTH
Arne Emilsson, Limträteknik AB, Falun

July 2001

Acknowledgement

The work presented in this diploma project had been carried out at the Division of Structural Engineering at Lund University / Sweden in spring 2001 and was accepted as a diploma thesis at the Technical University of Hamburg-Harburg (TUHH) / Germany.

The project was initiated by Mr. Arne Emilsson of Limträteknik AB in Falun / Sweden who also served as a supervisor during the project.

Supervisors at the Division of Structural Engineering were Prof. Dr. Sven Thelandersson, Dr. Tord Isaksson and Mr. Martin Hansson.

First, I would like to thank Prof. Dr. Valtinat from the Division of Steel and Timber Structures at TUHH that he made it possible for me to write my diploma thesis at a university in Sweden.

Also, I would like to thank my supervisors for endless discussing the problems, Mr. Per-Olof Rosenkvist and Mr. Martin Hansson for helping me in the laboratory with the tests and all the staff at Division of Structural Engineering for always having an ear for my questions.

Lund, July 2001

Eva Frühwald

Abstract

In certain types of glulam roof structures with large spans, reliable methods for design with respect to instability are lacking. One example is a three-hinged roof truss with steel tension rods as shown in Figure 1.
The types of structures shown in Figure 1 are investigated in the diploma project with the purpose to evaluate and improve the currently used design methods and detailing. Calculation methods and design principles to predict the load-bearing capacity with respect to stability are developed. A theoretical model was created in the frame analysis software Microstran with the purpose to do a parameter study with different variables, e.g. the inclination of the roof, the number of studs, the stud length, the type of joint (stiffness) and the different structures shown in Figure 1.
Additionally, several tests of a part of a scaled roof structure and their joints were performed and compared with the theoretical model.

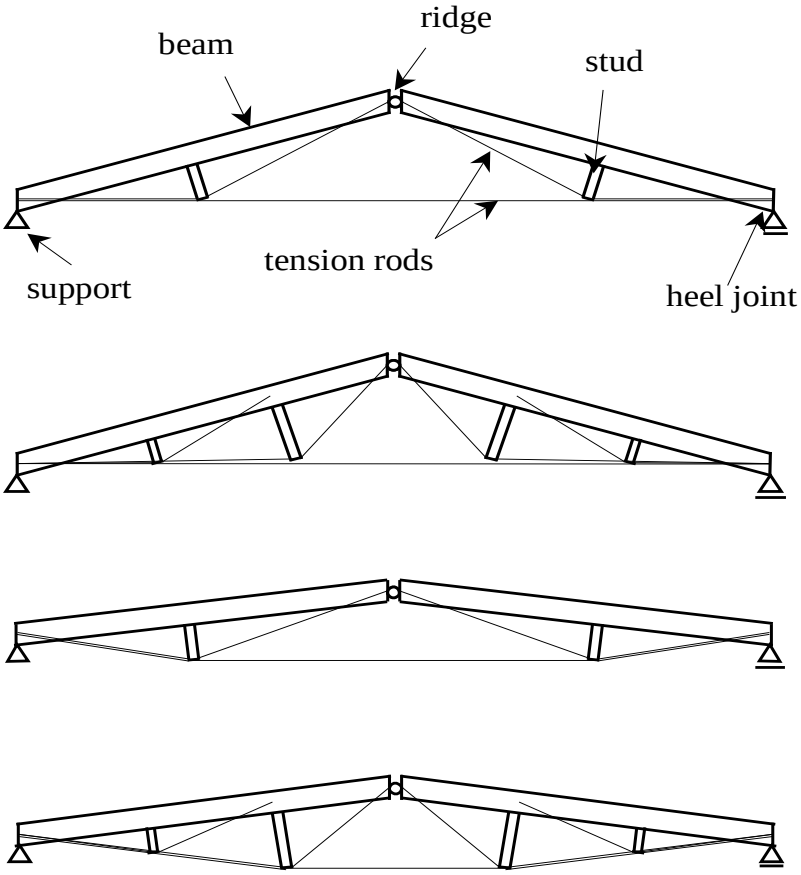

Figure 1: Investigated roof trusses.

Most of the structures with trussed beams are braced out of plane or are built three-dimensional because of the risk for out of plane buckling. In this study, the buckling length of the stud was investigated and found to be close to $\beta L = 1.0L$, which is the Euler case 2 (simply supported beam) instead of a cantilever, which is normally used when determining the axial load capacity. With the studs buckling length being much shorter than expected, the risk for out of plane buckling decreases and the load carrying capacity increases.
Due to the time restriction, only a limited number of tests could be performed. To ensure the correctness of the results achieved in this study, more tests with a different stud length, joint stiffness, initial deflection and initial inclination as well as varying prestressing of the tension rods should be performed.

1 Introduction

Glulam beams with steel tension rods (trussed beams) are often used for large span constructions. Three-hinged roof trusses can be built with or without steel tension rods between the two supports with spans of 15-50 m. For spans exceeding this range, tension rods between support and ridge are necessary (additionally to the ones between the two supports). In this way, roof trusses with spans of up to 100 m can be produced. However, spans exceeding 60 m are unusual due to transportation limitations.
For roof trusses and bridges with large spans, different kinds of constructions are possible. One possibility is to use a single span beam and to adjust the beam dimensions to the section forces. If this is done, usually large dimensions are needed which further increase the section forces (especially the bending moment) by their weight. Another way to cope with large spans is to decrease the maximum bending moment in the beam. By introduction of one or more elastic intermediate supports (studs), the static system changes from a single span beam to a double span beam or even to a continuously supported beam. The intermediate support, a glulam stud, and the steel tension rods change the behaviour of the glulam beam, which now is a trussed beam. The bending moment between the supports decreases while the bending moment at the intermediate supports builds up, see Figure 1-1. The intermediate support is elastic, as the stud and tension rods deflect under loading, they are deformed: The length of the stud is decreased due to the axial compression force, whereas the tension rods get longer. Due to these deformations, the beam is not fixed vertically at the intermediate support to the same extent as at the regular supports at its two ends.

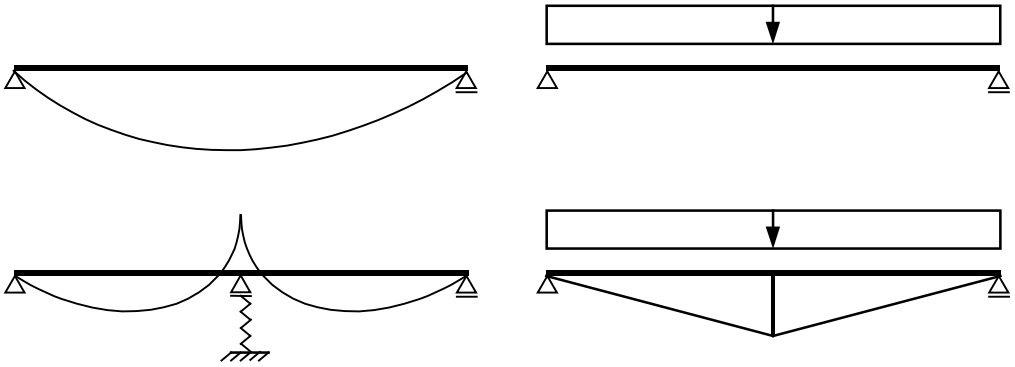

Figure 1-1: Bending moment reduction by introduction of an elastic intermediate support. Bending moment distribution (left) for different static systems (right) with uniformly distributed load.

The axial force in the individual construction component increases if one or several additional supports are introduced: At the supports, equilibrium of the forces has to be fulfilled. The tension force in the steel rod evokes a compression force in the timber beam. Of course, the interaction of compression force and bending moment in the beam has to be considered when determining the dimensions. Other failure modes like column buckling, lateral beam buckling and the stud buckling out of plane can occur, compared to regular beams. The bending moment reduction results in lower stresses in the beam leading to smaller dimensions or larger spans compared to a simple beam structure.

The detailing for a roof truss with trussed beams is of course different from that of a simple roof structure made of timber, a so-called trussed rafter, see Figure 1-2.

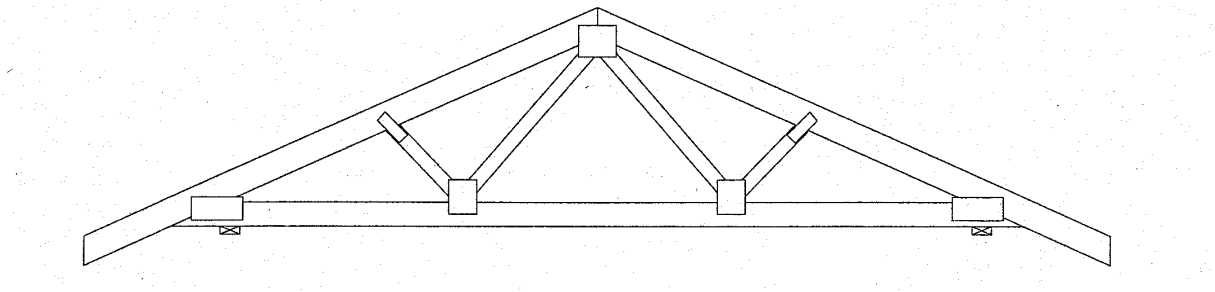

Figure 1-2: Trussed rafter with Punched Metal Plate Fasteners, from Nielsen 2001.

The trussed rafter consists of upper and lower chord and diagonals of timber, which are joined with punched metal plate fasteners. For this kind of construction, dimensions for both timber members and joints are already estimated for different loads and the values can be taken from tables in the literature. A glulam roof truss with trussed beams consists of glulam beams and studs and steel tension rods. Two materials with different cross-sections are used in one construction. The solid glulam members have a rectangular cross-section whereas the slender steel members usually are circular. Therefore, the connections between timber members and steel tension rods have to be specially designed: The details for roof heel, ridge and joint between stud and tension rod are not needed in usual roof trusses and therefore no standard details are available. For the detailing of these joints, see chapter 3.
Additionally, a more complicated analysis has to be used: Simple roof trusses (trussed rafters) are braced by plates or purlins. Usually they hold no or a rather small risk for instability, as the diagonals are fixed between the braced upper chord and the lower chord, the tension chord which cannot deflect out of the trusses plane. However, roof trusses with trussed beams very often are calculated with second order analysis to consider the large risk for instability due to the fact that the cantilever ends of the studs are not braced, as well as the high axial forces in all construction elements.
Trussed beams can be used successfully in inclined roof structures, whereas framework with parallel upper and lower chord and diagonals usually is used for flat roof structures.

In certain types of trussed glulam roof structures, reliable methods for design with respect to instability are lacking. A three-hinged roof truss, “beam truss”, (see Figure 1-3) was investigated in the diploma project, being one of the most-used systems.

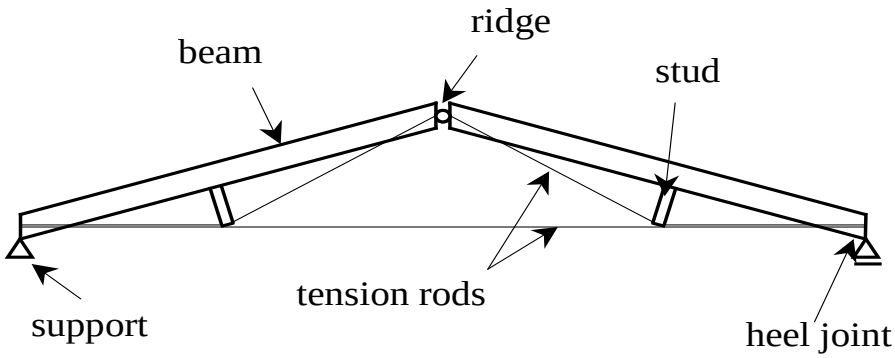

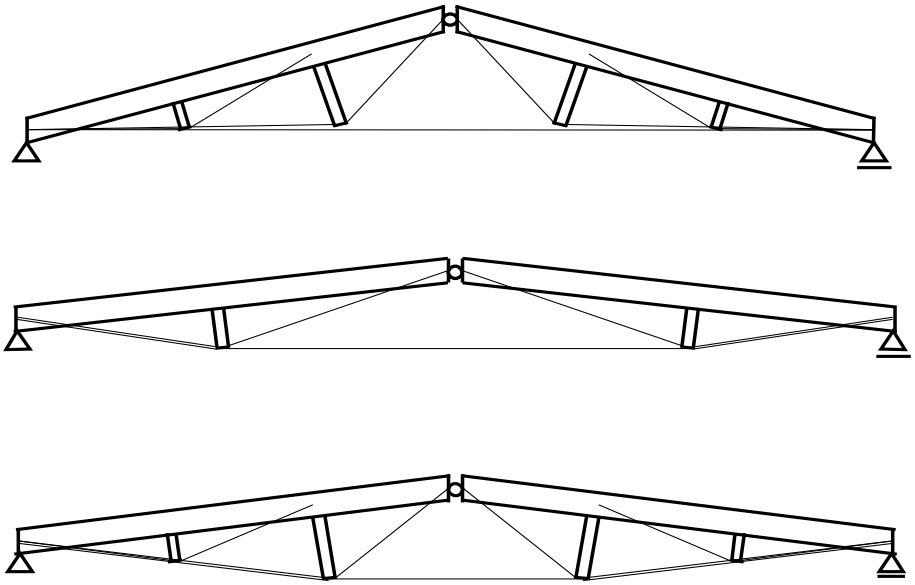

Figure 1-3: Investigated roof trusses.

The purpose with this project is to evaluate the currently used design principles and detailing and develop calculation methods and design principles to predict the load-bearing capacity with respect to stability. On the one hand, this is achieved by a theoretical model in a frame analysis software (Microstran) and on the other hand by different tests in the laboratory. A parameter study was performed with the help of the computer program, varying parameters such as roof inclination, number of studs, length of the studs, stiffness of the joint and comparing the different structures shown in Figure 1-3. Due to different problems (free space in the laboratory, type of loading and dimensions of the structure), a scaled-down three-hinged roof truss could not be studied. Instead, half of the system was studied, having one horizontal trussed beam, see Figure 1-4. This system is only subjected to vertical loads, i.e. there are no load components parallel to the beam as there are in inclined structures. This means that the axial compression forces in the beam are lower in the horizontal test structure than in a comparable inclined structure. The actual buckling risk for the beam (column buckling and lateral beam buckling) is therefore higher in an inclined structure, but as the beams are slender, different failure modes (also including buckling in the beams) are possible, so that the horizontal test system is sufficient.

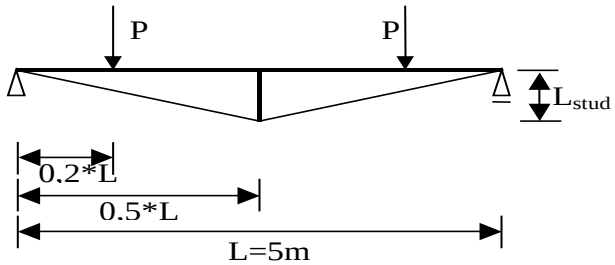

Figure 1-4: Test System.

2 Timber and glulam as a material

2.1 Timber

Timber is a highly anisotropic material. The properties vary significantly in the longitudinal (stem) and the transversal (cross) direction. In the transversal direction there are even differences between the directions radial and tangential to the growth rings. Due to this anisotropy, the orientation of timber in a construction and especially in a joint has to be considered carefully. Usually the strength and stiffness values are much higher parallel to the grain than perpendicular or at an angle to the grain.
Further, timber is a natural material that has defects, which have an effect on the strength: knots, grain deviation and compression wood as well as some other defects lead to a reduction of strength and stiffness values (Gustafsson 2001).
Also the length and the volume of a timber beam has an effect on the strength since there is a higher probability of having a weak zone (knot or group of knots) within a longer beam than in a shorter one. As a result, the bending moment capacity increases with decreasing beam length (decreasing beam volume). The load configuration also has a high influence on the capacity of a beam: For a uniform bending moment, the stressed volume is maximised, for a point load it is smaller and so is the probability of having a weak section at the one point of highest stress. This so-called volume- or size-effect is described mathematically by the Weibull-theory, the "weakest-link-theory". An assumption in this theory is that the whole beam fails if its weakest element (for example the section at a knot) fails. This theory gives especially good results for brittle failures such as tension failures and sufficiently good results for bending failure, which is composed of tension and compression, with compression failure being highly ductile. However, in most cases the failure will occur in the tension zone when subjected to bending stresses (Isaksson 2001).
For the influence of moisture content and moisture content change on the timber properties, see section 2.3.
Timber experiences creep like other materials, for example concrete, and also a duration of load effect (DOL). That means that for long-term loads (for example 10 year loading), a strength loss around 40 % in the timber elements is experienced (Hoffmeyer 2001).

Summarising some of the most important characteristics of timber:

- Strength depends on the angle between load and grain.
- Strength decreases with increasing moisture content.
- Strength decreases with increasing duration of load.
- Large variation in material properties (inhomogeneous material).

2.2 Glued laminated timber (glulam)

For glued laminated timber (glulam), the same influences on the material properties have to be considered as for regular timber since glulam is built up of timber boards. Timber as a natural material is only available up to certain dimensions. If larger dimensions are needed, special cross-sections have to be built up of timber elements. A simple way to produce large cross-sections is to glue graded timber boards together (under pressure) so that they work together as one beam. The advantages of glulam compared to normal timber are (according to Serrano, 2001):

- Improved strength and stiffness properties
- Freedom in the choice of geometrical shapes
- Possibility to match the lamination qualities in relation to expected stress levels (outer laminations with higher grading quality)
- Improved accuracy of dimensions and shape stability during exposure to moisture.

Due to the larger cross-sections, the probability that the cross-section contains a defect that initiates the (brittle) failure is higher than in smaller cross-sections or single boards and therefore the strength decreases. The so-called volume or size effect has to be considered for the estimation of the bending and tension strength of glulam beams.
Glulam is an industrialised product with higher strength and stiffness properties as well as lower variability of material properties than regular timber. In the Swedish Code BKR (BKR1999), lower partial safety factors γ_m are used for glulam (γ_m = 1.15) than for regular timber (γ_m = 1.25). If this is applied, then the material properties have to be controlled accurately, making sure that the variability of the glulam is low.

2.3 Moisture content and moisture content change

Wood or timber as a hygroscopic material is affected by the changing relative humidity. There is a continuous change of moisture content with the surrounding relative humidity. The moisture content and moisture content changes influence both strength and stiffness parameters. Normally the strength decreases when the moisture content increases, at least below the fibre saturation point. However, not only the moisture content, but also the fast changes in moisture content are of importance, because these moisture gradients evoke stresses perpendicular to grain that cause splitting of the timber. One example of splitting in timber is a joint between two timber parts whose grain directions are perpendicular to one another. As the moisture transfer across the grain is different from that along the grain, one of the timber members shrinks or swells more than the other one. If several fasteners are used with large distances between one another, fixing the two timber members, severe splitting can occur due to the different moisture movements.
Also, varying moisture content has a negative effect on the strength and stiffness of timber under long term loading. The influence of moisture on mechanical properties increases with an increase in grading quality (Ranta-Maunus 2001).
Moisture content changes lead to the so-called mechano-sorptive effect: deflections are larger for repetitive moisture content changes than for constant high moisture content. The reasons for this have not been clarified so far, but the mechano-sorptive effect cannot be left out, otherwise the deflection is underestimated (Ranta-Maunus 2001 and Mårtensson 2001).
The change of moisture content can be simulated in the theoretical computer model by a temperature load. Decreasing moisture content evokes shrinking, a decrease in length, whereas increasing moisture content leads to a length increase of the timber members. Due to the length change, the geometry of the system and the distribution of the section forces (axial and lateral forces as well as bending moment) change.

3 The properties of the beam truss

The beam truss has some special properties compared to regular trusses. The joints cannot be hinged, because then the structural system has a large risk for instability already at low loads. The semi-rigid joints have to be simulated in the theoretical model in a special way so that the section force distribution gets realistic.
The section force distribution in the truss depends on the ratio of the stiffnesses of the different structural members, the joint stiffness and of course the geometrical premises. A short stud for instance has both advantages and disadvantages: On the one hand, the studs buckling length and therefore the risk for buckling decreases with decreasing length. On the other hand, the axial compression force in the timber beam increases with decreasing angle between tension rod and beam (i.e. decreasing stud length), and therefore the risk for buckling and lateral buckling in the beam increases.

3.1 Instability

Due to the large spans, the resulting large dimensions and the type of section forces, there is a high risk for instability. Several instability modes can be found:

- Lateral buckling of beams: Slender beams (high height/width-ratio) tend to buckle laterally in the compression side, see Figure 3-1. They have to be supported preventing out of plane bending. This stabilisation is provided by purlins or steel sheathing fastened at certain distances to the compressed (usually the upper) edge of the beam. A bracing for a compressed lower edge, i.e. sections near or at intermediate supports of continuous beams, can for example be achieved with steel bars that are fastened to the purlins or roof sheathing and the beam, see Figure 3-2.

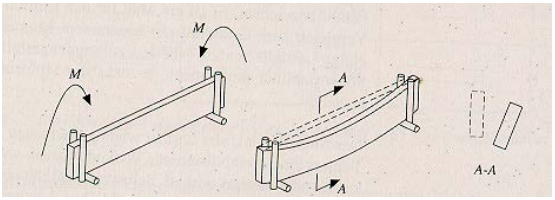

Figure 3-1: Lateral buckling of beams, positive bending moment (from: Step, B3).

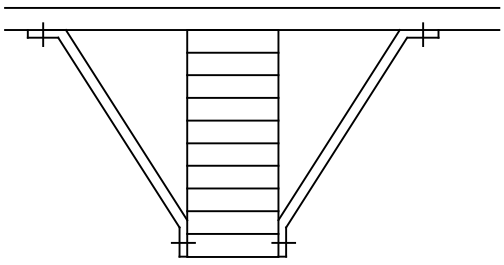

Figure 3-2: Possible bracing of the compressed beam edge (lower edge) at places with negative bending moment (according to Natterer et al, 1996).

For lightweight constructions also the lower edge can be compressed even for single span beams if the load combination wind and dead load is considered. Due to the large spans, resulting in large dimensions for the glulam beams, this case will not be of importance for this study.

- A second kind of instability can be of importance if the upper chord of a trussed beam is located straight between the supports. Already under very low load the stud buckles out of plane if the joint between beam and stud is hinged. If the joint between beam and stud is not located directly between the two supports, for example when giving the beam a precamber or having a bend in the beam (see Figure 3-3), then the stability of the system increases.

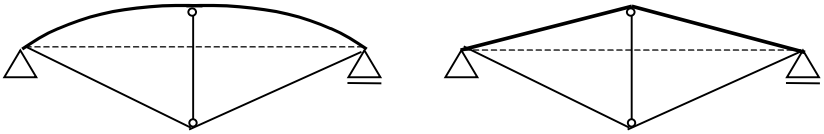

Figure 3-3: Trussed beam with precamber (left) or bend (right).

The resultant force in the tension rods is always directed to its joint with the glulam beam. If the glulam beam deflects under load and the joint between stud and beam is lower than the joint between tension rods and beam, the resultant force in the tension rods is directed more vertically and less horizontally than it would be if it followed the studs axis, see Figure 3-4 on the left. This means that the horizontal stabilising force component is rather small. If the joint between stud and glulam beam also under deflection due to load is located higher than the joint between tension rods and glulam beam, see Figure 3-4 on the right, then the stabilising horizontal load component is larger, as the resultant force is directed less vertical and more horizontal compared to the axis of the stud.

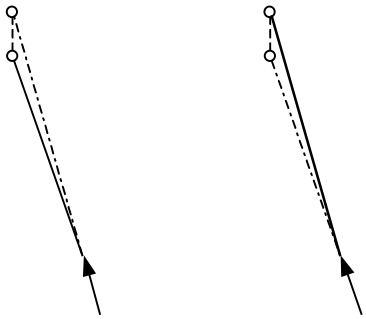

Figure 3-4: Stabilising horizontal force on the stud in trussed beams. On the left, the stabilising force is rather low, whereas it is large on the right. The stud is drawn with a solid line and the direction of the resultant force as a dashdot line.

If the joint between beam and stud is semi-rigid or rigid, then the buckling load increases compared to the hinged system. Decreasing the buckling risk by introduction of a precamber or a bend is unfortunately not practical in all cases. Kessel (1988) showed the phenomenon of stabilising horizontal force with tests and calculation, but constitutes that a precamber only increases the system stability if the precamber always is larger than the deformations due to load and long-term behaviour.

- The higher the loads and the resulting stresses, the higher is the risk for the tension rod and the stud to bend out of plane. Imperfections such as initial curvature of a

beam and initial displacement of points (e.g. supports and cantilever end) can influence the stability in a large rate. Several different imperfections are possible:

a) An initial crookedness of the whole roof truss (certain angle between vertical direction and truss plane),
b) a crookedness of the glulam beam itself (initial deflection in the roof plane),
c) an oblique assembling (beam is turned a little around its main axis),
d) an initial deflection in the stud or
e) an out-of-plane displacement of the cantilever end of the stud (joint with the tension rod).

Of course all these imperfections can happen solely but also simultaneously. Another kind of imperfection is the one concerning the material: Timber as a heterogenous material does not have the same material properties in every section. Usually, the design of timber structures is done with comparatively low strength and stiffness values, being on the "safe side", which leads to low coefficients of efficiency. Reliability studies can be performed to model a material (glulam, steel) that fits the reality best, e.g. by use of Monte Carlo Simulation. In this report, material imperfections such as knots, deviations from the grain direction and cracks are not considered separately. They are to some extent included in the suggestions for initial curvature and initial displacement as required in Eurocode 5, the interaction equations as well as in the partial safety factors.

3.2 Currently used design principles and detailing

3.2.1 Sweden

In Sweden, three-hinged roof trusses with trussed beams are used frequently since ca. 1850. In the beginning, the truss consisted of two parallel beams and the stud was fastened between them, for example with dowel type fasteners. The design of today is with only one beam and the stud is connected to the rafter by punched metal plate fasteners or aperture plates, forming a T-joint. Punched metal plate fasteners can only be used until certain timber dimensions, whereas aperture plates can be specifically designed for a truss and therefore be used for all truss sizes (Emilsson, 2001).

The section forces can approximately be calculated by a framework-analysis. For large spans and / or highly utilised tension rods a precise calculation may become necessary. This calculation can include deformations in the joints and the tension rods length change due to temperature change as well as loads (Carling / Johannesson, 1998).

The beams are designed for simultaneous compression and bending (interaction equations). Lateral instability and buckling are considered by using reduction factors that consider the length between the bracing on the compression side of the timber member as well as the beams slenderness.

The studs are supposed to be rigidly connected to the beam (which is not possible in reality) and they are also designed for simultaneous compression and bending. Special attention has to be paid to the studs buckling in plane and out of the trusses plane. One way to prevent buckling is to brace the joint between stud and tension rod, see Figure 3-5.

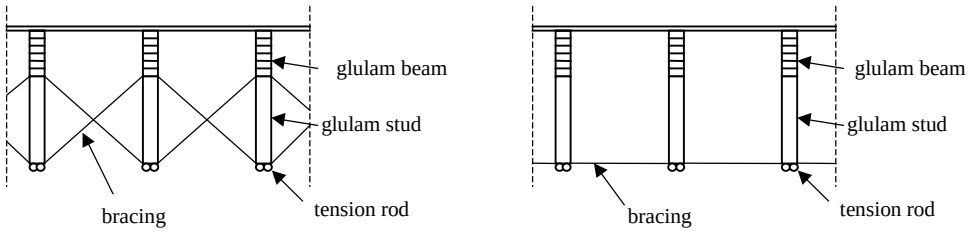

Figure 3-5: Bracing of the studs to prevent buckling. On the left with crossed steel rods, on the right with horizontal rods.

The deflection of the ridge of a roof truss with trussed beams can approximately be estimated as for a regular three-hinged truss which only has a tension rod between the supports (truss heel joints) (Carling / Johannesson, 1998).

3.2.2 Germany

The small-span trusses in Germany are of the same kind as in Sweden – punched metal plate fasteners are the usual way to manufacture joints. However, larger spans are not fabricated with nailed steel plates on the outside of the timber members, because these joints do not have a good fire resistance. Due to the need for better fire resistance, the joint is manufactured with slotted-in steel plates and dowel-type fasteners. Also, the construction type with double beams, fixing the stud between them with dowel-type fasteners is still used. Many constructions with trussed beams are built three-dimensional to avoid the risk of buckling. The stud can for example consist of several studs (see Figure 3-6) or be manufactured of timber plates forming a pyramid (Bauen mit Holz, no. 5/98). Most of the constructions that can be found in the literature (for example Natterer et al (1996), magazine “Bauen mit Holz”) are braced to prevent out of plane buckling.

3.2.3 Coping with instability

There are different ways to avoid failure due to instability of one of the roof structural members. Possible bracing for the stud is shown in Figure 3-5.
Three-dimensional roof trusses are a possibility to avoid instability: each truss stabilises itself. These roof trusses can for example consist of double beams with two or more studs (inclined in one or more directions) see Figure 3-6. A construction with timber material plates for both the beam and the studs (pyramidal form) is also possible – with the benefit of low dead load and fascinating and interesting construction (Bauen mit Holz, no. 5/98).

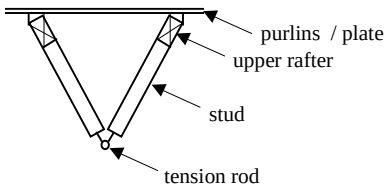

Figure 3-6: Three-dimensional roof truss.

Another way of reducing the buckling risk is to use stout studs, but they are neither economically nor aesthetically recommended.
Natterer et al (1996) shows different bracing methods for trussed beams, see Figure 3-7. The joint between beam and stud is braced so that no rotation can occur in the joint (top right, lower right in Figure 3-7) or the cantilevered end of the stud is braced (lower left in Figure 3-7).

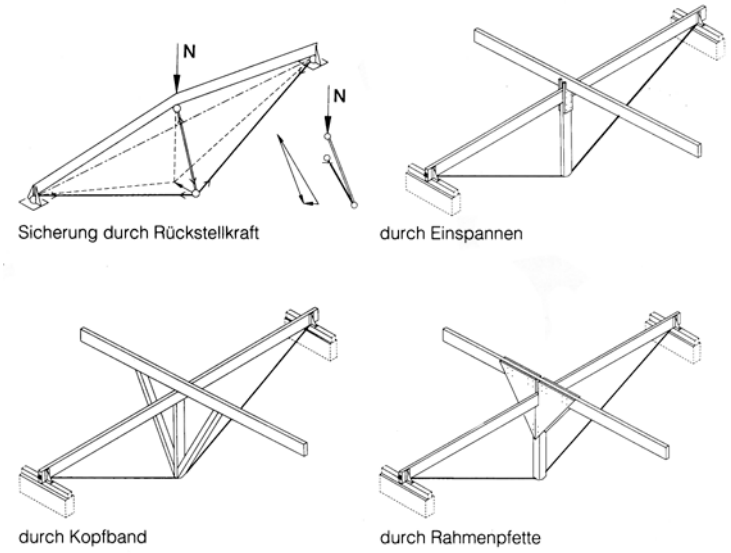

Figure 3-7: Out of plane buckling for trussed beams. Coping with instability by precamber (top left), rigid joint and restraint in purlin (top right), head band (lower left), frame corner (lower right) (from: Natterer et al, 1996).

The stabilisation of the beams upper edge is done with purlins or steel sheathing. If the lower edge of the beam is compressed (negative bending moment), it can be braced with steel tension rods or steel clamps, see Figure 3-2.

3.2.4 Problems with state of the arts design and detailing

One problem of today's design and detailing of roof trusses with trussed beams is that they usually are designed as a simple framework. In a precise analysis, other section forces are achieved due to the prestressed tension rods. The deformations of the whole construction also have a high influence on the stresses in the different members. Due to deflection of the ridge of a three-hinged roof truss, the beams experience much higher axial forces, which have a high influence on the chords capacity (interaction equations for bending and compression).
Also, the joint stiffness is not considered in a first order analysis. However, the joint stiffness is said to have an influence on the buckling length of the stud and therefore on the instability risk of the whole structure.
As trussed beam systems have not been established as "standard structural systems" like regular timber roof trusses, the so-called trussed rafters, yet, the joints between the timber members or timber and steel members have not become standard joints. These details have to be developed and designed for each structure, which is expensive and time-consuming.

3.3 Stiffness of joints

The stiffness of the joint between beam and stud has a high influence on the behaviour of the actual system. A perfect hinge would create an unstable system with the beam axis and the T-joint between beam and stud lying between the two supports (see also section 3.1), a perfect stiff joint is difficult to manufacture, also due to economical reasons. In reality, the stiffness of the joint will therefore be higher than for a hinge but lower than for a restraint.

A literature study has been performed to explain the influence of both single fasteners and fastener groups on the stiffness of a joint. Joint stiffness values were taken from reports on tests performed all over the world. Different joint types have been reviewed and compared with each other. The results are compiled in Table 3-1 andTable 3-2. They are then compared to the equations for joint stiffness given in Eurocode 5, section 7.1.
The equations given in EC 5 are different for the different joint types, and are valid for both timber-to-timber and panel-to-timber joints. The slip modulus K_{ser} is calculated per shear plane per fastener under service load (serviceability limit state, SLS) and can be transformed to the slip modulus for the ultimate limit state (ULS) K_u: $K_u = \frac{2}{3} \cdot K_{ser}$
For dowels, bolts without clearance, screws and nails with pre-drilling,
$K_{ser} = \rho_m^{1,5} \cdot \frac{d}{25}$ is valid, whereas for nails (without pre-drilling) $K_{ser} = \rho_m^{1,5} \cdot \frac{d^{0,8}}{30}$
has to be used. Initial values ρ_m in [kg/m^3] and d in [mm] give K_{ser} in [N/mm].

According to EC 5, section 7.1(3), the value for K_{ser} can be multiplied by two for steel to timber connections.

Some more equations for K_{ser} exist for staples, shear plate connectors, ring connectors and toothed connectors, but they are of no importance for this investigation.

In Figure 3-8 andFigure 3-9, the slip modulus K_{ser} per fastener is plotted against the fastener diameter. For joints with more than one fastener, the slip modulus of the joint was divided by the number of fasteners to get the slip modulus per fastener.

Stiffness for dowel-type fasteners

Table 3-1: Stiffness for dowel-type fasteners

reference										
	Racher / Step C1, tab. 4		Yasumura, Sawata / CIB 33-7-1			Jorissen / CIB 32-7-6				Haller / COST C1
Test										
tension / compression	x		x			x				x
bending moment										
fastener										
diameter [mm]	9 / 14 / 24		8 / 12 / 16 / 20			10.65 / 11.75 / 15.85 / 19.85				14
amount of fasteners	8 (9mm) 5 (14mm) 2 (24mm)		1			5				2
timber										
wood species	glulam GL24		picea jezonensis c.			european spruce				glulam (spruce)
density [kg/m^3]	-		390…450			378				507
moisture content [%]	-		-			-				14
dimensions [mm]	-		-			thickness t				thickness t=90
angle between load and grain	0		0 / 90			0				90
spring constant K_{ser}	d mm	k N/mm	d mm	k (α=0) N/mm	k (α=90) N/mm	t mm	t mm	d mm	k N/mm	k = 4200 N/mm with initial slip k = 6200 N/mm without initial slip k = 8000 N/mm according to equation $k = \rho^{1,5} \cdot \frac{d}{20}$
	8*9	53300	8	5920	3070	12	24	11,75	804	
	5*14	41500	12	5000	3070	24	48	11,75	1160	
	2*24	35600	16	5920	3070	36	48	10,65	1154	
			20	4900	4600	48	64	15,85	3616	
						60	80	19,85	4566	
						59	72	11,75	1582	
configuration	-		-			-				-
assumptions	spring constant values from table		spring constant values from diagram			spring constant values from table				spring constant values from table

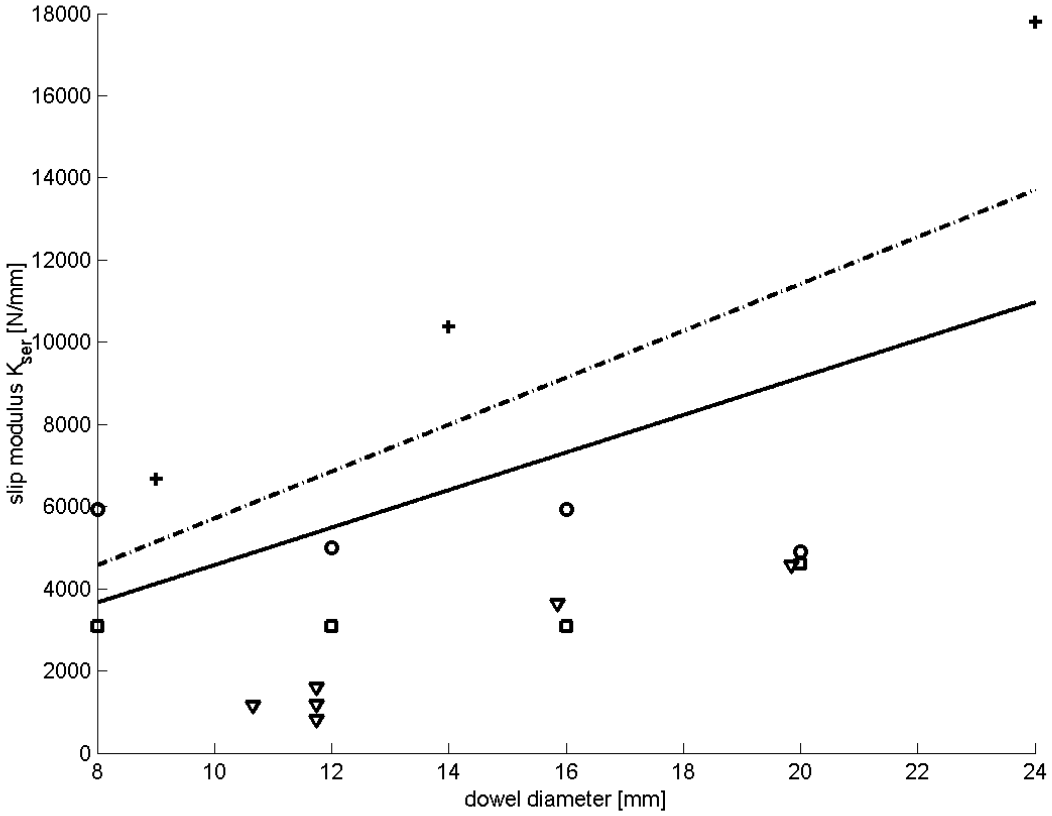

Figure 3-8: Slip modulus for joints with dowel-type fasteners. Legend: solid line – equation according to EC5; dashdot line – Haller/ COST C1; cross mark – Racher /STEPC1; circle mark – Yasumura, Sawata / CIB 33-7-1 (α=0); square mark – Yasumura, Sawata / CIB 33-7-1 (α=90); triangle mark – Jorissen / CIB 32-7-6.

Stiffness for nails and nailed plates

Table 3-2: Stiffness for nails and nailed plates.

<table>
<tr><th colspan="6">reference</th></tr>
<tr><td></td><td>Racher /
Step C1, tab. 4</td><td colspan="2">Norén</td><td>Whale, Smith, Hilson
/ CIB 19-7-1 Fig.7</td><td>Jensen /
SBI 238, p. 32/41</td></tr>
<tr><td>Test</td><td>nails</td><td colspan="2">nails</td><td>nails</td><td>nailed plates</td></tr>
<tr><td>tension /
compression</td><td>x</td><td colspan="2">x</td><td>x</td><td>x</td></tr>
<tr><td>bending
moment</td><td></td><td colspan="2"></td><td></td><td>x</td></tr>
<tr><td>fastener</td><td></td><td colspan="2">grooved wire nails</td><td></td><td>annular ring shanked
nail</td></tr>
<tr><td>diameter [mm]</td><td>34/80</td><td colspan="2">variable</td><td>3,35</td><td>40/35</td></tr>
<tr><td>amount of
fasteners</td><td>2</td><td colspan="2">1</td><td>-</td><td>-</td></tr>
<tr><td>timber</td><td></td><td colspan="2"></td><td></td><td></td></tr>
<tr><td>wood species</td><td>glulam GL24</td><td colspan="2">-</td><td>keruing</td><td>swedish spruce</td></tr>
<tr><td>density [kg/m3]</td><td>-</td><td colspan="2">-</td><td>670</td><td>375…437</td></tr>
<tr><td>moisture
content [%]</td><td>-</td><td colspan="2">-</td><td>-</td><td>16,6</td></tr>
<tr><td>dimensions
[mm]</td><td>-</td><td colspan="2">-</td><td>-</td><td>t = 2,5</td></tr>
<tr><td>angle between
load and grain</td><td>-</td><td colspan="2">-</td><td>0</td><td>0, 45, 90</td></tr>
<tr><td rowspan="15">spring constant
K_{ser}</td><td rowspan="15">59,9*10^3 N/mm</td><td>d [mm]</td><td>k [N/mm]</td><td rowspan="15">2,37*10^3 N/mm</td><td>α [°]</td><td>k [N/mm]</td></tr>
<tr><td>1,6</td><td>2150</td><td rowspan="2">0</td><td rowspan="2">480</td></tr>
<tr><td>1,6</td><td>1000</td></tr>
<tr><td>1,6</td><td>1290</td><td rowspan="2">45</td><td rowspan="2">490</td></tr>
<tr><td>2,2</td><td>5200</td></tr>
<tr><td>2,8</td><td>1640</td><td rowspan="2">90</td><td rowspan="2">700</td></tr>
<tr><td>3,1</td><td>1920</td></tr>
<tr><td>3,1</td><td>2250</td><td rowspan="9" colspan="2"></td></tr>
<tr><td>3,1</td><td>600</td></tr>
<tr><td>3,3</td><td>1650</td></tr>
<tr><td>3,7</td><td>2100</td></tr>
<tr><td>4,3</td><td>1300</td></tr>
<tr><td>5,1</td><td>7900</td></tr>
<tr><td>5,1</td><td>2100</td></tr>
<tr><td>configuration</td><td>-</td><td colspan="2">-</td><td>-</td><td>-</td></tr>
<tr><td>assumptions</td><td>service class 1;
climate class 1;
spring constant
values from
table</td><td colspan="2">spring constant
values from table</td><td>spring constant values
from figure</td><td>spring constant
values from figure</td></tr>
</table>

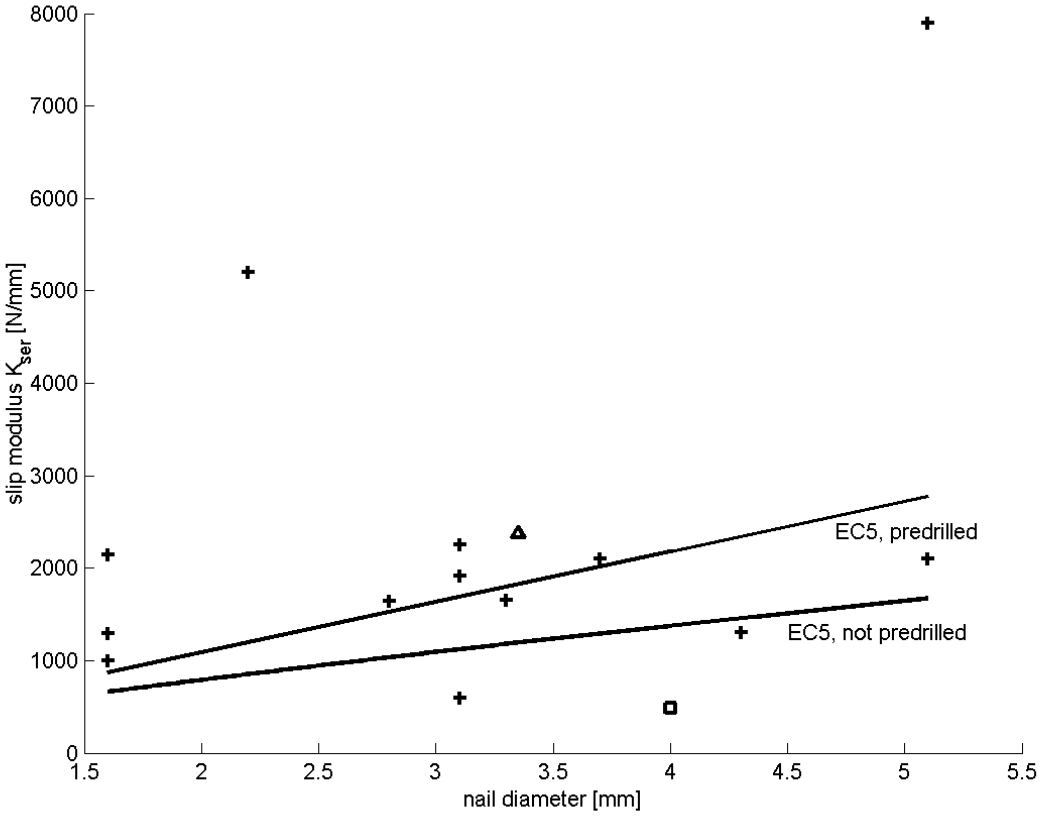

Figure 3-9: Slip modulus for nails and nailed joints. Legend: Solid lines – equation according to EC5; cross mark – Norén; triangle mark – Whale, Smith, Hilson / CIB 19-7-1; square mark: Jensen / SBI 238.The test value from Racher / STEP C1 is not included in the diagram because it lies in a totally different range.

3.3.1 Conclusions

From the diagrams can be seen that a large variability / scatter exists in the test results for the slip modulus for all joints studied. The equation according to Eurocode 5 does not always give conservative results. Especially does it give high values for dowel-type fasteners.

It is difficult to compare the different test results with each other since each test depends on its very special boundary conditions, such as timber member thickness, timber density, angle between load and grain, number of fasteners in a joint, type of joint, duration of load and so on. For some test results, information is lacking so that the accuracy of the evaluation cannot be taken for granted. Also the values for slip moduli calculated according to the equations from EC 5 are a little bit problematic. The failure mode of a joint depends for example also on the thickness of the steel plates used, so a multiplication with 2 for the value of K_{ser} perhaps is not on the "safe side" for every steel-to-timber joint. Additionally, the equation for K_u has been changed from the First Draft (dated 1999-06-29) to the Final Draft (dated 2001-04-09). Earlier, $K_u = \frac{1}{2} K_{ser}$ was valid, now it is $K_u = \frac{2}{3} K_{ser}$.

To make sure that the comparative calculations of test results and the theoretical model do not diverge too much, tests of the joint stiffness were performed for the nailed joints used in the test structure.

3.4 Theoretical Model

Theoretical models for trussed beams and roof trusses with trussed beams were created in the frame analysis software Microstran. This programme works like a regular frame analysis software, but can also handle three-dimensional systems, out of plane buckling and semi-rigid joints.
The different system members are put in as beams with different material properties and cross-sections. The semi-rigid T-joints are simulated by a combination of a rigid offset between the end of member A and the neutral axis of member B and a spring constant (rotational springs around two axes) at the end of member A, defining the joint stiffness, see Figure 3-10.

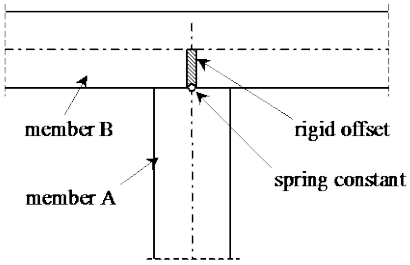

Figure 3-10: Simulation of a T-joint between two members A and B in the theoretical model.

If no rigid offset would be used, then the joint would be assumed to lie in the interception of the neutral axes of the two members joined with each other. However, joints always include eccentricities that have to be considered to model the real behaviour.
The tension rods can be modelled best with non-linear elements, so-called cable elements. These elements demand non-linear analysis, but give more reasonable results than regular (linear) elements, especially for the deformations,.
Different models for the whole three-hinged roof truss with trussed beams or only for the horizontal test system of one trussed beam (see section 3.5, Figure 3-11 andFigure 3-12) have been analysed with second order analysis as well as with elastic critical load analysis (ECL). The initial analysis in the ECL-analysis was also a second order analysis.

3.5 Finding the test structure

Tests of the actual structure of a roof truss with trussed beams and a comparison with theoretical results are a part of the diploma project. It was planned to test a real roof truss with trussed beams with the same structural system as the large span roof trusses but scaled down. A test model with 5 m span that has the same ratio of bending stiffness in the single members as a real-scale roof truss was designed. To achieve a comparable behaviour between the test structure and the computed calculation for a real truss, the single members of the structure have to have the same degree of utilisation in the model and in the real (large-scale) structure.
In reality, the roof truss is loaded with different types of uniform loads: dead load, snow load and wind load. In the test, uniform loads cannot be applied on the inclined beams. That is why a loading with point loads, producing the same stresses in the structure (maximum values of bending moment, normal force and lateral force), has to be applied. The designed scaled-down model is shown in Figure 3-11.

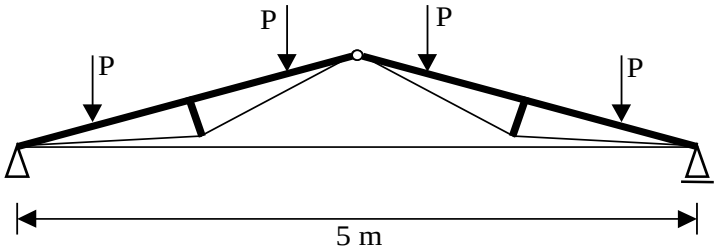

Figure 3-11: Test structure, whole roof truss with trussed beams. Loading with point loads.

Unfortunately, the scaled-down roof structure happens to have a too slender stud. This stud should be (due to comparative calculations for a 5 m and a 60 m span roof truss) have dimensions which are smaller than 20 by 20 mm, which makes it impossible to manufacture a joint. For a nailed joint with steel side plates, being easiest to assemble for a small structure, the distances between nails as well as end and edge distances have to be considered. The edge distance for a 4 mm grooved nail is for example 14 mm (see EC5, Tab 8-1), which makes it impossible to assemble a structure that resembles an actual roof truss. Furthermore does the structure have to have a minimum width of 42 mm which is the slenderest glulam beam that is produced. Due to the joint type (nail plates on both sides of the timber), the beam and the stud have to be of the same width. The reason for this diploma project is that designers and constructors are worried about the out of plane buckling of the studs. To simulate this, out of plane buckling should coincide with bending / buckling in the weak direction. A stud with at least 42 x 42 mm^2 would be very stiff compared to the beams so that the buckling of the stud perhaps would not be the failure mode. A larger truss to avoid this problem by increasing the studs length could not be designed because of the free space in the laboratory as well as the maximum height in the testing machine.

Due to the problems with the dimensions, it was decided to test only half of the roof truss. A simply supported beam with stud and tension rods, a so-called trussed beam, see Figure 3-12, was tested. This structure has a span of 5 m and the horizontal beam makes it easier to apply the point loads, because the structure is symmetric and the deflections in the loading points do not diverge so much. Of course, this assumption is only valid if there are no large variations in the material properties.

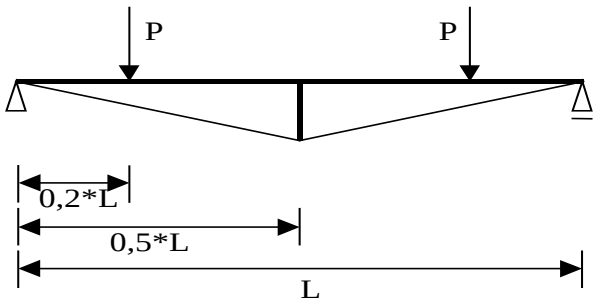

Figure 3-12: Test structure, simple span trussed beam.

Lacking knowledge for buckling of trussed beams, the stiffness of the joint between beam and stud is thought to be an important factor for the stability of the whole structure. That is why this was varied. For different structural systems, the joint stiffness affects the buckling length of the cantilever: the lower the spring constant, the longer is the buckling length of the

cantilever. However, the buckling length for the stud of a trussed beam is different, as will be seen from the test results and the calculations.
The test system was loaded with two vertical point loads, located 0,2L from each end of the beam. This loading results in a similar bending moment distribution as a uniformly distributed load, compare Figure 3-13.

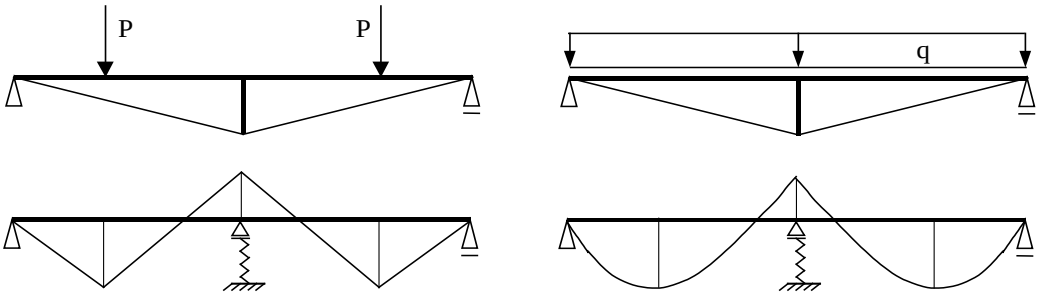

Figure 3-13: Bending moment figure for loading with two point loads (left) and for uniformly distributed load (right).

3.5.1 Dimensions for the test structure

To ensure that the test system fails in the same way as the real roof structure, the dimensions for the different components are determined for special utilisation factors.
The probable buckling loads and the dimensions (length of the stud, cross-section of beam, stud and tension rods) were investigated with calculations of equilibrium of the system at certain points. In the beginning, the stud was assumed to be a cantilever for out of plane buckling, i.e. the buckling length factor is $\beta = 2.0,$ giving the buckling length to $\beta L = 2L$.
The assumption was made that the bending moments in the bay and at the intermediate support (stud) have the same values. As a result, the beams bending moment capacity is optimal utilised. When the structure is only loaded with the two point loads P, then the bending moment in the bay is larger than the bending moment at the stud as the stud only is an elastic intermediate support which deflects under load. To achieve $\left|M_{\sup}\right| = \left|M_{bay}\right|$, the tension rods have to be prestressed with a certain value, producing a linear bending moment distribution in the beam with maximum value at the intermediate support. From equilibrium equations for the system and the boundary condition $\left|M_{\sup}\right| = \left|M_{bay}\right|$, the section forces can be calculated. The total tension force in the steel rods is then the tension force due to the loading plus a prestressing that has to be guessed. Iterative calculations are performed until $\left|M_{\sup}\right| = \left|M_{bay}\right|$.
The dimensions of the system are chosen with respect to the desired failure mode. As the studs buckling out of plane was most interesting, the highest degree of utilisation was chosen for the stud, whereas the beam and the tension rods were designed more conservative, having a margin.
The desired axial force in the stud is the critical buckling load. The system is loaded with two point loads P and the tension rods are prestressed with a certain value, together evoking the critical buckling load in the stud.

3.6 Stabilising effect of the tension rods on the studs

According to the Microstran-analysis of the test structure, the stud did not buckle at the load N_s, which is the buckling load for a buckling length $\beta L = 2L$. In fact, the stud can tolerate much higher loads, as the prestressed tension rods have a positive effect on the studs buckling length.

To clarify the stabilising effect of the tension rods on the studs, several simple systems (see Figure 3-14) were studied:

1. Cantilever
2. Cantilever with tension rods, fastened in fixed supports
3. Cantilever with tension rods, fastened in fixed supports, together with a prescribed displacement of the restraint. (The actual test system of the trussed beam, see Figure 3-12, bends under prestressing and the point loads so that the stud is displaced in the direction of the tension rods.)

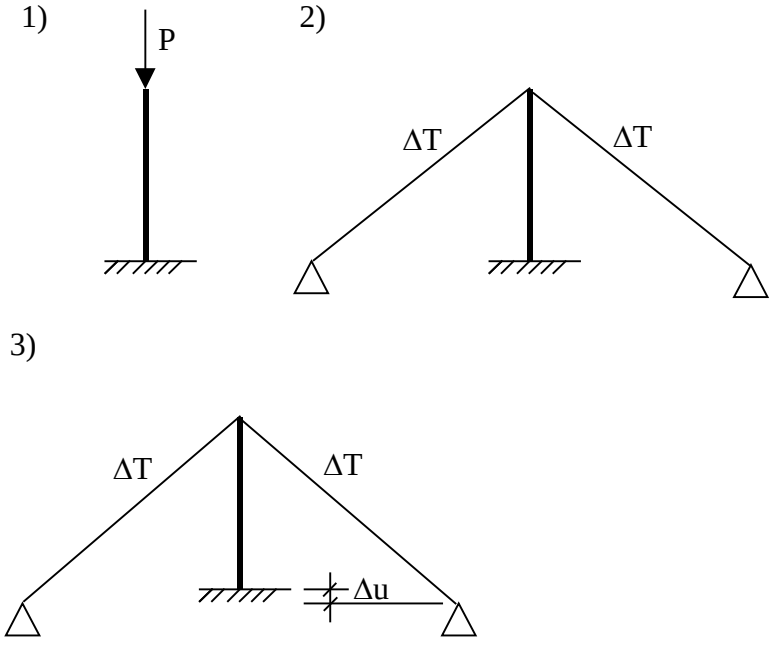

Figure 3-14: Systems to clarify the effect of the tension rods on the buckling length of the stud.

The calculations were done in Microstran, and non-linear-analysis was used because of the tension rods being non-linear cable elements. A temperature load, a negative temperature on the whole length of the member, which causes shortening, simulates the prestressing of the tension rods.

The three systems were loaded until the buckling load was reached. Output values of the ECL-analysis are the buckling length factor β and the axial load in the stud. They can be found in Table 3-4. The buckling length factor was calculated from the following equation, using the axial load in the stud at the moment of buckling:

$$N_{s,cr} = \frac{\pi^2 EI}{(\beta L_{stud})^2} \quad \text{where}$$

$N_{s,cr}$ is the axial force in the stud when the system becomes unstable [kN] and
L_{stud} is the length of the stud [m]

The results can be seen in Table 3-4.
Boundary conditions and assumptions for the comparative calculations of the three systems are

- L_{stud} = 0.86 m
- P = variable
- ΔT = variable
- Simple fixed supports for the tension rods
- Linear analysis for system 1 (cantilever), non-linear analysis for systems 2 and 3 due to the non-linear elements for the tension rods (cable elements)
- The comparative calculations were also made with rigid and semi-rigid joints for the cantilever. Different nailed joints were designed, using a varying number of nails. The stiffness of the joint is then evaluated by the rotational spring constants around the two axes of the cross-section of the cantilever. The rotational spring constants are composed of the spring constant K_u for the single nail, multiplied with the square of the distance of this very nail from the centre of the joint: $k_{m,y/z} = \sum K_{u,i} \cdot r_i^2$. The spring constants and descriptions of the different joints used can be found in Table 3-3.

Table 3-3: Different joint types used in the study of the 3 systems.

type	nails	k_y [kNm/rad]	k_z [kNm/rad]
rigid-offset	-	∞	∞
Joint A	9 x 2 x 2	9.130	57.9
Joint B	8 x 2 x 2	8.115	40.48
Joint C	7 x 2 x 2	7.100	27.34
Joint D	6 x 2 x 2	6.085	17.48
Joint E	5 x 2 x 2	5.070	10.30
Joint F	4 x 2 x 2	4.055	5.52
Joint G	3 x 2 x 2	3.045	2.455

Table 3-4: Buckling length factors β and axial load in the stud for the different systems, output values of Microstran ECL-analysis.

	buckling length factor β for system no.			axial load in the stud at the moment of buckling [kN]		
joint type	1	2	3	1	2	3
rigid-offset	2.0	1.127	1.131	-12.2	-38.783	-38.523
Joint A	2.869	1.203	1.214	-5.95	-34.026	-33.403
Joint B	2.963	1.216	1.227	-5.58	-33.294	-32.721
Joint C	3.084	1.234	1.247	-5.15	-32.379	-32.721
Joint D	3.239	1.262	1.277	-4.67	-30.916	-30.161
Joint E	3.435	1.301	1.319	-4.15	-29.088	-28.284
Joint F	3.725	1.367	1.388	-3.53	-26.344	-25.555
Joint G	4.34	1.479	1.508	-2.60	-22.502	-21.630

As can be seen in Table 3-4, the tension rods have a positive effect on the stability of the stud: They reduce the studs buckling length from that of a cantilever nearly to that of a beam that is simply supported at both ends (systems 2 and 3, "rigid offset"). For the semi-rigid joints, the positive effect is even more evident as for the rigid joint ("rigid-offset"): the lower the spring

constant of the joint, the higher is the reduction of the buckling length caused by the tension rods. The highest reduction can be observed for the weakest joint (Joint G) and has a value of 65.3% (reduction from system 1 to 3). According to Kessel (1988), see also section 3.1, the prescribed displacement of the restraint in system 3 should have a negative effect on the stability of the system. However, the buckling length factors for the systems 2 and 3 are nearly the same, i.e. the negative effect of the joint of the stud being deflected in relation to the joint of the tension rods is only small for semi-rigid joints.

The usual Euler case 1 (cantilever) deals with a cantilevered beam loaded with a vertical point load pointing towards the cantilevers axis, see Figure 3-15a. When the cantilever deflects due to the load (and possible initial deflections and inclinations), then the load remains vertical, i.e. there is an angle between load direction and the neutral axis of the cantilever, compare Figure 3-15b. This results in second order effects, leading to an increasing deflection and finally to failure.

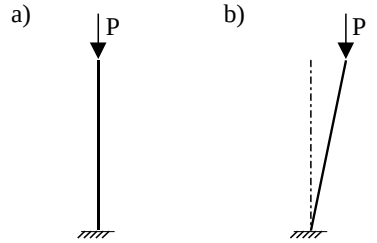

Figure 3-15: Euler case 1, cantilever with vertical load.

The observed phenomenon that the buckling length of the stud is shorter than expected for Euler case 1 can be explained with non-conservative buckling, see Figure 3-16.
The tension force in the rods, which in theory can be replaced by a vertical point load, results in an axial force in the stud. When the stud (cantilever) begins to buckle, a small displacement arises at the "free end". The point load changes its direction: It is always directed to the fixed support. Due to this, there is a horizontal load component that counteracts the displacement of the stud.

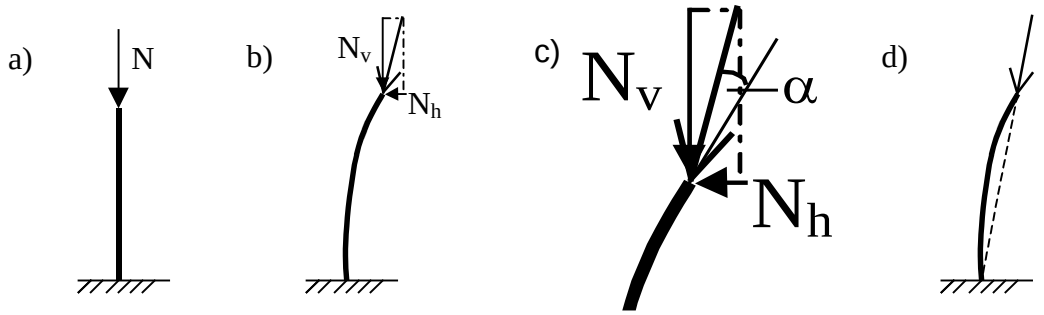

Figure 3-16: Non-conservative buckling. a) Cantilever without deflection; b) cantilever with deflection and resulting load pointing to the fixed support; c) detail of the load components in the different directions, there is an angle α between the resultant load and the axis of the cantilever; d) actual buckling mode.

According to Pettersson (1971), buckling length factors β can be as low as $\beta=0.7$ for a cantilever with non-conservative buckling. The lowest values for β are achieved if there is no angle $(\alpha = 0^\circ)$ between the load N and the cantilever end, i.e. the load is tangential to the cantilever end. In the case with the tension rods, the load always points towards the joint

between tension rod and beam. For this special case, the buckling mode resembles Eulers second buckling mode, see Figure 3-16, d) with βL=1.0L.

4 Tests

4.1 Test material

The test structure is composed of glulam beams and steel tension rods. The glulam beams have the nominal size 42 mm x 225 mm and are of the swedish glulam strength class L 40 which resembles strength class GL 32 from prEN 1194. The studs were sawn to 42 mm x 60 mm from short beams of the same cross-sections and strength class as the beams used in the test. Two steel tension rods with 12 mm diameter of steel quality S 355 were used. This quality would not have been necessary, but the rods had to be threaded and the material properties deteriorate under this process (Emilsson, 2001).

4.2 Test A: Determination of the material properties

When test results shall be compared with theoretical calculations, then the actual material properties (mean values for the different structural members) have to be investigated and used for the calculations. The mean value for the modulus of elasticity (MOE) was obtained by testing the beams and studs in the laboratory. Actually, the testing has to be done according to EN 408:1995, providing several special boundary conditions.

- The test piece shall be symmetrically loaded in bending at two points over a span of 18 times the depth as shown in Figure 4-1.
- Lateral restraint shall be provided as necessary to prevent buckling. This restraint shall permit the test piece to deflect without significant frictional resistance.
- Load shall be applied at a constant rate. The rate of movement of the loading-head shall not be greater than $v = 0.003 \cdot h$ [mm/sec] with h being the depth of the test piece.
- The maximum load applied shall not exceed the proportional limit load or cause damage to the test piece.
- Deformations shall be measured at the centre of a gauge length of five times the depth of the section.

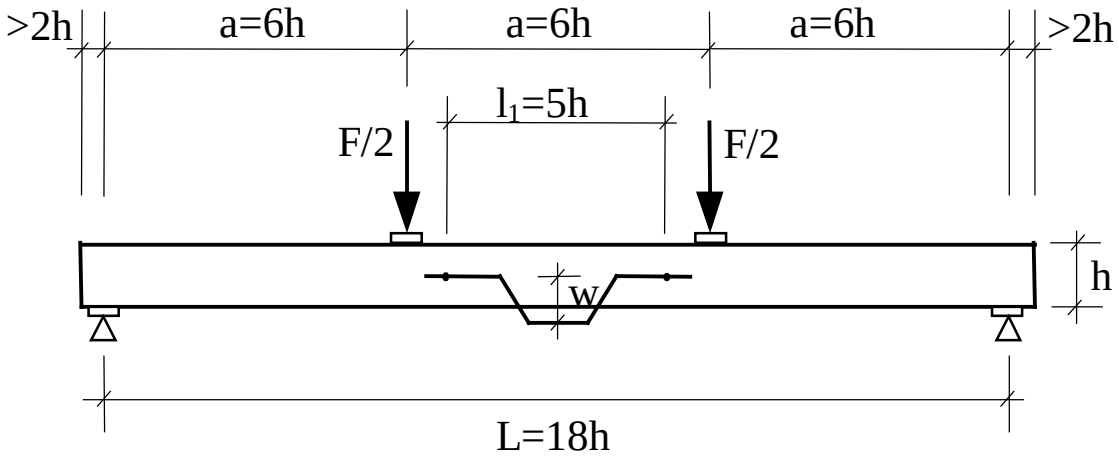

Figure 4-1: Test arrangement for measuring the modulus of elasticity in bending according to EN 408:1995.

The modulus of elasticity in bending E_m is then given by the equation

$$E_m = \frac{a l_1^2 (F_2 - F_1)}{16 I (w_2 - w_1)}$$

where

F_2-F_1 is an increment of load on the straight-line portion of the load-deformation curve [N] and

w_2-w_1 is the increment of deformation corresponding to F_2-F_1, in [mm]

For the beams, the following values are valid:

h = 225 mm

a = 6h = 1350 mm

l_1 = 5h = 1125 mm

L = 18h = 4050 mm

$v \le 0.003 \cdot h = 0.003 \cdot 225 = 0.675 mm/\sec$, chosen value: $v = 0.2 mm/\sec$

The beams were loaded with 3 – 4 kN, which corresponds to circa 25 % of the bending moment capacity (design values). By this low loading, the beams were not damaged as well as no high plastic deformations were obtained.

Under the testing only very small deformations could be measured, for example 0.3 mm for 4 kN load. These small deformation values cannot be taken as correct, because of the deformation gauge accuracy, which is about 3/100 of a millimetre.

The small deflections of about 0.3 or 0.4 mm are due to the high stiffness of the test pieces (highest strength class for glulam and large height). The load-deflection diagrams for testing according to the code did not show a clear linear relationship, but several jags, i.e. load uptake of up to 0.7 kN without deformation. Very high differences in the values for MOE were obtained when changing the increment of load (F_2-F_1) and the increment of deflection (w_2-w_1). As an example, MOE-values ranging from about 10000 MPa up to approximately 24000 MPa were obtained for one beam, the value just depending on the choice of increment.

The load-deflection diagrams would look better and more linear in a minor scale, i.e. if the specimens were tested to a higher load, for example 10 kN. Then the curve would not look so rough but more smooth and linear. But some jags would occur anyhow, that is why it was decided to test the specimens in a different way.

To be able to measure reasonable values for the deflection of the beams, the deflection was measured for the whole span, see Figure 4-2. The other boundary conditions, such as span (18h), two point loads located 6h from the supports, remained the same as claimed in EN408:1995. With this type of test, a linear relationship between load and deflection could be obtained, see Figure 4-3. The MOE was calculated from the equation for deflection of a simply supported beam with two point loads,

$w = \frac{Fa}{24EI}\left(3l^2 - 4a^2\right)$ with a being the distance between load and support.

$\rightarrow E_m = 103.5 \cdot 10^3 \frac{\Delta F}{\Delta w} \cdot \frac{12}{b}$ for a rectangular cross-section with all distances according to code.

With this test arrangement, the deformations measured consist of bending and shear deformations. The size of the shear deformation is not known, but the shear deformations were regarded as not important for this study.

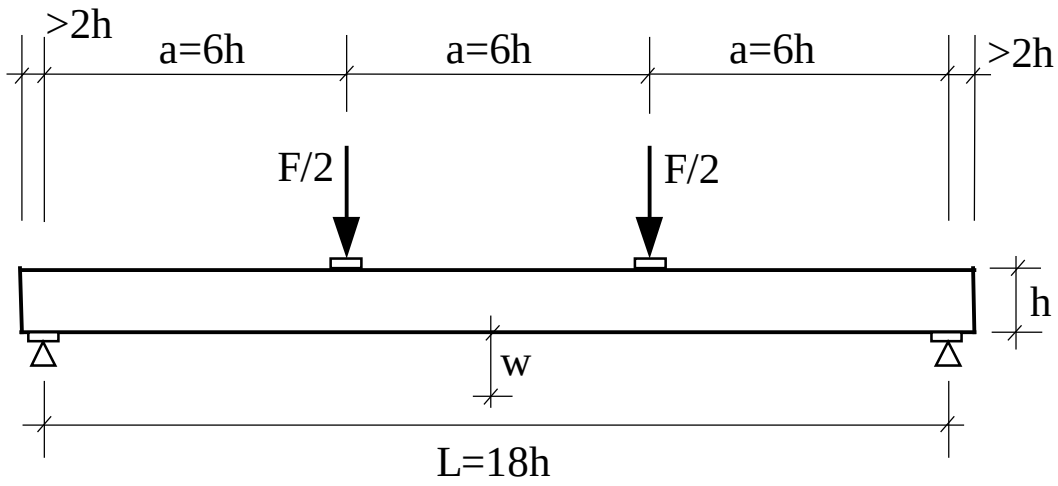

Figure 4-2: Actual test arrangement for measuring modulus of elasticity in bending.

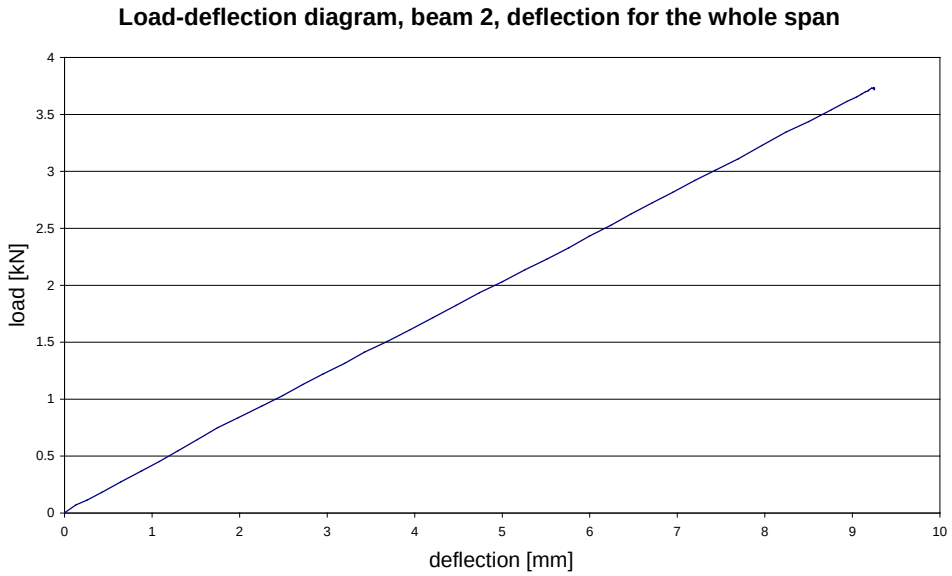

Figure 4-3: Load-deflection diagram for beam 2, deflection measured for the whole span.

The results of the MOE-tests for seven beams are shown in Table 4-1.

Table 4-1: Modulus of elasticity obtained for the beams in edgewise bending tests.

beam number	depth [mm]	width [mm]	MOE [MPa]
1	223.5	41	12350.8
2	224	41	12150.1
3	224	41	12370.1
4	224	41	11656.9
5	223	41	11027.6
6	223.5	41	11414.0
7	223	41	12174.8

A statistical evaluation of the test results of the seven beams can be found in Table 4-2.

Table 4-2: Statistical evaluation of the MOE-test results of the beams.

mean value μ	standard deviation σ	coefficient of variation COV
11878 MPa	518.8 MPa	4.4 %

The same problem as for the beams also appeared for the studs, here it was even more obvious that the stiffness of the test specimens was too high to measure the deflection according to the code. In several tests according to EN 408:1995, negative deflections (deflection upwards) or no deflection at all were measured. That is why the deformation for the studs also was obtained for the whole span.
As it is not clear, in which way the studs will fail in the following tests of the whole system, the MOE has to be measured both for the strong direction and the weak direction (edgewise and flatwise bending). Furthermore, each piece has to be tested in the two strong and two weak directions, i.e. 4 tests are performed on each test piece.

For the studs, the following values are valid:

for bending in the strong direction:
h = 60 mm
a = 6h = 360 mm
L = 18h = 1080 mm
$v \leq 0.003 \cdot h = 0.003 \cdot 60 = 0.18 mm/\sec$, chosen value: $v = 0.1 mm/\sec$

for bending in the weak direction:
h = 42 mm
a = 6h = 252 mm
L = 18h = 756 mm
$v \leq 0.003 \cdot h = 0.003 \cdot 42 = 0.126 mm/\sec$, chosen value: $v = 0.1 mm/\sec$

The results of the bending tests for the studs can be seen in Table 4-3.

Table 4-3: Modulus of elasticity obtained for the studs in edgewise and flatwise bending tests. Studs with highest MOE marked in grey.

MOE [MPa]	bending in the strong direction		bending in the weak direction	
Stud no.	up	down	up	down
1	9879.1	9169.9	9785.0	10482.7
2	10705.5	10457.4	9471.0	10413.9
3	8810.0	9018.2	9330.6	9265.9
4	11502.6	10695.1	10218.3	11751.9
5	9119.4	9193.0	8917.8	8370.3
6	12368.1	12322.0	11206.4	11271.7
7	10129.8	10578.2	10167.7	10526.0
8	9301.3	9734.9	8940.8	8640.1
9	7942.0	8753.9	9382.3	9515.1
10	7662.7	7656.5	8119.9	8065.5
11	9828.4	10183.5	11795.1	13228.8
12	8728.2	8953.1	10573.8	9351.6

A statistical evaluation of the studs test results (12 specimens, 48 tests performed) can be found in Table 4-4.

Table 4-4: Statistical evaluation of the MOE-test results for the studs.

	mean value μ	standard deviation σ	coefficient of variation COV
strong direction	9695.5 MPa	1271.1 MPa	13.1 %
weak direction	9949.7 MPa	1272.5 MPa	12.8 %

To exclude other failure modes than buckling, the strongest, i.e. stiffest studs are used for further tests. As 7 system-tests are possible, only seven studs will be needed, and the 5 studs with minor stiffness will not be used at all. The seven studs with the highest MOE are marked grey in Table 4-3. As the stiffness is composed of EI, the second moment of inertia also has to be considered when determining the "stiffness" of a stud. Due to the differences in the cross-section values, a specimen with high MOE must not have a high stiffness (EI) as well.

The studs were sawn from beams with the cross-section area 225x42 mm (nominal values). The lamella thickness in the glulam is 45 mm. To achieve homogenous material, the studs were sawn in such a manner that each stud consists of two lamellas with the same thickness of 30 mm (studs numbered 1 to 8). From the rest of the material, 4 studs with 2 lamellas of different thickness, 45 mm and 11 mm, were obtained. These studs are supposed to have not such a good performance as the "symmetrical" studs.
The cross-section values for the different studs can be found in Table 4-5.
The six stiffest studs are obtained from the sample with the "symmetrical" studs. The seventh stud is stud number 11 instead of number 8, because it has a higher stiffness in the weak direction. As it is assumed that out of plane buckling will occur, bending in the weak direction will be crucial.

Table 4-5: Cross-section values for the studs.

Stud numbers	width [mm]	depth [mm]	$I_{strong.direction}$ [mm^4]	$I_{weak.direction}$ [mm^4]
1 to 8	41	60	738000	344605
9 to 12	41	56	600021.3	321631.3

The other material properties like bending and compression strength used for the comparative calculations also have to be mean values. These values are adjusted to the mean value for the modulus of elasticity of the single test specimen. For glulam beams, a relation between the modulus of elasticity and the bending strength can be found to $f_m = 0.0035 \cdot MOE - 6.3$ (in: Grazer Holzbaufachtagung 1995). As there does not exist a relation between the MOE and the compression strength of glulam or between the bending strength and the compression strength, further investigation had to be done. A relation between MOE and f_c can be found in Curry / Fewell (1977). The tests performed in this study were done with polish redwood (pinus sylvestris), not for glulam, but the results seem quite good when comparing them to interpolated values from tables given in the swedish code BKR (BKR1999) and EC5 (STEP). The table values can be shown in a diagram plotting compression strength f_c against MOE for different glulam strength classes, see Figure 4-4. The equation from Curry / Fewell gives slightly conservative results for high MOE, being on the "safe side".

In this study, the bending strength is obtained by the relation taken from Grazer Holzbaufachtagung 1995,
$f_m = 0.0035 \cdot MOE - 6.3$ [MPa].

The compression strength parallel to the grain can be taken from the equation from Curry / Fewell (1977),

$f_c = 0.00148 MOE + 10.41$ [MPa].

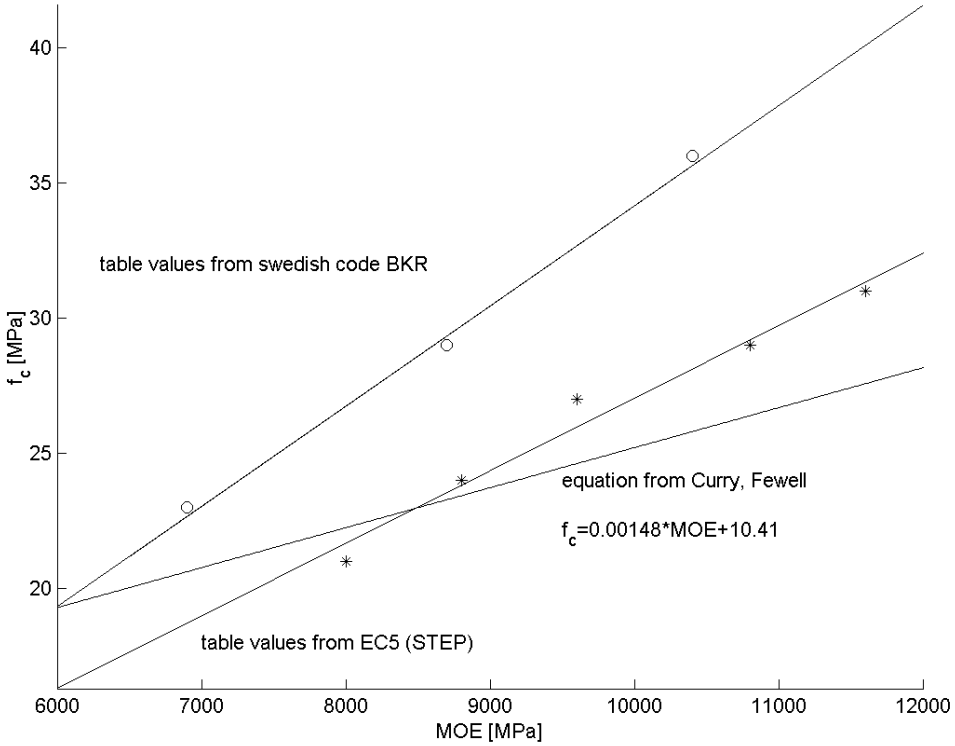

Figure 4-4: Relationship between MOE and compression strength f_c. Table values and regression lines from Swedish code BKR and EC5 as well as relation from Curry / Fewell, 1977.

For the studs, the material properties bending and compression strength are adapted to the MOE that is apparent during the system test. For example, for a stud bending in the weak direction "up", the values for f_m and f_c obtained from the MOE for this direction are used.

The mean strength and stiffness values for the steel tension rods are estimated from the characteristic values by basic statistics (Blom 1994), since no tests concerning the steels properties have been done. An assumption is made that all material properties are normally distributed. The coefficient of variation (COV) for steel is about 5 % (Degerman 1981).

For normal distributions applies $f_k = \mu - 1{,}64 \cdot \sigma$

with f_k = characteristic value
σ = standard deviation
μ = mean value

$COV = \frac{\sigma}{\mu}$ $\quad \sigma = \mu \cdot COV \rightarrow f_k = \mu - 1{,}64 \cdot (\mu \cdot COV)$

$\mu = 1{,}09 \cdot f_k$

$E_k = 205000 MPa \rightarrow E_{mean} = 1{,}09 \cdot 205000 = 223450 MPa = 2{,}2345 \cdot 10^6 MPa$

f_{yk} *= 355 MPa (S355)* $\rightarrow f_{y,mean} = 1{,}09 \cdot 355 = 387 MPa$

f_{uk} *= 490 MPa (S355)* $\rightarrow f_{u,mean} = 1{,}09 \cdot 490 = 534 MPa$

4.3 Test B: Joint Stiffness

The stiffness of the joint between beam and stud has to be tested so that it is possible to compare the final test results (test of the whole system) with the analysis in the computer program. For the test, different nailed joints were manufactured and the stiffness, i.e. spring constant value was tested for bending of the stud in plane and out of plane.

The tested joints are steel-to-timber joints according to EC 5. The following materials / dimensions were used:

- steel plate: t = 2 mm
  l = 400 mm
  b = 60 mm
  steel plates on both sides of the timber members

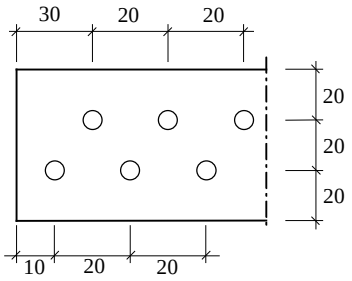

Figure 4-5: Nail plate used in the tests. Dimensions in [mm].

- nails: l = 40 mm
  d = 4 mm
  annular ring shanked nail

Several different joints were manufactured. The number of nails influences the stiffness of the joint. The stiffest joint (A) with this kind of nail plate has 9 nails per plate and joint half, i.e. a total of 9 x 2 x 2 = 36 nails.
The nail plate has 20 holes possible for nailing. The two holes in the middle of the plate cannot be used due to too small edge and end distances.
EC 5 gives minimum values for nail spacing and distances (EC 5, table 8-2) to prevent splitting of the timber members and embedment failure, compare Table 4-6.

Table 4-6: Nail spacings and distances – values according to EC 5, table 8-2. α is the angle between force and grain direction, d is the nail diameter. The factor 0.7 may be used for steel-to-timber connections.

Nail spacings and distances	minimum distance	on the stud [mm]	on the beam [mm]
a_1 (parallel to grain)	$0.7(7+8\cdot\cos\alpha)d$	42	19.6
a_2 (perpendicular to grain)	$0.7\cdot 7d$	19.6	19.6
$a_{3,t}$ (loaded end)	$0.7(15+5\cdot\cos\alpha)d$	56	42
$a_{3,c}$ (unloaded end)	$0.7\cdot 15d$	42	42
$a_{4,t}$ (loaded edge)	$0.7(7+5\cdot\sin\alpha)d$	33.6	19.6
$a_{4,c}$ (unloaded edge)	$0.7\cdot 7d$	19.6	19.6

Not all the requirements for the nail spacings and distances are fulfilled in the test. This was done to create a really stiff joint by using many nails. By comparison with weaker joints (less nails), the influence of the joint stiffness on the systems behaviour can be studied.

Four different test systems were created with two different joints. Tests 1 and 3 were done with a nailed joint with 9 x 2 x 2 nails (nailed from both sides, Joints A and C), Tests 2 and 4 were performed with weaker joints with 4 x 2 x 2 nails. The difference between joints A and C is an initial inclination out of plane for joint C (circa L_{stud}/1000). Joints B and D are exactly the same, with the difference of the stud in Test 4 (joint D) being only half as long (0.60m) than in Test 2 (joint B, 1.20m).

4.3.1 Stiffness-Test B1: Joint stiffness out of plane

4.3.1.1 Test set-up

The beam and the stud are nailed together, forming a T-joint. Then the beam is placed horizontally in a testing machine, on top of a steel beam and two steel plates, see Figure 4-6. On the timber beam, steel plates are placed next to the joint, another timber beam is put on top of this and loaded with a hydraulic jack. By loading the timber beam with a hydraulic jack, the beam is fixed in its position, i.e. it cannot move or twist. By placing steel plates beneath and above the timber beam next to the joint, the timber beam is fixed next to the joint, but the joint is free to rotate, as it is in reality. The horizontal stud is loaded 1.0 m (0.55 m for the short stud) from the joint by the hydraulic jack of another testing machine. Two deflection gauges are placed next to the load, to measure the deflection of the cantilever end.

Figure 4-6: Test set-up for testing the joint stiffness for bending out of plane. The manually controlled jack in the testing machine to the right applies the load on the stud. The beam is fixed in the testing machine to the left, but the joint is left free to rotate.

4.3.1.2 Testing procedure

The cantilever (stud) is loaded by a manually controlled jack. Load and deflection are measured every second and a load-deflection diagram is produced on the testing computer. The stud is loaded up to a total deflection of about 30 to 40 mm, which corresponds to a load of about 300 N. The spring constant *k* is tested in both directions ("upwards" and "downwards", referring to the designation in the MOE-testing), obtaining two values for *k*. Then the mean value of these two can be calculated, giving a more reasonable value compared to just one testing. Another advantage of testing in both directions is that deviations from straightness, which result from the testing, can be minimised. If the testing in both directions is done to approximately the same deflection of the stud, then the remaining angle Θ in the joint will be nearly zero.

4.3.1.3 Test results

The results obtained in the test have to be modified, since the total deflection measured consists of two parts: bending in the stud and rotation in the joint.
The deflection due to bending in the stud (see Figure 4-7) can be calculated from basic statics to $\delta_{bending} = \frac{PL^3}{3EI}$.

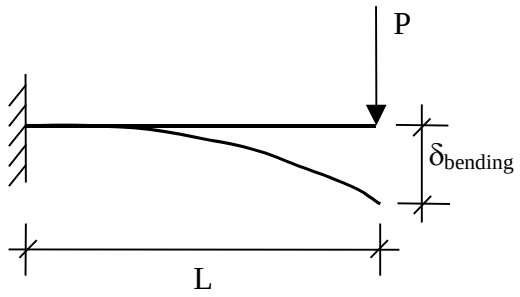

Figure 4-7: Deflection of the cantilever due to bending in the cantilever (stud).

The deflection due to rotation in the nailed joint (see Figure 4-8) can be estimated with $M = \Theta \cdot k$, with *k* being the spring stiffness of the joint. For small angles $\sin\Theta = \Theta = \frac{\delta_{jo}}{L}$ is valid. These two equations lead to

$$\delta_{jo} = \Theta L = \frac{M}{k} L = \frac{PL}{k} L = \frac{PL^2}{k}.$$

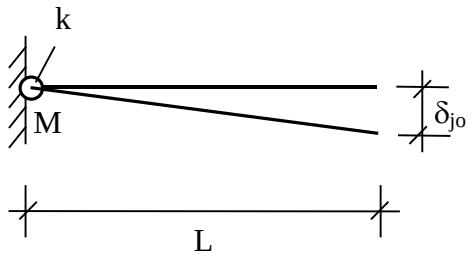

Figure 4-8: Deflection in the cantilever due to spring constant k in the joint.

The total deflection (see Figure 4-9) is
$\delta_{tot} = \delta_{bending} + \delta_{jo}$.

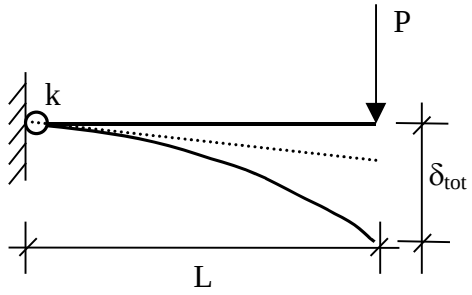

Figure 4-9: Total deflection in the cantilever, due to bending in the cantilever and spring constant k in the joint.

Using the expressions for $\delta_{bending}$ and δ_{jo}, the spring constant k can be calculated as follows:

$$\delta_{tot} = \delta_{bending} + \delta_{jo}$$

$$\delta_{tot} = \frac{PL^3}{3EI} + \frac{PL^2}{k}$$

$$k = \frac{PL^2}{\left(\delta_{tot} - \frac{PL^3}{3EI}\right)}$$

The measured load and deflection are used to create a load-deflection diagram.
The spring constant k is calculated using a section of the linear portion of the load-deflection diagram. Then the equation for k looks like this:

$$k = \frac{\Delta PL^2}{\left(\Delta\delta_{tot} - \frac{\Delta PL^3}{3EI}\right)}$$

The spring constants k are tested and calculated for the different joints and can be found in Table 4-7.

Table 4-7: Spring constant k in [kNm/rad] for bending out of plane (weak direction) obtained from tests and k_{ser} calculated according to EC 5.

Test no.	Joint	number of nails	k [kNm/rad] "upwards"	k [kNm/rad] "downwards"	k [kNm/rad] mean value	k_{ser} according to EC5, [kNm/rad]
B1a	A	9 x 2 x 2	9.7	5.5	7.6	13.70
B2a	B	4 x 2 x 2	2.8	2.3	2.6	6.08
B3a	C	9 x 2 x 2	4.5	6.1	5.3	13.70
B4a	D	4 x 2 x 2	1.9	2.1	2.0	6.08

Large differences can be found in the spring constants between the test results and the spring constant k_{ser} calculated according to EC 5. In general, the value from EC 5 is much higher than the tested ones.

4.3.2 Stiffness-Test B2: Joint stiffness in plane

The joint stiffness in plane is tested nearly in the same way as out of plane, but the test set-up is slightly different. The equation for spring constant *k* presented in section 4.3.1.3 is also valid for bending in plane.

4.3.2.1 Test set-up

The beam is put upside-down in one of the testing machines, so that the stud (cantilever) is sticking up, see Figure 4-10. The beam is loaded with a hydraulic jack to ensure that no movement occurs in the beam itself, preventing slipping on the testing machine, when the cantilever is loaded horizontally. Putting woodblocks between the beam and the frame of the testing machine ensures bracing to prevent tilting and torsion. The cantilever is loaded horizontally by a manually controlled hydraulic jack. One deflection gauge is placed on the jack to measure the horizontal deflection of the cantilever at the loading point. Another deflection gauge is placed on the testing machine, measuring the slip of the beam on the testing machine.

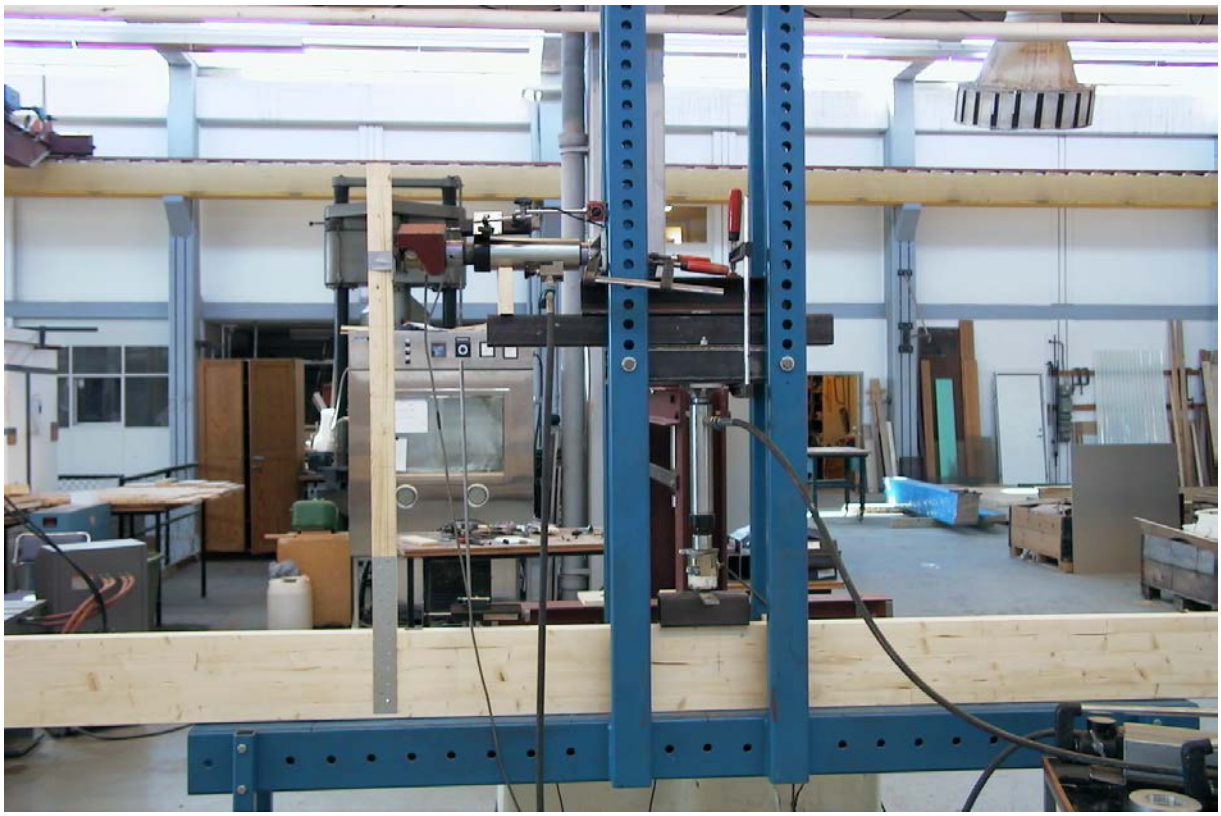

Figure 4-10: Test set-up for testing the joint stiffness for bending in plane. The beam is fixed in the testing machine (loading and woodblocks). The horizontal jack applies the load on the stud.

4.3.2.2 Testing procedure

See the statements in 4.3.1.2.

4.3.2.3 Test results

The spring constants *k* are tested and calculated for the different joints and can be found in Table 4-8.

Table 4-8. Spring constant k in [kNm/rad] for bending in plane (strong direction) obtained from tests and k_{ser} calculated according to EC 5.

Test no.	Joint	number of nails	*k* [kNm/rad] "upwards"	*k* [kNm/rad] "downwards"	*k* [kNm/rad] mean value	k_{ser} according to EC5, [kNm/rad]
B1b	A	9 x 2 x 2	31.1	33.6	32.4	85.63
B2b	B	4 x 2 x 2	2.5	2.2	2.34	8.28
B3b	C	9 x 2 x 2	17.8	40.8	29.3	85.63
B4b	D	4 x 2 x 2	2.8	2.9	2.8	8.28

As in the preceding test of the joint stiffness in the weak direction, the differences between test results and the spring constant calculated according to EC 5 are large. Here, the calculated values for the spring constant *k* are more than twice as large than the tested ones. For the comparison of test results of the system tests and the theoretical model, the test values of the joint stiffness will be used.

The movement of the beam on the testing machine (slipping due to the horizontal loading of the cantilever) is measured during the whole test. No movement in any special direction can be noticed. The beam performs a kind of oscillation around an equilibrium point with a maximum amplitude of $\Delta w = 0.0323 mm$ (which can be claimed to be no movement).

4.4 Test C: System Tests

4.4.1 Objective

The aim with the system tests is to test trussed beams (see Figure 4-11) and then compare the test results with the calculations of the theoretical model. As the main problem in the theoretical model was the elastic critical load analysis (ECL) and the determination of the buckling length of the different structural members, the focus in the test was on the problem of the stud buckling out of plane.

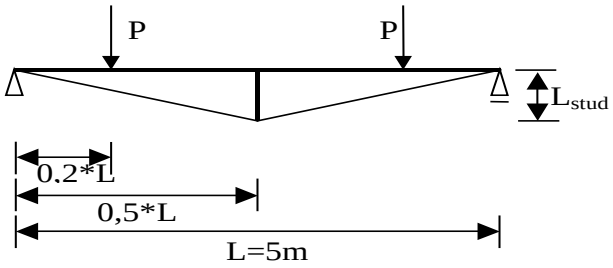

Figure 4-11: Tested system (trussed beam).

4.4.2 Material

For the structural system, the jointed timber members (compare section 4.3) are used. Additionally, tension rods, steel plates, a C-steel-profile as well as some bolts, screws and nuts were needed.

- glulam beam, L = 5.20 m, h = 225 mm, b = 42 mm (nominal values)
- glulam stud, L = 1.20 m, h = 60 mm, b = 42 mm (nominal values)
- tension rods, 2 pieces, L = 6.20 m, diameter 12 mm, strength class S355
- steel plates, 2 pieces, h = 150 mm, b = 100 mm, t = 10 mm, holes with diameter 13 mm for the anchorage of the tension rods and smaller ones to screw the plate onto the timber beam
- C-steel profile, U30, h = 30 mm, b = 33 mm, L = 60 mm, t = 5 mm, holes to screw it onto the stud and to insert a security bolt
- bolts, screws, nuts

4.4.3 Test set-up

The timber parts used in the system test were already tested in the tests A (MOE) and B (joint stiffness, compare sections 4.2 and 4.3). To be able to put the system together, the tension rods had to be bent by hand. The C-profile was fixed on the studs lower end by screws and the tension rods were inserted. A bolt holding the rods in place secures the joint between tension rods and stud, see Figure 4-12.

Figure 4-12: Joint between stud and tension rods.

An inclination had to be sawn in the beam-ends to screw the steel anchorage plate on the beam end so that the inclined tension rods are perpendicular to the plate. The 6.2 m long tension rods were threaded at the ends, inserted in the anchorage plates and fixed with nuts, compare Figure 4-13.
Two tension rods instead of just one are used for the test structure for two reasons: First, they have to be bent, and smaller diameters are easier to bend. Secondly, the joint between beam and tension rod would be more complicated with just one tension rod. This tension rod would have to be in the systems axis, i.e. in the beams neutral axis. A hole would have to be drilled through the beam end to fix the tension rod in the beam axis. Due to the small dimensions (the width of the beam is only 42 mm), one tension rod with 16 mm diameter would cause problems when drilling a hole with 17 or 18 mm diameter. Splitting of the timber would occur for sure. However, for larger structures with much larger dimensions, joints with tension rods going through the timber are no problem.

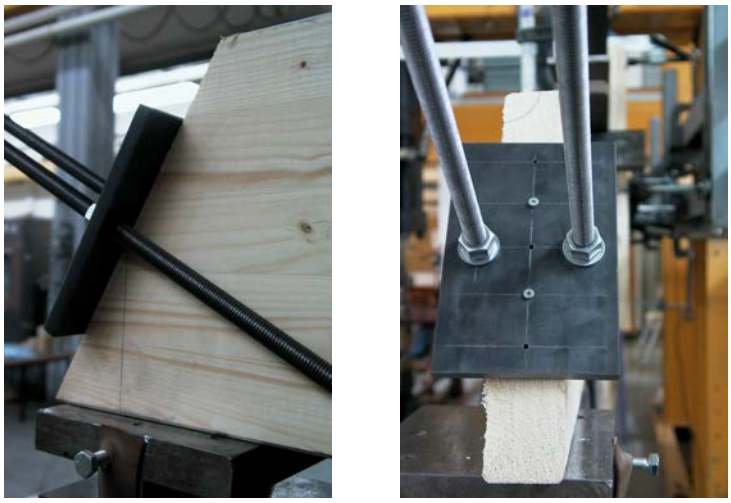

Figure 4-13: Joint between tension rods and glulam beam.

The timber beam was put on the supports (5 m span) and secured against translation out of plane by clamps in three points equidistant with 1.25 m. No fork supports were used since they are not very usual in large span constructions. If a fork support is used at the supports, then it does not have a high influence on the torsion of a long beam. On the length of the beam, fork supports are not possible. The bracing obtained by purlins or steel sheathing can just prevent a translation of slender beams, not torsion.
Two strain gauges were glued on each tension rod, one on each half of the system. The strain gauges measure the strain in the rod when the prestressing is applied and during the test. The prestressing is applied from both sides of the system by fastening or loosening the nuts, with the purpose to have a uniform strain in both tension rods and in both sides of the tension rods. As the tension rods were bent to be fixed to the studs end, there is a salient point in the rod. Additionally, friction occurs between the rods and the steel profile being fixed to the stud.

When applying the tension force on the steel rods, great attention has to be paid to an even prestressing in order not to incline the stud in plane.
The loading of the test system was supposed to consist of two point loads located 0.2L = 1.0 m from the supports. This loading meets the bending moment distribution of a uniform load best. To be able to apply two point loads of the same size with one jack, a single span steel beam was needed to distribute the point load of the jack, see Figure 4-14 and Figure 4-15. For this purpose, a 4.12m long IPE160 steel beam was chosen.

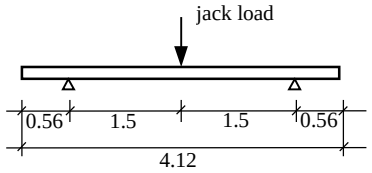

Figure 4-14: Single span steel beam IPE160 used to distribute the jack load to the glulam beam.

This beam can handle a point load in the centre of about 40 kN, then the characteristic yield limit is reached. Even if the beam may yield a little when exposed to higher loads, it was chosen due to its relatively low dead load. The steel beam is put on the glulam beam in the right position and secured with a crane to prevent falling down and crushing the test system and the measuring devices when the system fails, see Figure 4-15.

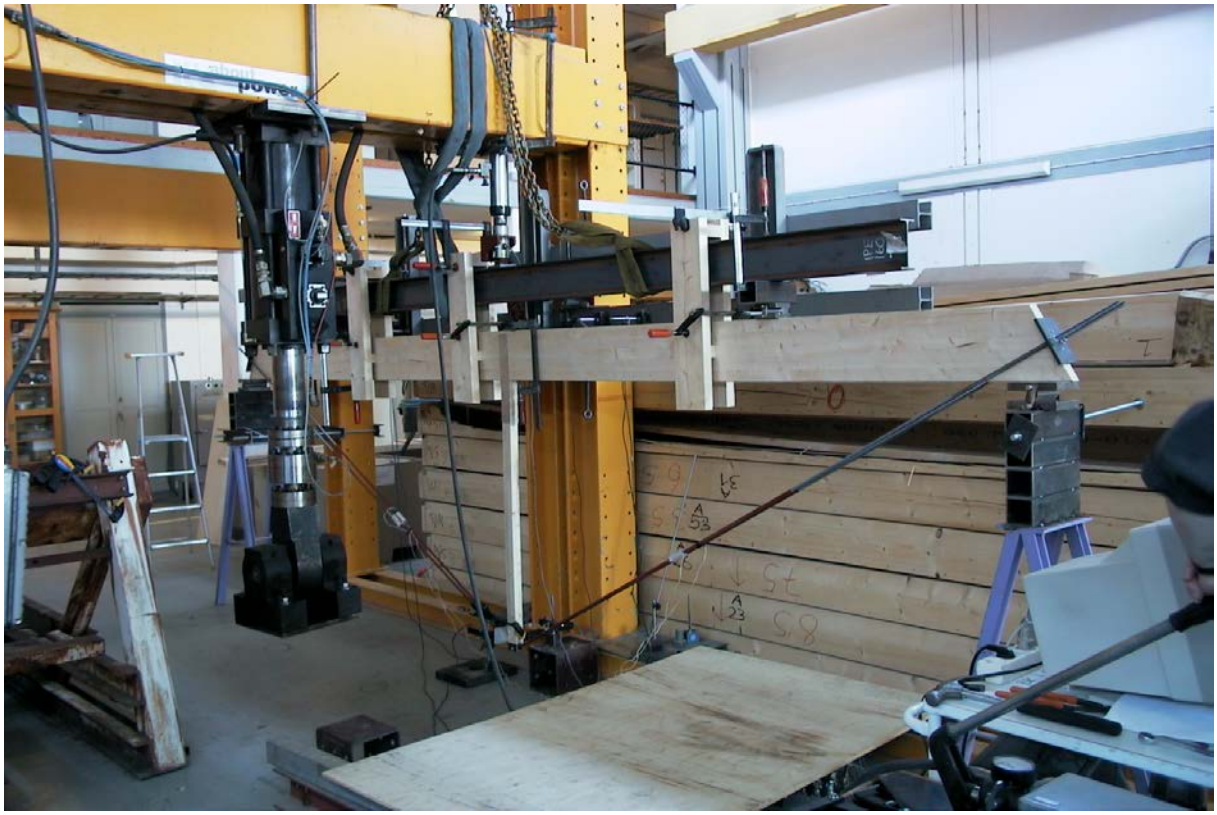

Figure 4-15: Test set-up for the system tests.

The first test (Test C1-1) was performed with the steel beam only being braced at midspan. At a load of about 30 kN, the load uptake was stopped since the steel beam twisted and the reaction forces of the steel beam could not be transferred to the glulam beam. The stud was bending out of plane, but the buckling load of the system was higher than the 30 kN applied.

As a consequence, the bracing of steel beam and glulam beam were connected to each other, providing 3-point-bracing for both beams for the following tests, see Figure 4-16.
The glulam beam was fixed against translation out of plane in its neutral axis. The steel beam was left free to deflect independent of the beams movements. A small gap between the bracing device and the steel beam ensured that the two beams could behave independently of each other, but on the other hand, the steel beam was prevented from twisting.

Figure 4-16: Bracing device for steel and glulam beam.

The loading of the test system is done with a manually controlled jack with a low load rate in order to achieve a high number of measuring points as well as to notice all the deflections in the system.
The deflections at certain points of the system are measured with deflection gauges with 100 mm and 200 mm measuring length respectively. The deflection gauge with the longest measuring length (200mm) is placed at the lower end of the stud as this point is assumed to deflect most in horizontal direction. The deflection gauges with 100 mm measuring length are placed at the studs end for deflection in plane and at different places on the beam for vertical and horizontal deflection. The torsion of the beam is measured using one deflection gauge at the neutral axis and two gauges located 45 mm from the upper and lower edge of the beam.
From the second to the last test, another deflection gauge measured the studs deflection out of plane at the half of the stud length. By comparing the deflections at the end and in the middle of the stud, the bending in the stud can be estimated, see Figure 4-17. With this bending, the buckling length of the stud can be estimated with help of the so-called “Southwell-Plot” (Trahair and Bradford, 1991). This method is used to extrapolate the elastic critical load from tests (tests can be non-destructive).

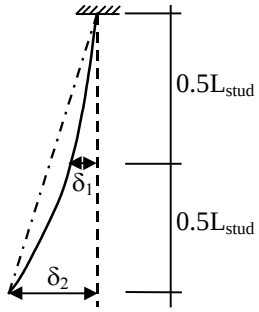

Figure 4-17: Estimating the bending in the stud from the measured deflections δ_1 and δ_2.

The bending in the stud is approximately the difference between the two measured deflections. Without bending, $\delta_1 = 1/2\,\delta_2$ is valid. With bending in the stud, δ_1 gets smaller, and $\delta_{bending} = 1/2\,\delta_2 - \delta_1$ approximates the bending in the middle of the stud. The result is not totally correct, as the stud is inclined and the deflection is measured horizontally instead of perpendicular to the stud axis. For further research in this field, this problem could be either solved geometrically in the evaluation of the test data or directly in the test set-up. For this study, the achieved values were assumed to be sufficiently accurate.

In the Southwell-plot, the ratio of central bending deflection and axial load in the stud ($\delta_{bending} / N_s$) is plotted against the central deflection ($\delta_{bending}$), see Figure 4-18. A linear correlation line fitting the measured values best is inserted. The slope of this straight line gives an estimation for the elastic critical load of the stud. The initial crookedness δ_0 of the stud can be estimated by the intercept on the horizontal axis.

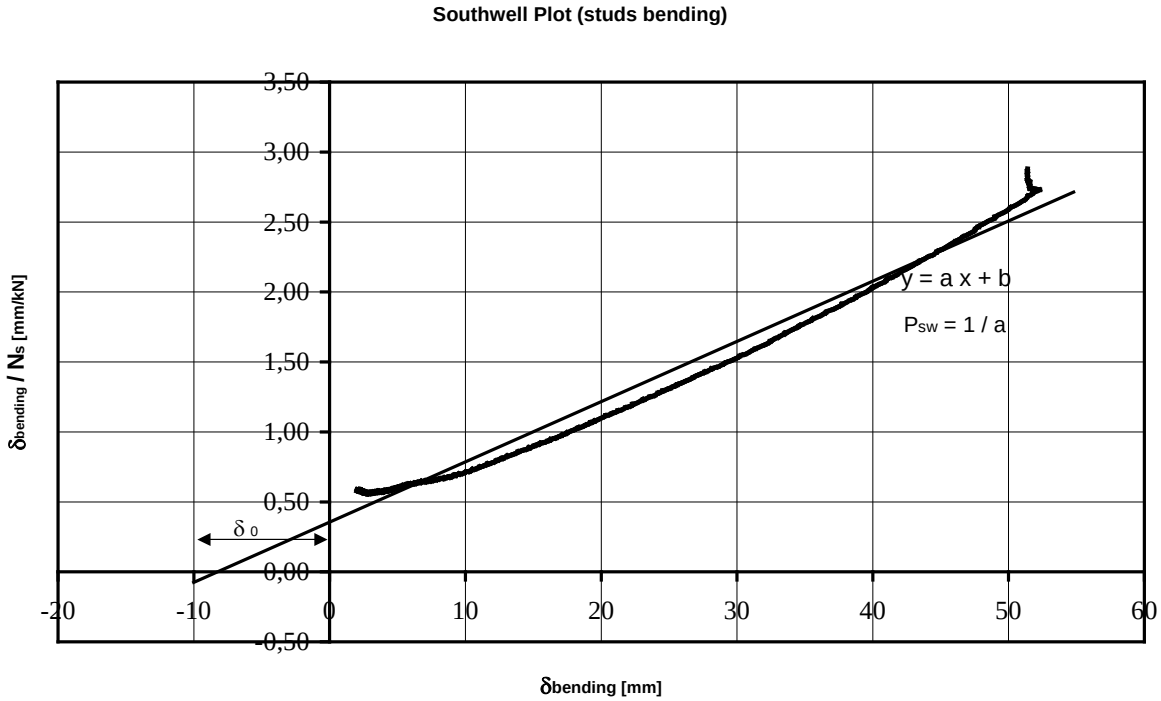

Figure 4-18: Southwell-Plot.

During the test, the deflections at different points, the load and the strain in the tension rods were recorded every second. From these measured values, diagrams can be created showing load – deflection as well as load – strain relations, see for example Figure 4-20. The strain in the steel tension rods can be transformed to the actual tension force by multiplying the strain value with the extensional stiffness: $F_{t,i} = \varepsilon_i EA$

For estimation of the axial force in the stud, the sum of all tension forces in the steel rods is needed. The axial load in the stud is then calculated from the geometrical relation $N_s = \sum F_t \cdot \cos\varphi$, φ being the angle between the stud and the tension rods.

Using the equation for Eulers critical load, the buckling length of the stud as well as the buckling length factor β can be estimated:

$$N_{cr} = \frac{\pi^2 EI}{(\beta L)^2}, \text{ assumption } N_s = N_{cr} \rightarrow \beta = \frac{\pi}{L}\sqrt{\frac{EI}{N_s}}$$

The different values for the deflection gauges and the jack are visible during the whole testing on the computer, so that certain actions can be taken in time. For example, one deflection gauge measuring the horizontal deflection of the cantilevers end has to be removed when it is obvious in which direction the stud bends. The other deflection gauge (on the “safe” side) is left there to measure the deflection.

In the evaluation of the test results, an additional load was considered for the dead load of the steel beam and the rest of the loading equipment (supports, clamps, steel plates and so on). The steel beam has a dead load of G = 0.65 kN. Then 0.1 kN was added for the rest, giving a total additional load of $G_{additional}$= 0.75 kN.

Many photos have been taken during the testing procedures, showing the set-up, the deflection under load and the failure. Additionally, a video was taken to be able to see the actual failure moment.
The test data were evaluated and are presented in the following. However, not all the diagrams and photos of the test can be shown. For those interested in this test data (test files, diagrams as well as photos), a CD is available.

4.4.4 Overview of the system tests

The boundary conditions for the different tests, such as stud length, type of joint and initial inclination of the stud out of plane are reviewed in Table 4-9.

Table 4-9: Boundary conditions for the different system tests.

Test no.	stud length [m]	joint	inclination
C1-5	1.2	A (stiff)	-
C2-2	1.2	B (weak)	L_{stud} / 100
C2-4	1.2	B (weak)	L_{stud} / 24
C3-1	1.2	C (stiff)	L_{stud} / 150
C4-1	0.6	D (weak)	L_{stud} / 50
C4-4	0.6	D (weak)	L_{stud} / 9.5
C4-5	0.6	D (weak)	L_{stud} / 3.6

4.4.5 Test C1-5

The first system test was performed with stud no. 1 and beam no. 6, together forming the first "test-system", see Figure 4-19. The stud is 1.2 m long, the beam has a span of 5.0 m. The angle between the steel tension rods and the beam is 28 degrees. Joint A, the "stiff joint", was used.

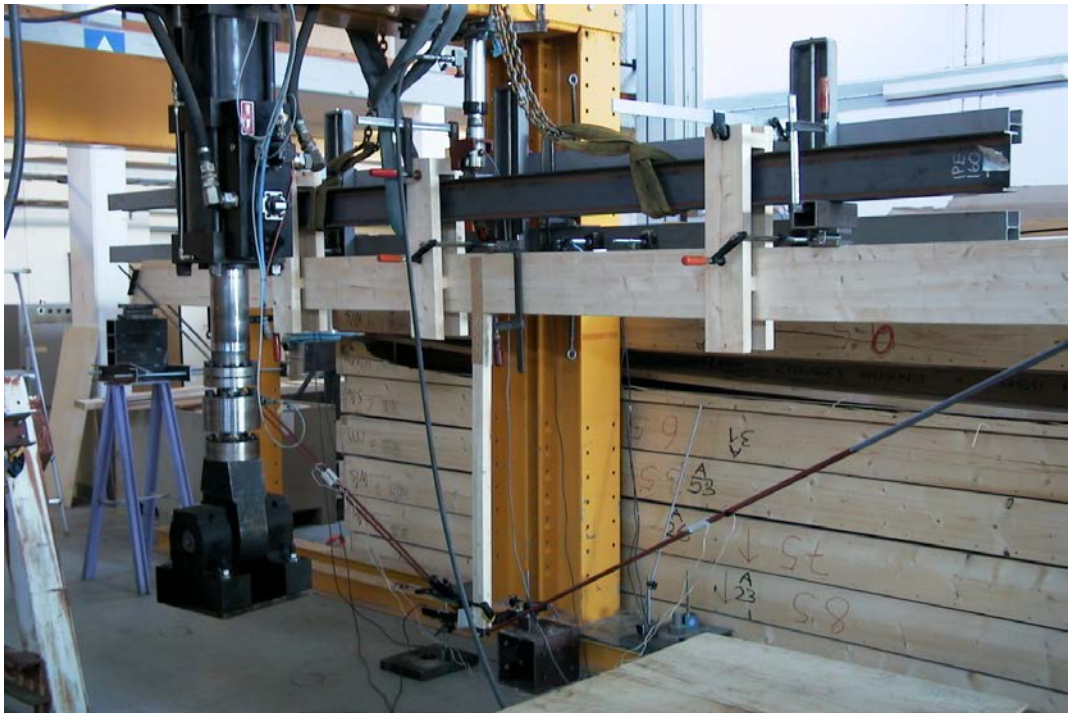

Figure 4-19: Test set-up for system test 1-5.

A calculation of the test system was done before testing with Microstran. It gave a total load for out of plane buckling of the stud of P_{tot} = 12 kN. This seemed to be a quite low load, but since the buckling length is a problem in the computer calculations, it was taken as a starting value. The prestressing of the tension rods was done with about F = 0.56 kN. This force results in equal values for bending moment (negative and positive) in the beam for a total load of P_{tot} = 12 kN. When prestressing the tension rods it was made sure that the stud did not deflect in plane due to uneven prestressing from both sides of the system. Then the system was loaded. As expected, the stud deflected out of plane with increasing load. In the beginning, the stud deflected about 1 mm for each kN of load on the system. At a load of about P = 37 kN, the deflections increased in relation to the load-increase, see Figure 4-20. The maximum load posed on the test system is P = 41.6 kN. After reaching this maximum load, the load uptake stopped and the stud buckled out of plane at a load of $P_{failure}$ = 41.5 kN. The failure mode found was bending failure in the stud. The stud buckled at its midspan (about 53 cm from the jointed end). From this failure mode can be concluded that the buckling length of the stud is lower than $2L_{stud}$, since a stud with that buckling length would have experienced larger deformations in the joint. Additionally, it would have buckled at a much lower load.
The steel beam bent laterally (see Figure 4-22), i.e. it twisted under the load and produced an uneven pressure on the timber beam at the steel beams supports, see Figure 4-23. The glulam beam itself did not twist much, as can be seen in Figure 4-21: The two deflection gauges on the right half of the beam were placed on the lower and upper edge of the glulam beam. “Upper edge” means here one lamella (45 mm) from the upper edge and “lower edge” one lamella from the lower edge respectively. The deflection gauges could not be placed nearer to the edge since the beam also deflects vertically. There was always the risk that the upper deflection gauge would not measure during the whole test, but jump off the glulam beam. Due to the uneven pressure on the beam, the glulam beam twisted slightly to the end of the test – the horizontal deflection at the lower edge increases much more than on the upper edge.

Figure 4-20: TestC1-5, studs deflections out of plane and in plane in relation to the total load P on the system. One deflection gauge measuring out of plane buckling was removed to prevent damage, the deflection gauge measuring in plane deflection jumped off the measuring plate when the deflection out of plane increased too much.

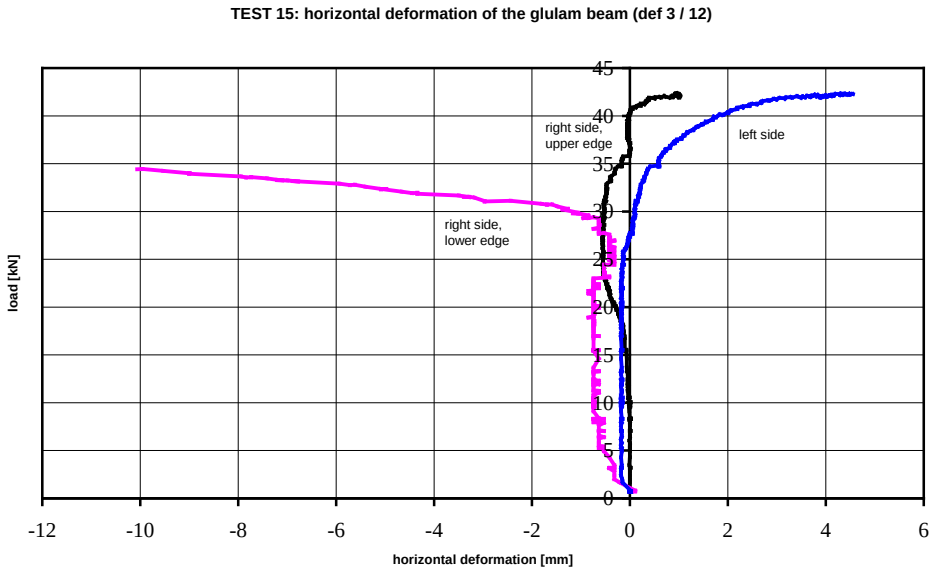

Figure 4-21: Test C1-5, horizontal deflection of the beam.

Figure 4-22: The stud bends out of plane, the steel beam experiences lateral buckling.

Figure 4-23: Uneven load-transfer due to the twisting of the steel beam

The axial force in the stud at the moment of failure can be estimated to $N_{s,\,failure} = 20.53kN$. With the stiffness value (EI) for the stud (bending "weak up") and the stud length, the buckling length factor β can be calculated to $\beta = \frac{\pi}{1.2}\sqrt{\frac{3.372}{20.53}} = 1.061$, which is close to $\beta = 1.0$ (Euler-case 2). An assumption was made that the stud is a perfect Euler-column. As the stud is not perfect – initial inclination and crookedness – it failed at a lower load and the buckling length factor is somewhat higher than $\beta = 1.0$. The system did not fail at the maximum load but at a little lower load, which means that the buckling length factor can also be estimated for the maximum load to $\beta = 1.043$. The failure of the system was due to

bending in the stud, occurring at a section with a defect, which locally decreases the stiffness, see Figure 4-24. So perhaps an even higher load would have been possible if the stud had been defect free in the failure zone.

Figure 4-24: Detail of the failure in the stud. The failure happened almost in the middle of the stud at a section with a large defect (knot), which locally reduces the strength..

This test result, giving a buckling length factor for the stud that is almost 1.0 as for Euler case 2 (simply supported beam) proves the hypothesis that the tension rods have a large stabilising effect on the stud and also on the whole system of the trussed beam.

After removing the tension rods, the beam was loaded to failure, see Figure 4-25. This was done to check the assumptions made for the relation between MOE and bending strength in section 4.2.

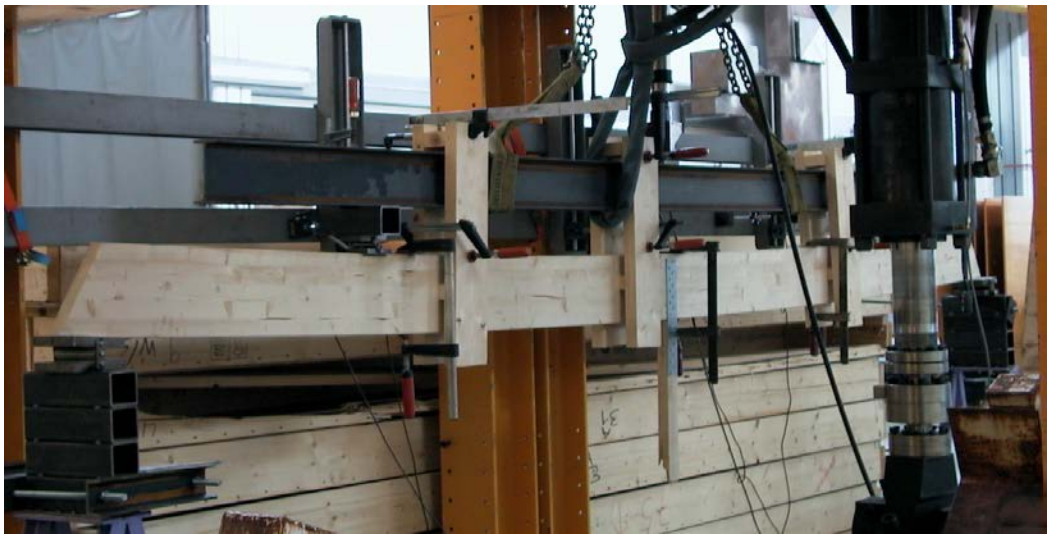

Figure 4-25: Testing the glulam beam to failure.

The maximum bending moment for the beam loaded with two point loads can be estimated as $\max M = \frac{Pa}{2}$, P being the total load being imposed on the system and a being the distance between support and loading point. The bending moment capacity is $M_R = f_m W$. For this beam, $M_R = 11.486 kNm$ gave an expected failure load of $P_{\exp} = 22.97 kN$. When loading the system, the beam experienced large deformations (see Figure 4-25) and failed at a load of

$P_{failure} = 22.91kN$, only 0.3% lower than the expected failure load. This result affirms the correctness of the relation between MOE and bending strength used in this study. The failure mode was a combination of bending and shear failure in the beam and tension failure in a finger joint in the lowest lamella, see Figure 4-26.

Figure 4-26: Failure in the beam. Combined bending and shear failure in the timber (left) and tension failure in the finger joint (right).

The increase in load from the regular beam to the trussed beam was 181% in this test. That means that the trussed beam can carry almost twice as much load as the regular beam.

4.4.6 Test C2-2

The second system test was performed with stud no. 6 and beam no. 7. The stud is 1.2 m long, the beam has a span of 5.0 m. The angle between the steel tension rods and the beam is 28 degrees. Stud and beam are put together with joint B, the weaker joint used in these tests, containing 2 x 2 x 4 nails, see Figure 4-27. The tension rods were prestressed with about 0.56 kN. The stud has an inclination out of plane of about $L_{stud}/100$.

The system was set up and loaded as described above. With increasing load, the stud deflected out of plane and the glulam beam as well as the steel beam twisted. Due to the twisting, uneven pressure was put on the glulam beam at the steel beam supports. As a consequence, the load could not be increased any longer.

The failure mode was lateral buckling in both the steel and the glulam beam, see Figure 4-28.

Figure 4-27: Joint B, used in Test C2-2,C 2-4 and C2-6.

Figure 4-28: Testing system 2-2.Failure due to lateral buckling in both the steel and the glulam beam.

The stud deflected out of plane with almost no visible bending in the stud itself. Large deformations occurred in the nailed joint (bending in the steel side plates).

The consistency between the buckling length factors directly obtained from the test and from the Southwell-plot is fairly good (6% deviation), see Table 4-10 and Figure 4-29. During the test, the buckling load for the stud was not reached as the beams bent laterally and the load uptake was stopped. This means that the buckling length factor β_{test} is too high as $N_s < N_{crit}$. The buckling length factor obtained from the Southwell-plot seems reliable. As the failure mode was not buckling of the stud, it can be concluded that the buckling load of the stud is even higher than the one obtained in the test. This means that the buckling length factor gets even closer to $\beta = 1.0$, which is valid for the ideal pin-ended Euler-column.

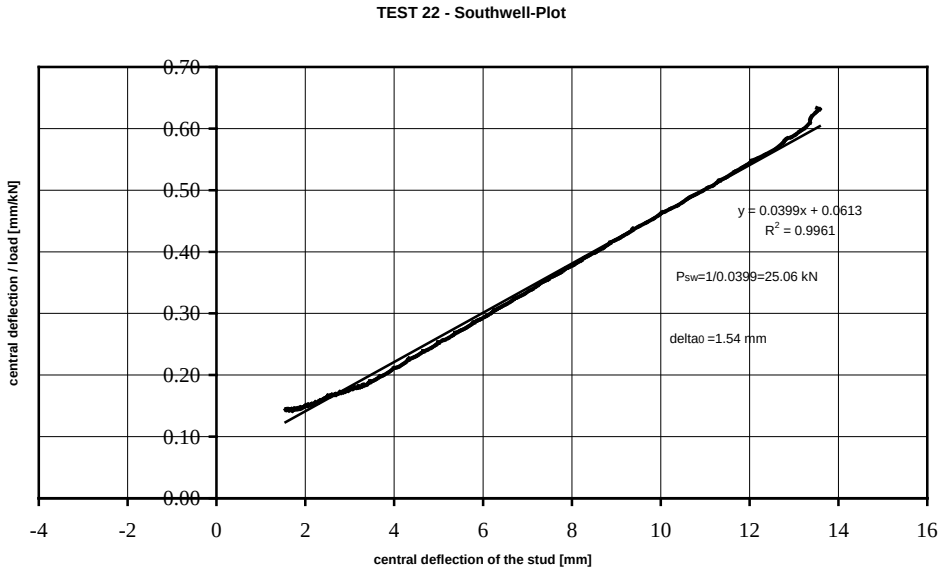

Figure 4-29: Southwell-Plot to estimate the buckling load of the stud. The maximum Southwell-load P_{sw} is the reciprocal value of the slope, the initial crookedness equals the interception on the horizontal axis.

Table 4-10: Evaluation of the test results for system test C2-2.

maximum load	max P [kN]	42.9
maximum tension force in the steel rods	max N_t [kN]	47.3
maximum axial force in the stud	max N_s [kN]	22.2
buckling length factor (test)	β_{test}	1.095
maximum Southwell-load	max $N_{s,sw}$ [kN]	25.1
buckling length factor (Southwell)	$\beta_{Southwell}$	1.03

4.4.7 Test C2-4

As the system did not fail due to instability reasons in test C2-2, the system was loaded again. Due to the high loading in test C2-2, plastic deformations were achieved in the joint so that the stud was inclined with about $L_{stud}/24$. This test system can therefore be regarded as a system with imperfection.
To avoid the failure mode of lateral buckling of the glulam beam, the supports of the steel beam were changed, see Figure 4-30. The compressed area on the glulam beam was increased to reduce the risk of an inclination due to locally high compression perpendicular to the grain.

Figure 4-30: Increased support area to avoid oblique supports due to locally high compression perpendicular to the grain.

When loading the system, the stud bent out of plane. Again, there was almost no central bending visible in the stud. The stud bent so much, that the deflection gauge (200 mm measuring length) did not last for the large deflections. At a deflection of about $\delta_2 = 462mm$, the stud came in contact with the steel portal frame that housed the whole test structure, see Figure 4-31. The stud could not deflect more, and shortly after it reached the portal frame, the load could not be increased any longer.


Figure 4-31: Test C2-4. On the left, the stud begins to deflect out of plane; on the right, the maximum horizontal deflection (462 mm) is reached when the stud touches the steel portal frame and no further deflection is possible.

The system was unloaded without bending or buckling failure in the stud. Large plastic deformations were visible in the joint (bending in the steel plates), see Figure 4-32. The nails are inclined and there is a gap between the glulam member and the steel plates as the embedding strength of the glulam is exceeded.

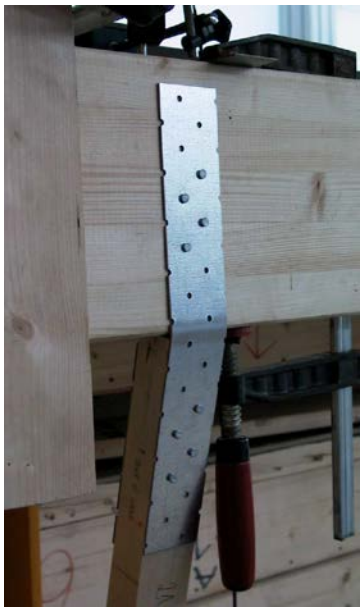
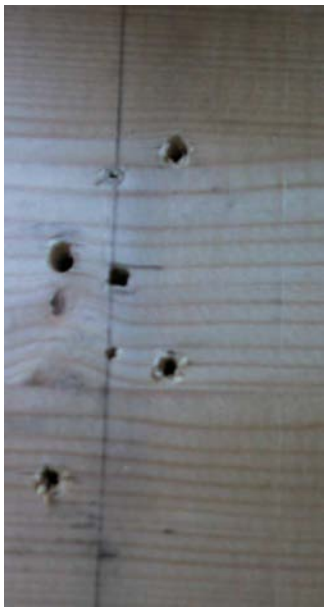


Figure 4-32: Nailed joint after system test C2-4. The steel plates bent (left, right), the stud is compressed inclined in the beam (left). The deformation in the joint is possible by deformation in the nails (bending) and by compression perpendicular to the grain in the glulam beam, exceeding the embedding strength of the nails (middle).

The system was not loaded to the failure load in this test. The load uptake was stopped when the stud reached the portal frame and could not deflect horizontally any longer. As the maximum load observed is not the "right" failure load, the buckling length factor obtained from the test (by assuming $N_s = N_{cr}$) is not correct. The value for β obtained from the Southwell-plot seems logical and also shows a much higher buckling load for the stud (max)$N_{s,sw}$, see Table 4-11. As it is unknown, at which load the stud would have buckled and

the whole system would have collapsed, the buckling factor obtained in the test is too high, it could even be closer to $\beta = 1.0$.

Table 4-11: Evaluation of the test results for system test C2-4.

maximum load	max P [kN]	40.4
maximum tension force in the steel rods	max N_t [kN]	38.2
maximum axial force in the stud	max N_s [kN]	17.9
buckling length factor (test)	β_{test}	1.218
maximum Southwell-load	max $N_{s,sw}$ [kN]	23.15
buckling length factor (Southwell)	$\beta_{Southwell}$	1.07

After unloading the system and removing the stud, the beam was loaded to failure. The failure mode was tension failure in the finger joint in the lowest lamella which occurred at $P_{failure}$ = 22.87 kN, a lower failure load than expected ($P_{expected}$ = 24.68 kN). The difference of only 7 % in the expected and achieved failure load is tolerable, as the value for bending strength was estimated by a relation between MOE and f_m and there is always spreading in the material properties.

4.4.8 Test C3-1

The third system test was performed with stud no. 4 and beam no. 1. The stud is 1.2 m long, the beam has a span of 5.0 m. The angle between the steel tension rods and the beam is 28 degrees. Stud and beam are put together with joint C, the stiffer joint used in these tests, containing 2 x 2 x 9 nails. An initial inclination of the stud was used to simulate a geometrical imperfection.

The inclination of the stud out of plane is $L_{stud}/150$. Before testing the joint stiffness, it was tried to have an inclination of $L_{stud}/1000$. But after testing the joint – which causes a deformation in the joint – and after setting up the whole system, the inclination was larger, and it was decided to test the system with this inclination.

The tension rods were prestressed with about 0.56 kN.

When loading the system, see Figure 4-33, the stud bent out of plane in the same direction as the initial inclination. Large bending deformations occurred in the joint. The system failed at a load of P = 43.0 kN. The failure mode was a combination of several failures, see Figure 4-34 andFigure 4-35: On the one hand, there was bending failure in the stud, directly under the joint. Tension (bending) failure on one side of the stud (tension side) could be observed as well as compression failure on the compressed side. On the other hand occurred shear failure in the glulam beam and tension failure in a finger joint in the lowest lamella of the beam.

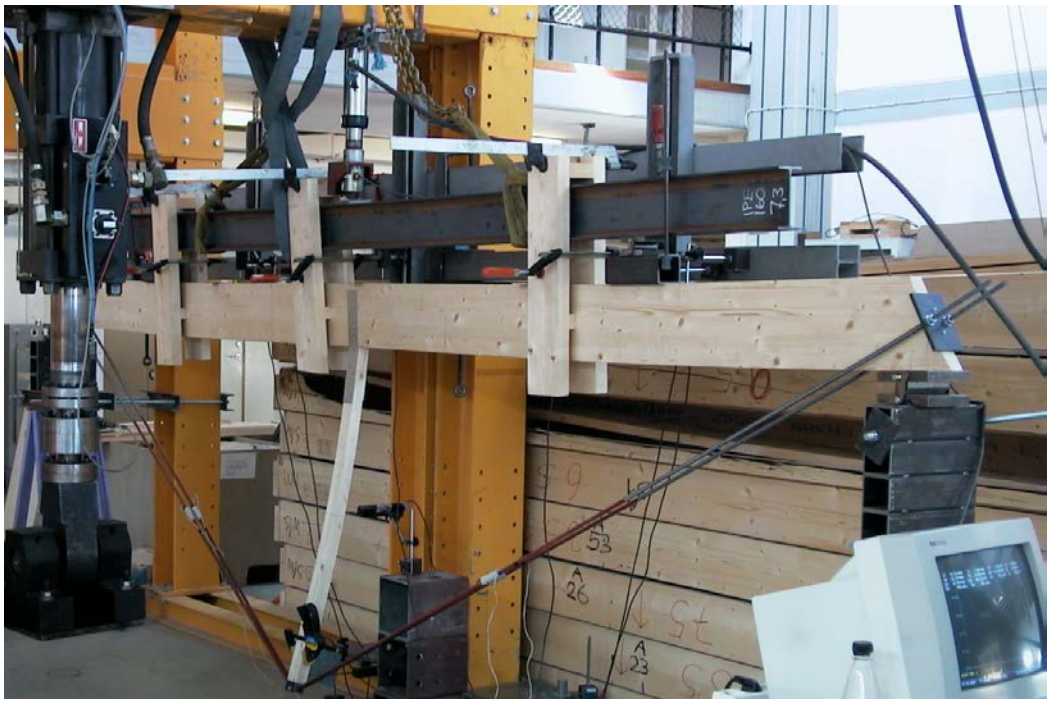

Figure 4-33: Out of plane bending of the stud in system test C3-1.

The joint of this test system experienced large deformations. First, the steel side plates bent (see Figure 4-35, left) and the stud moved in relation to the beam so that a gap between steel plates and stud appears. A small gap can even be seen between the beam and the (inclined) stud. The nails were bent and pulled out to some extent. As annular ring shanked nails with high withdrawal capacity were used, they were not pulled out completely. The stud itself experiences bending failure, the timber cracks parallel to the grain. Due to the comparatively stiff joint, the rotation in the joint itself is minimised and the rotation in the timber stud under the joint is maximised. This is why the failure occurred directly under the joint. The stud did not contain large defects on the tension side that could have lead to a failure at a different section of the stud.

Figure 4-34: Failure modes in system test C3-1: Bending failure in the stud, bending failure in the glulam beam and tension failure in a finger joint in the beam.

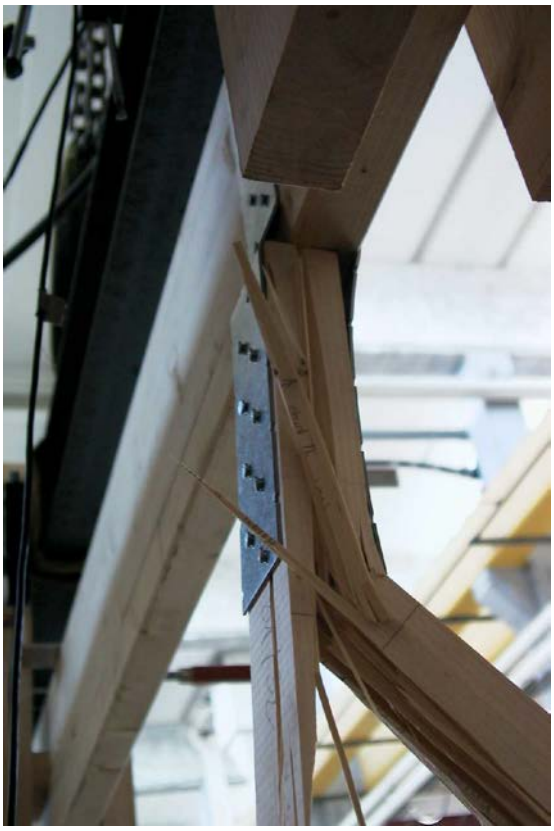

Figure 4-35: Failure modes in the joint and the stud. Large bending in the steel plates, withdrawal and bending of nails (left), bending failure in the stud (right).

When the stud deflects out of plane, the tension rods have to follow along. That means that the steel plate, which connects tension rods and glulam beam, rotates slightly around the beams strong axis. The transfer of the tension force from the steel rods by compression stress under the steel plate to the glulam beam is not uniformly any more, see Figure 4-36.

Figure 4-36: Joint between tension rods and glulam beam after the test.

In this test with failure in the stud, the difference between β_{test} and $\beta_{Southwell}$ is quite large (7.6%), see Table 4-12. The difference can be explained with the fact that the whole system failed: both beam and stud. It can only be guessed what initiated and finally caused the total failure. If the failure occurred first in the beam, then perhaps the critical load in the stud had not been reached yet and the stud failed due to the sudden large deflection when the beam failed. That is why the buckling length factor $\beta_{Southwell}$ seems more reliable than the value obtained directly from the test.

Table 4-12: Evaluation of the test results for test C3-1.

maximum load	max P [kN]	43.0
maximum tension force in the steel rods	max N_t [kN]	42.2
maximum axial force in the stud	max N_s [kN]	19.8
buckling length factor (test)	β_{test}	1.104
maximum Southwell-load	max $N_{s,sw}$ [kN]	23.2
buckling length factor (Southwell)	$\beta_{Southwell}$	1.02

4.4.9 Test C4-1

The last test series (C4-x) was different from the first 3 ones (C1-x to C3-x) as the stud length was only half the length as in the other tests, see Figure 4-37. The length was chosen to L_{stud} = 0.60 m, so that the angle between tension rods and beam decreased to α = 14 degrees. This set-up corresponds better to a real roof structure, as the roof inclination usually is not so large for trusses with large spans and therefore the stud is shorter.
Stud and beam are put together with joint D, the weaker joint used in these tests, containing 2 x 2 x 4 nails. This joint is the same as the one used in system tests C2-x (joint B). The inclination of the stud out of plane is L_{stud}/50. The tension rods were prestressed with approximately 0.56 kN.

Figure 4-37: Test set-up for test series C4-x. The stud is 0.60 m long.

When loading the system, the stud bent out of plane exactly as in the other tests.
However, the failure did not occur in the stud but it was failure due to compression perpendicular to grain at the right support of the glulam beam. The fibres were compressed, giving the beam an inclination, and rotating the support, see Figure 4-38. Due to this failure, the load could not be increased any longer as too large deformations were obtained (the systems resistance against the load was too small). The system was unloaded and the right support was moved further in, so that the total span decreased for the next test.

Figure 4-38: Failure due to compression perpendicular to the grain at the right support of the glulam beam. Seen from the front (left) and the back of the system (right).The fibres are squashed and the support rotates, increasing the beams deflection.

Neither the buckling length factor β_{test} nor $\beta_{Southwell}$ give good results in this test, see Table 4-13. The high value for β_{test} can be explained with the comparatively low load on the system. The other systems with a 1.2 m long stud carried loads of about 40 kN, whereas this system only was loaded with 32.7 kN. The shorter the stud, the higher is the buckling load, i.e. the stud was not loaded to a high extend of its capacity and was just beginning to deflect. The value for the buckling length factor obtained from the Southwell-Plot is also high compared to the earlier test series (C1-x to C3-x). One explanation can be that this plot only gives sound results for systems that are loaded with comparatively high ratios of test load to buckling load for the failure mode being buckling in the stud. The buckling length factors obtained in this test will not be considered in the further evaluation.

Table 4-13: Evaluation of the test results for test C4-1.

maximum load	max P [kN]	32.7
maximum tension force in the steel rods	max N_t [kN]	69.7
maximum axial force in the stud	max N_s [kN]	19.3
buckling length factor (test)	β_{test}	2.23
maximum Southwell-load	max $N_{s,sw}$ [kN]	20.2

buckling length factor (Southwell)	$\beta_{Southwell}$	2.18

4.4.10 Test C4-4

The test set-up is the same as for system test C4-1 with the exception that the right support was moved 0.175 m to the left, see Figure 4-39. The total span was then 2.5 + 2.325 = 4.825 m. By doing this, the material could be used for an additional test. Due to the pre-loading in test C4-1, the stud had an inclination out of plane of $L_{stud}/9.5$.

Figure 4-39: The support was moved in with 17.5 cm. Total span of the trussed beam is now 4.825 m.

When loading the system, the stud continued to deflect out of plane. At the same time, the glulam beam bent laterally in one bow between the supports, having the shape of a large "banana". As the beam moved away under the steel beam, the load could not be increased any more at a certain point as the beam just deflected sideways. The loading was stopped and the system was unloaded. The stud itself did not experience large bending stresses. The joint rotated as bending occurred in the steel plates, see Figure 4-40.

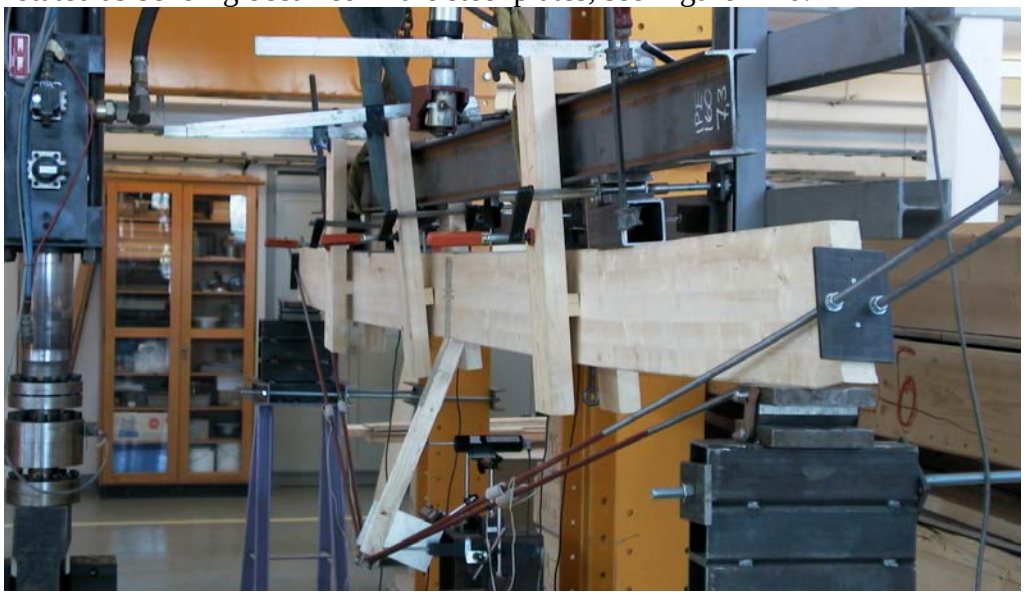

Figure 4-40: Stud buckles out of plane, beam bends laterally.

As in test C4-2, the results for the buckling length factors are quite disappointing, see Table 4-14. They can only be explained with the low axial force in the stud, compared to the buckling load. It cannot be evaluated whether perhaps the beam instead of the stud would have failed at a higher load. The buckling length factors obtained in this test will therefore not be considered in the further evaluation.

Table 4-14: Evaluation of the test results for test C4-4.

maximum load	max P [kN]	38.7
maximum tension force in the steel rods	max N_t [kN]	63.3
maximum axial force in the stud	max N_s [kN]	17.6
buckling length factor (test)	β_{test}	2.34
maximum Southwell-load	max $N_{s,sw}$ [kN]	24.6
buckling length factor (Southwell)	$\beta_{Southwell}$	1.98

4.4.11 Test C4-5

As the system was not tested to complete failure in test C4-4, the system was modified to be tested again. The clamps that brace steel and glulam beam were moved downwards as much as possible (about 7 cm) to increase the bracing effect on the glulam beam.
Due to the pre-loading in test C4-1 and especially in test C4-4, the stud had an initial inclination of 16.5 cm deflection out of plane, which is about $L_{stud}/3.6$. This inclination is due to the large plastic deformation in the steel plates of the joint.
When loading the system, the stud continued to bend out of plane while the glulam beam buckled laterally again. As in test C4-4, the load could not be increased any longer as the beam moved laterally under the steel beam, which suddenly tilted and almost fell of the glulam beam, see Figure 4-41. The system was unloaded.
The joint experienced large deformations, compare Figure 4-42. The steel plates are bent and the stud is inclined in relation to the beam which it compresses locally perpendicular to the grain. The nails are slightly inclined, giving room for deformation. The amount of displacement obtained in the joint can be seen from the lines drawn on the joint before the test.

Figure 4-41: The glulam beam buckles laterally, the steel beam tilts. The load cannot be increased.

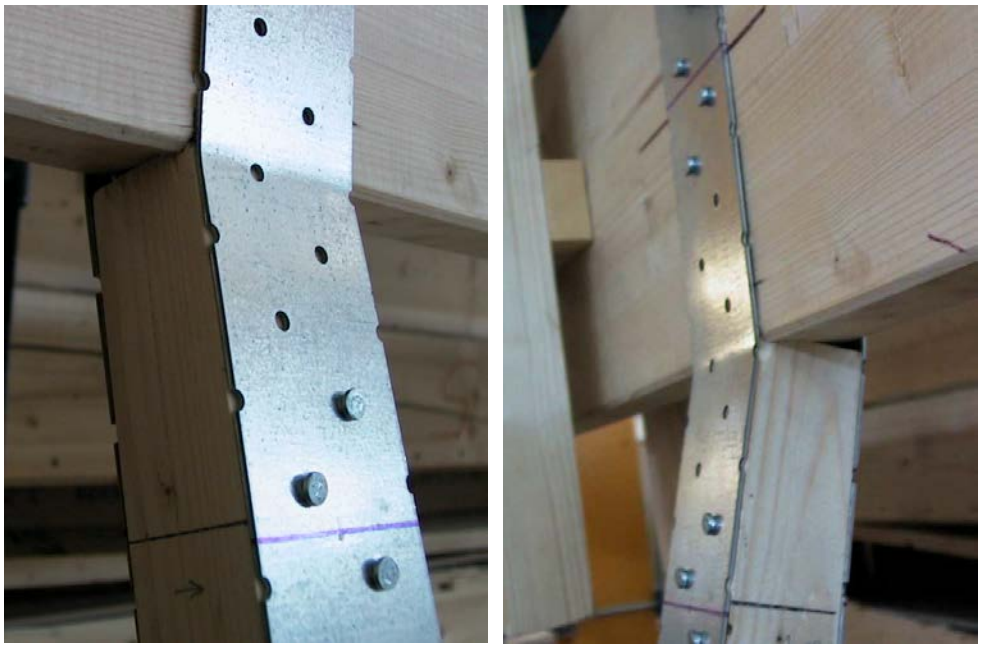

Figure 4-42: Deformation in the joint. Bending in the steel plates, inclination in the nails, making a large slip possible (compare the lines drawn on the plates and the timber).

As in the other tests of this series (C4-x), the buckling length factors obtained for the system with the short stud are not satisfactorily, compare Table 4-15. The reasons are the same as in tests 4-1 and 4-5. Therefore, the buckling length factors obtained will not be considered in the further evaluation.

Table 4-15: Evaluation of the test results for test C4-5.

maximum load	max P [kN]	40.8
maximum tension force in the steel rods	max N_t [kN]	63.1
maximum axial force in the stud	max N_s [kN]	17.5
buckling length factor (test)	β_{test}	2.34
maximum Southwell-load	max $N_{s,sw}$ [kN]	32.5
buckling length factor (Southwell)	$\beta_{Southwell}$	1.72

4.4.12 Summary of the system tests

To be able to compare the test results of the different system tests with each other and also with the theoretical model, the section forces in the various members are estimated by geometrical relations. Then a "design" of the different timber members is done, using interaction equations according to Eurocode 5 and the mean values for the glulam material properties obtained in the preceding tests. By comparing the degree of utilisation for the different design equations, a potential failure mode can be estimated and be compared to the actual failure mode obtained in the test.
For the design of the test system, different interaction equations according to EC 5 have to be fulfilled. All timber members are subjected to combined stresses, i.e. compression and bending. The combinations that have to be checked are

- eq. 6.17: combined bending and axial compression → stud, beam

$$\left(\frac{\sigma_c}{f_{cd}}\right)^2 + \frac{\sigma_{m,z}}{f_{md,z}} + k_m \frac{\sigma_{m,y}}{f_{md,y}} \le 1.0 \qquad \text{with } M_y = 0 \rightarrow \sigma_{my} = 0$$

- eq. 6.22 / 6.23: members subjected to compression and bending / stability → stud, beam

$$\frac{\sigma_c}{k_{c,z} f_{cd}} + 0.7\frac{\sigma_{m,y}}{f_{md,y}} + \frac{\sigma_{m,z}}{f_{md,z}} \le 1.0 \text{ (strong direction)}$$

$$\frac{\sigma_c}{k_{c,y} f_{cd}} + \frac{\sigma_{m,y}}{f_{md,y}} + 0.7\frac{\sigma_{m,z}}{f_{md,z}} \le 1.0 \text{ (weak direction)}$$

- eq. 6.33: lateral torsional buckling of beams → beams

$$\frac{\sigma_{mz}}{k_{crit} f_{mz}} + \frac{\sigma_c}{k_{cy} f_{cd}} \le 1.0$$

The test results are summarised in Table 4-16. The bottom line indicates the conformity of the failure modes observed in the test and the calculated ones. This has to be taken with care. The design equations in EC 5 use stiffness and strength parameters for the single timber members to estimate the capacity and the coefficient of efficiency respectively. The stiffness value MOE was obtained from tests, the strength parameters f_m and f_c were calculated with relation equations. The correctness of the correlation between MOE and f_m and f_c respectively cannot be guaranteed. Members showing a coefficient of efficiency of 90% and higher for the actual failure mode are marked with “yes/no” even if another coefficient of efficiency was higher but did not fit the failure mode that was obtained in the test.

Table 4-16: Summary of the system tests.

system test no.							
Test	1-5	2-2	2-4	3-1	4-1	4-4	4-5
failure mode	buckling in the stud	lateral buckling in the beam	bending in the stud to max value	buckling in the stud, bending in the beam	compression perpendicular to the grain (support)	lateral buckling in the beam	lateral buckling in the beam
maxP [kN]	41.5	42.9	40.4	43.0	32.7	38.7	40.8
$maxN_t$ [kN]	43.8	47.3	38.2	42.2	69.7	63.3	63.1
$maxN_s$ [kN]	20.5	22.2	17.9	19.8	19.3	17.6	17.5
P_{sw} [kN]	-	25.1	23.2	23.2	20.2	24.6	32.45
β_{test}	1.061	< 1.095	< 1.218	1.104	< 2.23	< 2.34	< 2.34
$\beta_{southwell}$	-	1.03	1.07	1.02	< 2.18	< 1.98	< 1.72
coefficient of efficiency in the stud for buckling out of plane with the assumption of $\beta = 1.0$, according to EC 5, equation 6.22							
η_{stud}	0.957	0.901	0.728	0.884	0.346	0.314	0.313
coefficient of efficiency in the glulam beam according to EC 5, equations 6.17, 6.22, 6.23 and 6.33							
eq. 6.17	0.95	0.87	0.92	0.92	0.65	0.86	0.95
eq. 6.22	1.03	0.95	0.98	0.99	0.76	0.97	1.06
eq. 6.23	0.89	0.84	0.82	0.84	0.81	0.93	0.99
eq. 6.33	1.16	1.01	1.05	1.08	0.78	1.09	1.25
conformity of observed and estimated failure mode (yes / no)							
	yes/no	yes	no	yes/no	no	yes	yes

The buckling length factors β achieved in the last test series (tests C4-x) diverge largely from the results achieved in the preceding tests. At least for the β-values obtained from Southwell-plots, this difference can be explained with the fact that the central deflection (bending) in the stud is different for a stud that buckles and for a test where the beam fails, compare Figure 4-43 andFigure 4-44. For the stud failing, the relationship shows two different sectors: In the first sector, the stud deflects only little with increasing load. In the second sector, the deflection / load ratio develops much higher (see Figure 4-43). In the beginning, the slope of the curve is large, at a certain load it turns and the slope develops much lower. At beam failure, when the stud is not loaded near its buckling load, then the graph is more even, the slope is almost constant, see Figure 4-44.

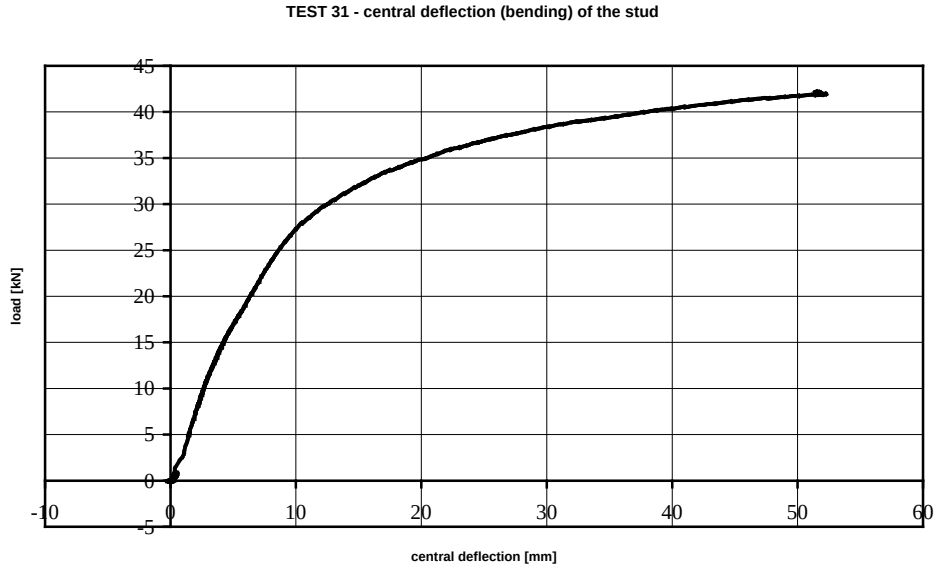

Figure 4-43: Central deflection (bending) in the stud. Failure mode is buckling in the stud.

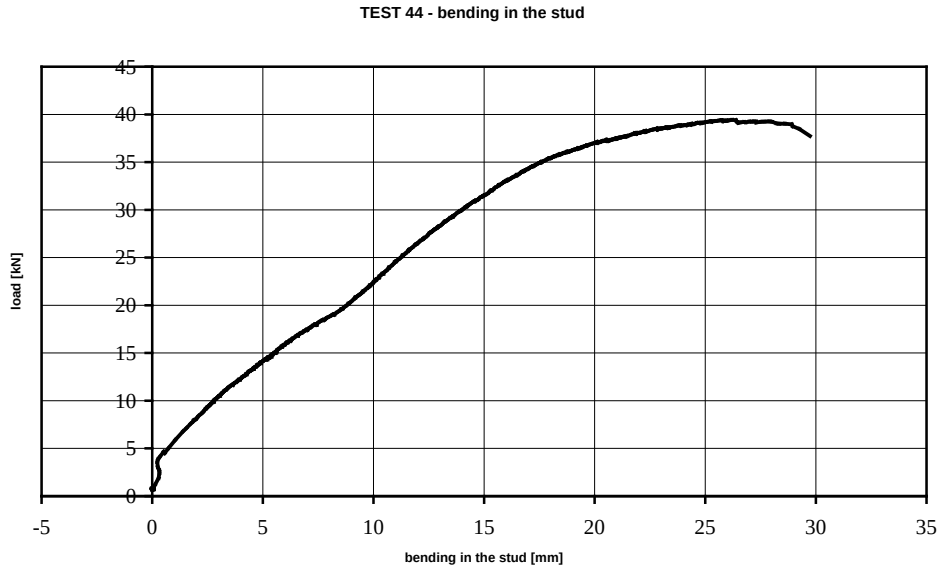

Figure 4-44: Central deflection (bending) in the stud. Failure mode is lateral buckling of the beam (test C4-4).

If test data for central deflection are plotted against the ratio of central deflection and axial load in the stud, the slope as seen in Figure 4-43 andFigure 4-44 shows a large influence on the results of the Southwell-plot. This is due to the fact that the correlation between test data

and regression line has a poor agreement for failing in the beam (see Figure 4-45), whereas the agreement for failing in the stud is quite good, see Figure 4-46.

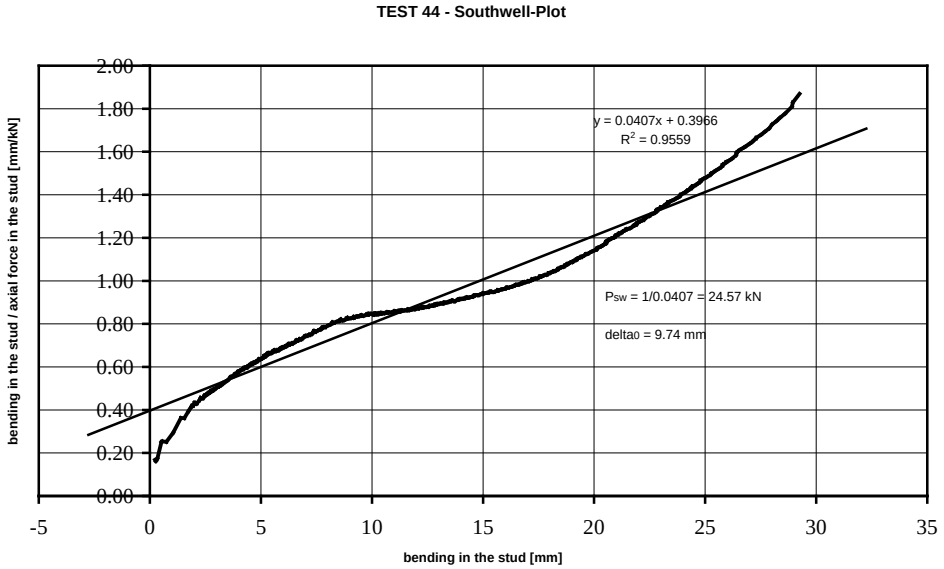

Figure 4-45: Southwell-plot for test C4-4 (beam failing). Rather poor agreement between test data and regression line.

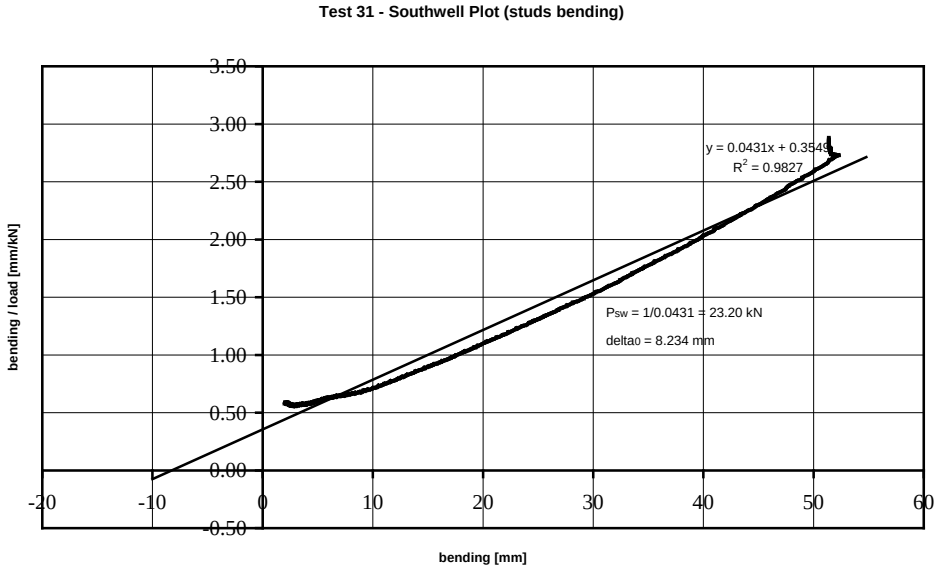

Figure 4-46: Southwell-plot for test C3-1 (stud failing). Good agreement for test data and regression line.

The buckling length factors obtained from the section forces in the test and from the Southwell-plot differ slightly. This proves that the buckling length factor in the Soutwell-plot is estimated without imperfections whereas the test buckling length factor includes the imperfections, giving higher buckling length values for inclined studs.

4.4.13 General observations and conclusions

The studs bending out of plane is slow with increasing load in the beginning, circa 1 mm deflection per 1 kN load increase. When reaching the failure load, then the deflection rate increases, see Figure 4-47. For low ratios ($P_{actual}/P_{buckling}$), the serviceability of the trussed beam is good: For ($P_{actual}/P_{buckling}$) of about 0 to 0.75, almost no deflection is achieved.

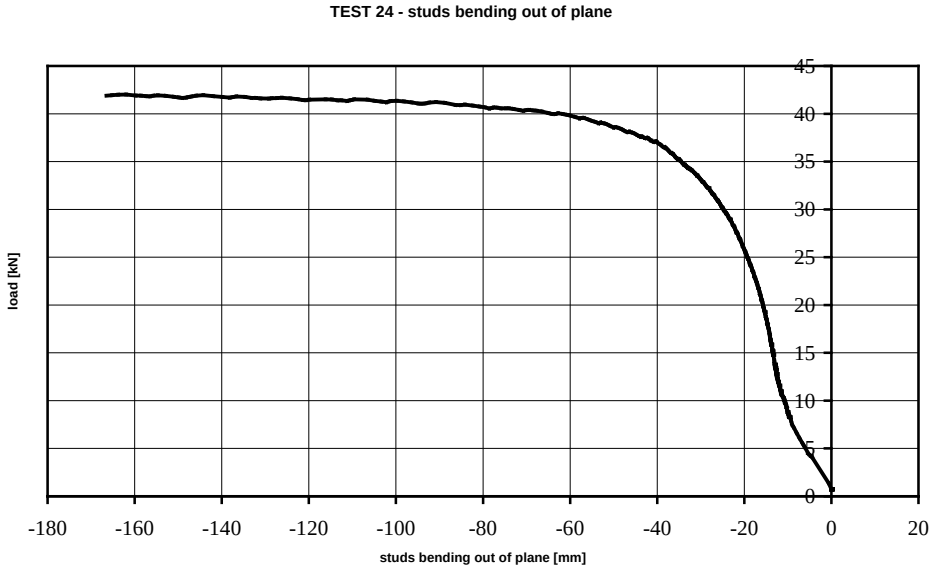

Figure 4-47: Out of plane deflection of the stud at different loads. The horizontal deflection increases much at higher load levels, shortly before reaching the failure load. At this very test, the deflection increased to 462 mm before the system failed at P=40.4kN.

The vertical deflection of the trussed beam is different from the deflection in a regular single span beam. The elastic intermediate support (stud) minimises the vertical deflection at midspan. Under load, the beam experiences a deformation that is similar to the third natural oscillation of a simply supported beam: the beam bends down at the point loads, and is supported by the stud, bending up at midspan. Due to the large total load and the low prestressing of the tension rods, the beam mid also deflects down. The deformed beam can be clearly seen in Figure 4-33 and Figure 4-40.

The importance of estimating the buckling length of the stud with help of the Southwell-Plot can be seen in all the tests where it was not the stud that failed, but for instance the beam that twisted or failed due to bending. In all these cases, the buckling load of the stud was not reached during the test, and with the assumption $N_s = N_{crit}$, the buckling length is overestimated.

The stiffness of the joint seems not to have an influence on the buckling length of the stud. The buckling length value $\beta_{southwell}$ for the "stiffer" joint is 1.02, whereas for the "weaker" joint, values between 1.03 and 1.07 were achieved. In the test, many factors have an influence on the results, i.e. the stiffness and strength parameters, defects (knots, compression wood etc.), inclined set-up, loading rate and some more. More tests should therefore be performed to underline the results achieved in this study with a reliable statistical basis.

It became clear in all the tests that the steel tension rods have a stabilising effect on the system of the trussed beam. Even for relatively weak joints, excessive deflections out of plane were possible without an instability failure in the stud.
This stabilising effect can be explained with a restoring force that helps to “minimise” the deflections, compare section 3.6. The resultant force of the tension rods is always directed towards the joint between stud and beam, providing Euler case 2 with a buckling length of 1.0L independent of the stiffness of the joint.

Also, the total deflection of the trussed beam does not seem to have a negative effect on the stability of the system. Kessel (1988) claims that the precamber always has to be larger than the total deflections during the systems lifetime if a stabilising effect of the tension rods on the stud shall be achieved. In this study, deflections at midspan of up to 26 mm for the long stud (L_{stud} =1.20 m) and even 50.7 mm for the short stud (L_{stud} = 0.60 m) were obtained due to the high loading and the low prestressing in the tension rods. Even for these large deflections, there is a high stabilising effect, which can be seen in the buckling length factors $\beta_{southwell}$ obtained for the stud.

5 Comparison of the theoretical model and the test results

In order to compare the test results and the theoretical model, some boundary conditions must be considered. The material and joint properties investigated in section 4.2 have to be input in the theoretical model as well as the same boundary conditions (restraints, supports) as in the tests performed. In the tests, only three lateral restraints could be used since only 3 of the special clamps needed were available. The beam is therefore braced laterally every 1.25 m, but not at the supports. In the three-dimensional theoretical model, the system behaves significantly different at places where no lateral bracing is provided: The beam buckles laterally, forming a banana, with large out of plane displacements at the supports, see Figure 5-1.

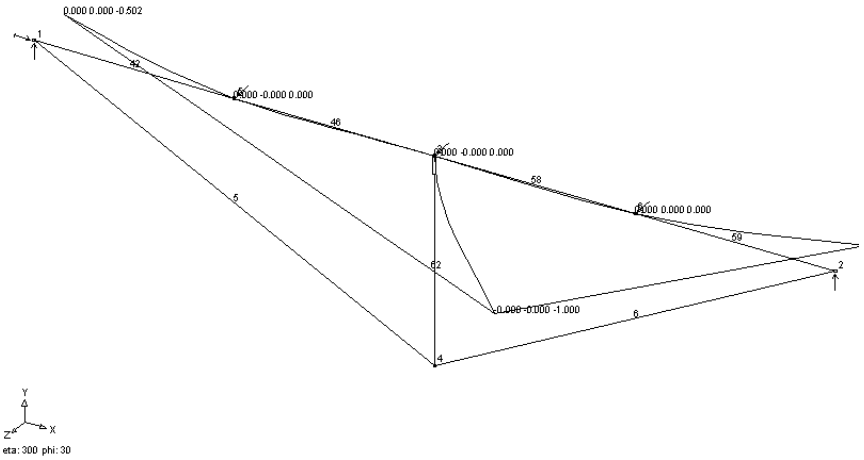

Figure 5-1: Lateral buckling of the beam if no lateral bracing is provided at the supports.

This kind of buckling did not happen in the tests, probably due to the high pressure at the supports (small support area since the beams are very slender) that caused high friction between glulam beam and the steel support. This friction provided some sort of lateral bracing. The theoretical model is therefore modelled with lateral restraints also at the supports to achieve the same buckling modes as in the tests. Further, the theoretical system is unstable if torsion is not prevented at at least one support. No fork support was used in the test and the beams did not rotate around their axis at the supports during testing. To compare the test results and theoretical model, a fork support is employed at the left support of the theoretical model.
The tension rods in the theoretical model are prestressed with $\Delta T = -45K$, giving the same tension force ($F_{prestress} = 0.56kN$) as provided during the tests.

The section forces in the different members of the test system were calculated for the maximum load as shown in section 4.4.12. The different test systems were analysed in the theoretical model for the same loading, calculating the section forces with second order analysis (due to the non-linear properties of the cable elements).
The section forces for the different system tests can be found in Table 5-1.
As system test C4-1 showed a failure mode (exceeding the compression strength perpendicular to the grain at the supports) that was significantly different from the other tests and the section forces also diverge very much, this test is not included in the evaluation of the differences between test results and theoretical model.

Table 5-1: Section forces for maximum load on the test system according to test and the theoretical model in Microstran.

		Section forces calculated from test results with geometrical relations					Section forces in the theoretical model (second order analysis)				
	Test	P_{max} [kN]	N_t [kN]	N_s [kN]	N_c [kN]	M_b [kNm]	M_s [kNm]	N_t [kN]	N_s [kN]	N_c [kN]	M_b [kNm]	M_s [kNm]
	C1-5	41.5	21.9	-20.5	-19.3	10.9	-4.5	26.46	-24.62	-23.51	9.78	-8.84
	C2-2	42.9	23.6	-22.2	-20.9	10.7	-5.9	25.88	-24.09	-22.99	9.58	-8.62
	C2-4	40.4	19.1	-17.9	-16.9	11.2	-2.2	24.42	-22.72	-21.69	9.00	-8.16
	C3-1	43.0	21.1	-19.8	-18.6	11.6	-3.3	25.91	-24.11	-23.02	9.61	-8.61
	C4-1	32.7	34.9	-19.3	-33.5	6.7	-7.8	32.61	-17.97	-31.41	7.61	-5.97
	C4-4	38.7	31.7	-17.6	-30.4	10.6	-2.6	38.36	-21.18	-36.96	9.11	-6.90
	C4-5	40.8	31.5	-17.5	-30.3	11.7	-1.4	40.43	-22.34	-38.96	9.65	-7.24

In general, the axial forces are larger in the theoretical model than in the test, whereas the determining bending moments are larger in the test than in the theoretical model.
This can be explained with the elasticity of the “support” provided by the stud. For a two-span beam with three rigid supports and two point loads located 0.4 L from each end of the beam, the intermediate support stands for 56.8 % of the vertical reaction forces, see Figure 5-2.

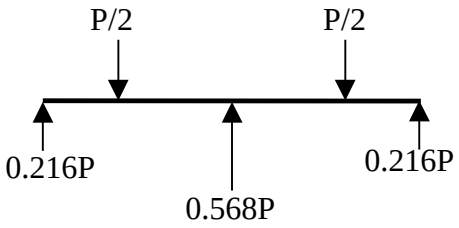

Figure 5-2: Vertical support reactions for double span beam with rigid supports.

In the theoretical model, the intermediate support is almost not elastic, as the support reaction (mean value) is $R = 0.560P$. However, in the test, the stud appears to be an elastic intermediate support, giving a vertical support reaction of $R = 0.467P$ (mean value) if test 4-1 is not considered (see reasons above). Due to the elastic support (i.e. lower axial force in the stud), the bay bending moment is not reduced as much as in the theoretical model, giving larger differences between the positive bay bending moment and the negative bending moment at the intermediate support. As the axial loads in all system components are related by geometry, they all decrease if one axial force decreases. That is why the differences between the section forces in the test and the theoretical model can be explained with the different degrees of elasticity of the intermediate support.

Reasons for the weaker support or higher elasticity of the intermediate support in the test can be found in the test set-up as well as in the material properties.

The most obvious reasons are gaps in all connections of the test system: the joint between stud and beam, the connection between beam and tension rods and the one between tension rods and the stud. Considering gaps at these locations, a certain load can be imposed on the system without resulting in large axial forces in the system components until the gaps are closed. Additionally, the tension rods were slightly bent after some tests, due to the studs bending out of plane and contact between the tension rod and the beam. The tension rods being not totally straight were prestressed with a certain load, but when loading the system, they straightened before taking up load, giving rise to further deflections and load-uptake without creation of high axial forces. Furthermore, the stud was pressed into the beam. As the compression stiffness perpendicular to the grain is quite small, the axial force in the stud caused deformations that have to be added to the deformations described above. For the different tests, the deformations perpendicular to the grain were some 0.5 to 1.0 mm. Deformations can also happen in the stud itself. The decrease in length can be estimated for a stud with $L = 1.2m$, $A = 0.041 \cdot 0.06 = 0.00246m^2$, $E = 10000MPa$ and an axial force $P = 20kN = 0.02MN$ to $\Delta L = \frac{PL}{EA} = 1mm$.

Of course, all these deformations are small, but if they are summed up, a certain deflection occurs under increasing load without increasing axial loads.

Additionally, the accuracy of the values for the material properties is not known. Both load cells and deflection gauges have tolerances, so that the actual MOE in the system test can differ from the one obtained from the earlier MOE-testing.

The accuracy of load cell and strain gauges can also contribute to the differences in section forces between the actual test system and the theoretical model. The load cell has a tolerance of $\pm$ 0.1 kN, the strain gauges one of $\pm$ 0.85 μm/m, giving $\pm$ 0.24 kN accuracy for the axial force in the tension rods.

If all these reasons are summed up, then the differences in the section forces between test and theoretical model can be explained.

The section forces obtained in the tests and the theoretical model give certain utilisation factors for the different design equations according to EC 5. The beams are designed with respect to combined bending and axial compression, column buckling and lateral buckling (beams). The studs are designed considering combined bending and axial compression as well as column buckling. The utilisation factors for the beams can be found in Table 5-2 andTable 5-3 and for the studs in Table 5-4 andTable 5-5 respectively.

Table 5-2: Utilisation factors for the beams according to testing.

Utilisation factors for the beams according to the test				
Test	bending/com-pression without buckling risk	column buckling (weak direction)	column buckling (strong direction)	lateral buckling
C1-5	0.95	1.03	0.89	1.16
C2-2	0.87	0.95	0.84	1.01
C2-4	0.91	0.98	0.82	1.05
C3-1	0.92	0.99	0.84	1.08
C4-1	0.65	0.76	0.81	0.78
C4-4	0.86	0.97	0.93	1.09
C4-5	0.95	1.06	0.99	1.25

Table 5-3: Utilisation factors for the beams according to theoretical modelling.

Utilisation factors for the beams according to the theoretical model, calculated with section forces obtained from second-order analysis				
Test	bending/com-pression without buckling risk	column buckling (weak direction)	column buckling (strong direction)	lateral buckling
C1-5	0.86	0.95	0.87	1.02
C2-2	0.78	0.87	0.79	0.88
C2-4	0.74	0.82	0.75	0.79
C3-1	0.77	0.85	0.78	0.86
C4-1	0.63	0.74	0.77	0.74
C4-4	0.75	0.88	0.92	0.97
C4-5	0.80	0.93	0.97	1.06

For the beams, the utilisation factors in the test are higher than in the theoretical model. The differences are between some 5% for buckling in the weak direction and 17% for lateral buckling. The bending moments are larger in the test, whereas the axial compression force is larger in the theoretical model. The bending moment very likely has a larger influence on the design of the beams than the axial compression force. As a real structure always contains imperfections – for example gaps in joints or defects in wooden members – the distribution of the section forces will resemble the one achieved in the test. The theoretical model over-estimates the load-carrying capacity, since the systems failed although the utilisation factors are comparatively low. If the section forces from the theoretical model were used to design the structure, then smaller cross-sections would be used to increase the degree of utilisation. Then the design can be on the “unsafe” side with the system failing.

As the section forces in the theoretical model were obtained from second-order analysis which already considers second-order effects and buckling length, the verification of the beams capacity could be sufficient with the design equation for axial compression and

bending – without taking buckling into account (see second column in Table 5-3). However, the load-carrying capacity is over-estimated in these comparative calculations when using this design. If buckling is taken into account, then the design is on the safe side, as buckling is considered in two ways. The "real" degree of utilisation will therefore be somewhere in between the low values without and the high values with consideration of buckling.

Table 5-4: Utilisation factors for the studs according to the test.

Utilisation factors for the studs according to the test			
Test	compression (without buckling risk)	column buckling (weak direction) out of plane	column buckling (strong direction) in plane
C1-5	0.34	0.96	0.50
C2-2	0.33	0.90	0.48
C2-4	0.27	0.73	0.38
C3-1	0.32	0.88	0.46
C4-1	0.31	0.35	0.32
C4-4	0.28	0.31	0.29
C4-5	0.28	0.31	0.29

Table 5-5: Utilisation factors for the studs according to the theoretical model.

Utilisation factors for the studs according to the theoretical model, calculated with section forces obtained from second-order analysis			
Test	compression (without buckling risk)	column buckling (weak direction) out of plane	column buckling (strong direction) in plane
C1-5	0.40	1.15	0.60
C2-2	0.36	0.98	0.52
C2-4	0.34	0.92	0.49
C3-1	0.38	1.08	0.56
C4-1	0.29	0.32	0.30
C4-4	0.34	0.38	0.35
C4-5	0.36	0.40	0.37

The design of the studs is done with a buckling length of $1.0L_{stud}$.
As all the axial forces are higher in the theoretical model than in the test, the utilisation factors for the studs are some 17% higher for the theoretical model compared to the test results. Designing the stud with the section forces from the second-order analysis in the theoretical model, one would choose a larger cross-section for the stud, being on the safe side.
Some utilisation factors in the test are lower than 1.0, but the stud failed nevertheless. This can be explained with local defects and the variation of the material properties.
According to the utilisation factors achieved in the theoretical model, the stud buckles out of plane for the first 3 test series (C1-x to C3-x), and in the last series (C4-x) the beam buckles or bends laterally. This does not fit the reality totally, as only in the first and third test series the stud buckled, whereas in the second series the beam buckled and the stud bent as much as it was possible (horizontal deflection was stopped when touching the portal frame). As it is not clear how the failure mode would have been if the stud could have deflected without influence of the frame, the consistency of the failure modes estimated in the theoretical model and in the test is quite good.

Just like for the design of the beams, buckling is considered twice in the design of the studs with the (second-order-analysis) section forces from the theoretical model and the consideration of the buckling length in the design equation. For second-order section forces a “regular” section-forces-control should be sufficient. As can be seen from the table values, the degree of utilisation for axial compression without consideration of buckling is very low, compared to the design including buckling risk and also compared to the actual test results. The “real” degrees of utilisation will be somewhere between the values obtained with or without bucking consideration. Since the studs buckled (Tests C1-5, C3-1) but the utilisation factors from the theoretical model (without buckling) are low, the buckling should be considered in the design so that the design is on the safe side.

6 Parameter Study

In a parameter study, the behaviour of different systems with trussed beams was evaluated and compared. Basis for the parameter study is a roof truss with trussed beams (see Figure 6-1) that has been designed as one part of the diploma thesis. For those interested in the design of the hall structure, please contact the author. Only one parameter was varied each time and the influence on the section forces was evaluated.

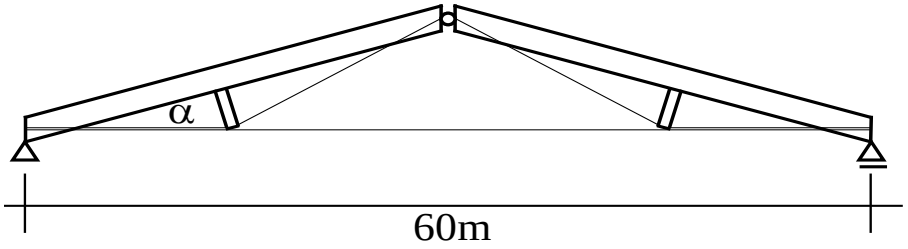

Figure 6-1: Basis-roof truss used for the parameter study.

Boundary conditions for the parameter study are:

- $L = 60m$
- $\alpha = 14^{\circ}$
- stiffness of the joint between beam and stud, spring constants k: k_y = 3343.3 kNm/rad, k_z = 23630.4 kNm/rad, estimated with $k_{y/z} = \sum K_{ser,i} \cdot r_i^2$
- one stud per beam
- simply supported roof truss
- cross-sections: beam 290 mm x 1035 mm
  stud 290 mm x 290 mm
  inclined tension rod A = 0.0033183 m^2
  horizontal tension rod A = 0.005281 m^2
- system is loaded with uniform loads (snow, dead load) and gravity-load case (dead load of the timber structure)
- non-linear analysis (second-order) of three-dimensional system

The parameters that were investigated are the joint stiffness, the length of the stud, the number of studs per beam, the roof inclination and the different structures that can be seen in Figure 1-3.

First, the effect of the joint stiffness was studied. The stiffness of the joint between stud and beam only has an influence on the section forces that result from imperfections, i.e. bending moments and shear forces in the studs. In a second order analysis without imperfections, there is no influence on the section forces. The smaller the spring constant, which determines the stiffness of the joint, the higher are the bending moments and shear forces in the stud. This can be explained with larger deflections out of plane and therefore higher second order effects for a weak joint. The bending moment can be plotted against the spring constant, see Figure 6-2 andFigure 6-3. To avoid all the absolute values, both the values for bending moment and spring constant were related to a base value, which is the spring constant given in the boundary conditions and its bending moment respectively.

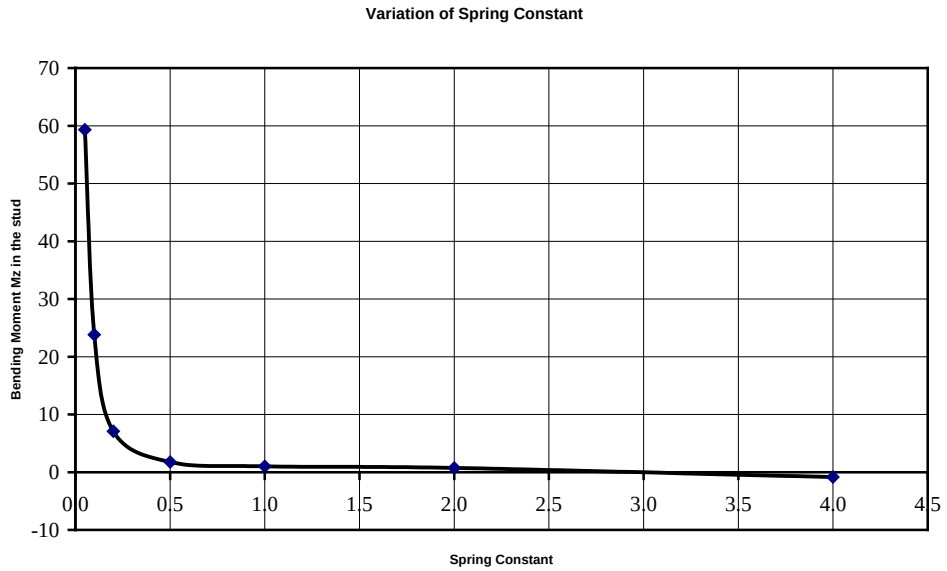

Figure 6-2: Variation of the Spring Constant. Bending moment M_z against spring constant (relative values). Second-order analysis and imperfections out of plane.

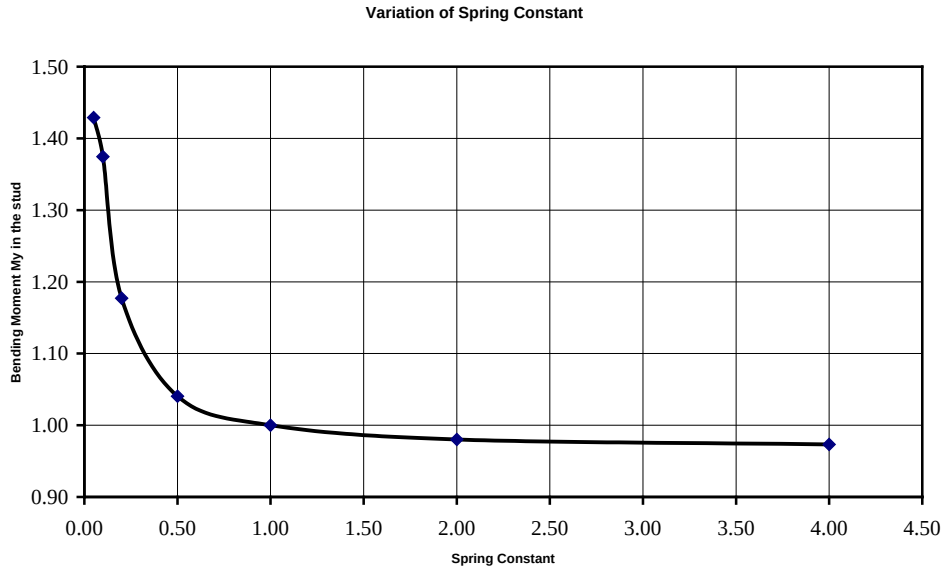

Figure 6-3: Variation of the Spring Constant. Bending moment M_y against spring constant (relative values). Second-order analysis and imperfections out of plane.

The joint stiffness does not have an influence on the section forces in the beam and the tension rods respectively. As the joint does not have high influence on the buckling length of the stud either, it only has to be designed in a way that the deformations do not get too large, otherwise the second order effects (bending moment) will cause the system to buckle.

A variation of the stud length has an influence on both the beam and the inclined tension rods. With decreasing length of the stud, both axial compression force and bending moment in the beam increase. There is also an influence on the other section forces (section forces due to second order effects) of the beam, but the variation is small and the overall values are small as well so that there are no changes with respect to the design of the beam. The axial force in the

stud is nearly constant for all lengths. Due to the increasing angle between stud and tension rods, see Figure 6-4, the tension force in the steel rods increase.

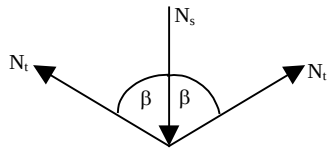

$$N_t = \frac{N_s}{2\cos\beta}$$

Figure 6-4: Geometric relation between axial compression force in the stud (N_s) and tension force in the steel rods (N_t).

At the supports, equilibrium of forces has to be fulfilled. With decreasing angle between tension rod and beam, a larger fraction of the tension force is taken up by axial compression in the beam, whereas a smaller portion is taken up by shear force in the beam.
The increase in bending moment and axial compression force in the beam and in tension force in the steel rods is almost linear to the decrease in the length of the stud, see Figure 6-5. Here, the stud length of L_0 = 3.38 m served as a basis value. For the parameter study, the length was decreased stepwise with $\Delta L = 0.25m$.

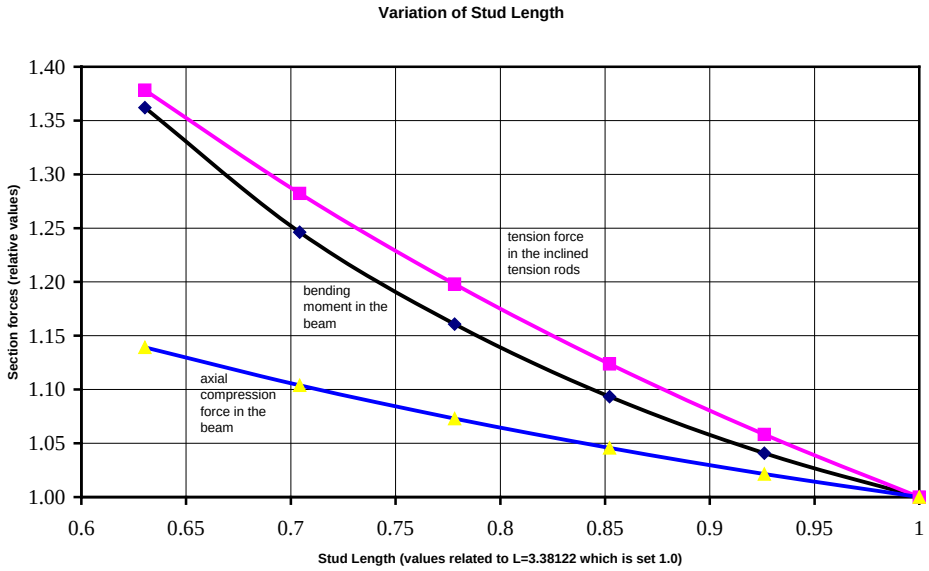

Figure 6-5: Variation of stud length. Relative values for bending moment and axial forces plotted against stud length (relative values).

As the section forces in the beam and the tension rod increase with decreasing length of the stud, this has a negative effect on the design of the system. Larger cross-sections are needed for both beam and tension rods, see Table 6-1.

Table 6-1:Cross-sections needed for beam and tension rods for different lengths of the stud.

Length [m]	L / L_0	cross-section beam [mm x mm]	diameter of tension rods (2 pieces) [mm]
3.38	1	290 x 1035	46
3.13	0.93	290 x 1035	46
2.88	0.85	290 x 1035	46
2.63	0.78	290 x 1080	46
2.38	0.70	290 x 1080	48
2.13	0.63	290 x 1125	50

The method of decreasing the length of the stud is advantageous for reducing the utilisation factor in the stud by reducing its buckling length. It can be combined with higher prestressing in the tension rods, which leads to somewhat lower bay bending moments, but on the other hand to higher axial compression in the beams. Therefore, the length of the stud and the amount of prestressing have to be determined accurately to achieve the most favourable result.

The number of studs on one beam of the roof truss has a large influence on the distribution of section forces. By introduction of more studs, the bending moment is reduced. The beam truss with one stud per beam (or truss-half) serves as a basis. Beam trusses with up to four studs per beam were analysed with second-order analysis (without imperfections) and compared to each other.

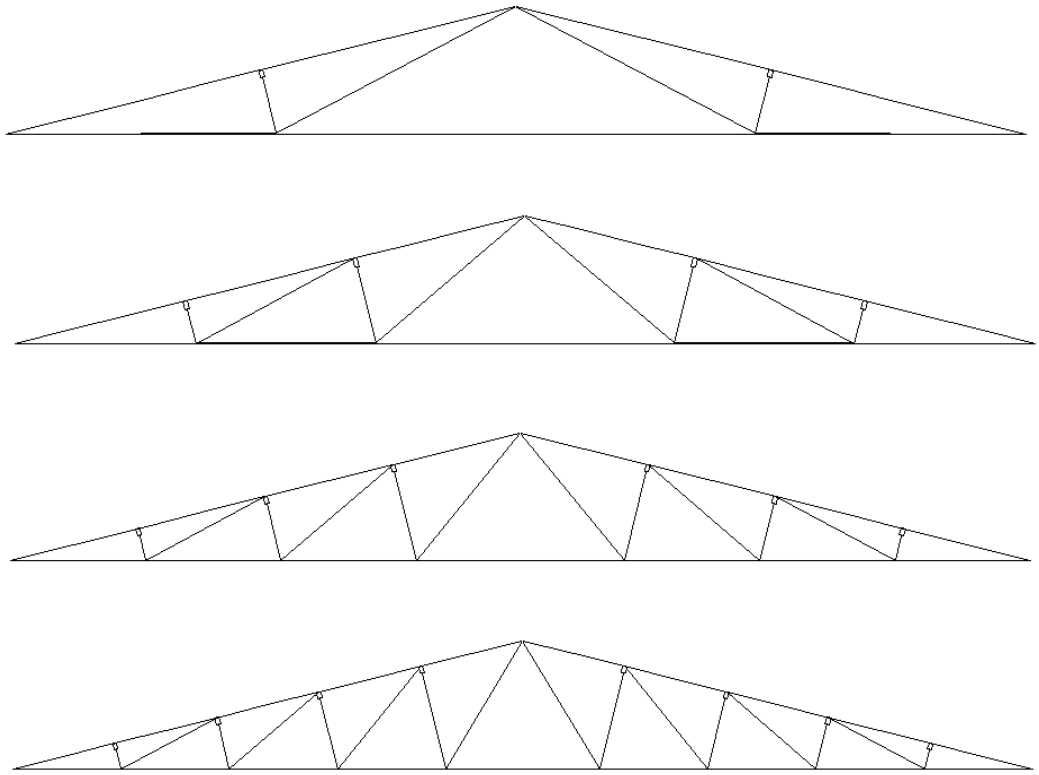

Figure 6-6: Variation of number of studs. One to four studs per beam.

In general, a stud or intermediate elastic support reduces the bending moment by reducing the span of the beam. The axial compression force in the beam increases with increasing number of studs, as more tension rods are used. In the case with one stud per beam, the axial force in the beam is nearly uniformly distributed throughout the beam length. It only increases a little towards the lower end because of load components in the beams axial direction resulting from outer loads, i.e. dead load etc. When more than one stud is used, then a discontinuity of normal force occurs in the beam at every joint between tension rod and beam, as the tension force has to be transferred into the beam. Maximum bending moment and axial compression force can be plotted against the number of studs, see Figure 6-7 andFigure 6-8. The section forces are related to the basis of one stud per beam, showing the increase and decrease respectively that results from introduction of one or more elastic intermediate supports (studs).

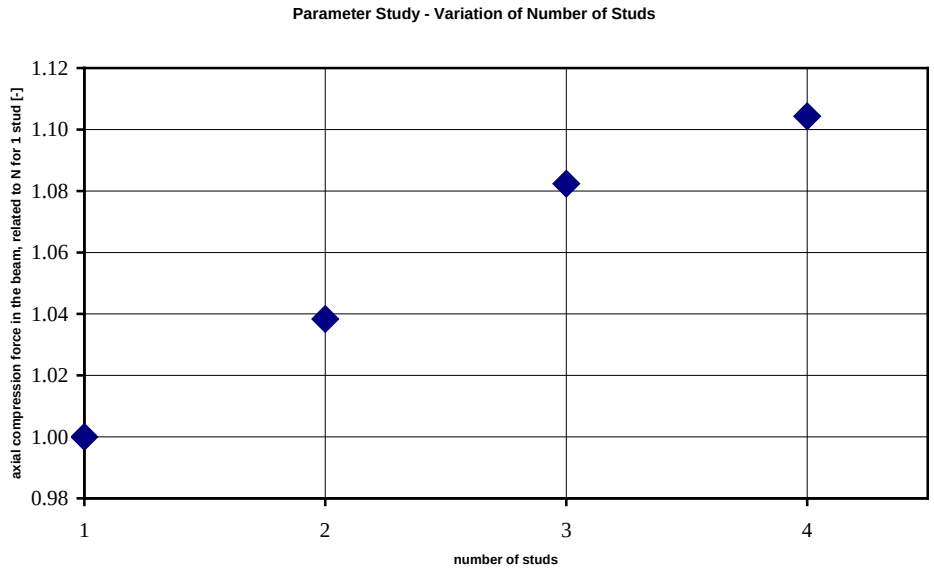

Figure 6-7: Maximum axial compression force in the beam for different number of studs on one beam. The values are related to the value of axial compression for one stud per beam.

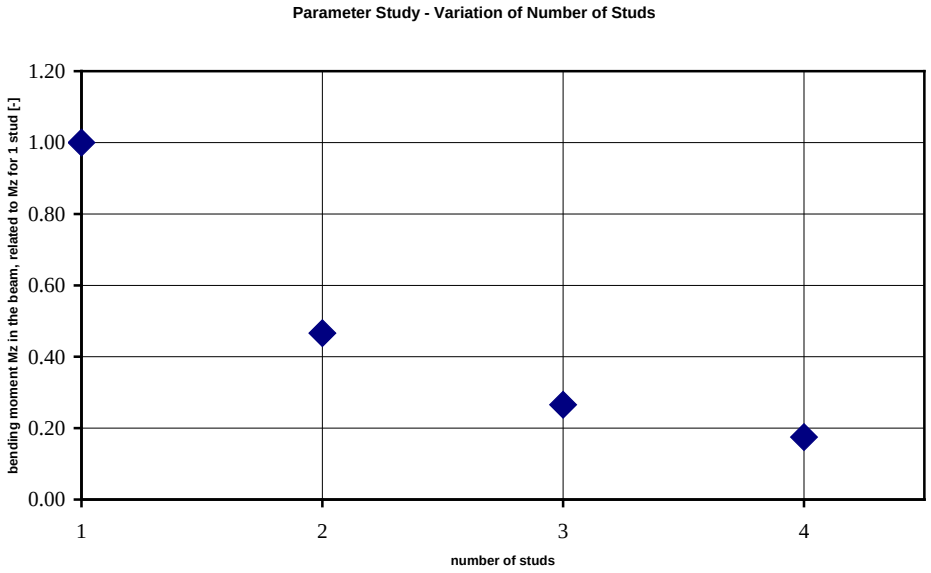

Figure 6-8: Maximum bending moment in the beam for different number of studs on one beam. Bending moment values are related to the value for one stud per beam.

The axial force increases about 4% for each stud introduced, being a nearly linear increase, whereas the bending moment decreases most with the introduction of the second stud on the beam. For the second stud introduced, the bending moment decreases approximately 53%. An additional decrease in bending moment of 20% and 9% results from the introduction of studs number 3 and 4 respectively. As the decrease in bending moment is much higher than the increase in axial compression force, the cross-section of the beam can be decreased.
For 1 to 4 studs per beam, the following cross-sections are sufficient, designing the beam with respect to combined bending and axial compression, column buckling and lateral torsional buckling, see
Table 6-2.

Table 6-2: Cross-sections needed for the beam for different number of studs on one beam. The beam volume reduction is related to every single stud that is additionally introduced to the beam.

Number of studs	Cross-section [mm x mm]	Volume reduction (per stud)
1	290 x 1035	0
2	265 x 810	28 %
3	265 x 765	6 %
4	265 x 675	12 %

The tension force in the steel rods is reduced by introduction of additional studs, as more rods are used to take up the loads, see Figure 6-9. The highest tension force occurs in the rod jointed to the longest stud. The rods supporting studs nearer to the heel joint experience much lower loads and their cross-sections can be drastically reduced. On the one hand, it is advantageous to have smaller diameters as standard steel rods can be used. On the other hand, the heel joint between tension rods and beam is more difficult to design and to manufacture, as more tension rods have to be anchored. In general, more joints have to be manufactured if more studs are used, which is both expensive and time-consuming and perhaps more severe than the benefit of the reduction in the beams volume.

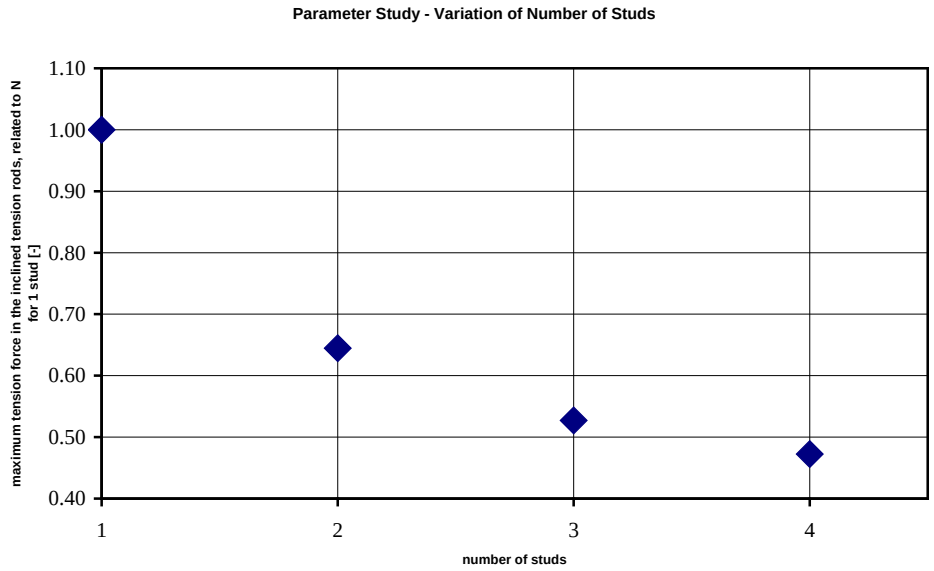

Figure 6-9: Maximum tension force in the tension rods for different number of studs on one beam. The values are related to the force in the tension rods when there is only one stud per beam.

As the tension force in the steel rods decreases if more than one stud is jointed with the beam, also the axial compression force in the glulam studs decreases as can be seen in Figure 6-10. The decrease in axial compression is between 12 and 15% for the longest stud (no. 2,3 and 4 respectively) and up to 43 to 68 % for the shortest stud (no.1).

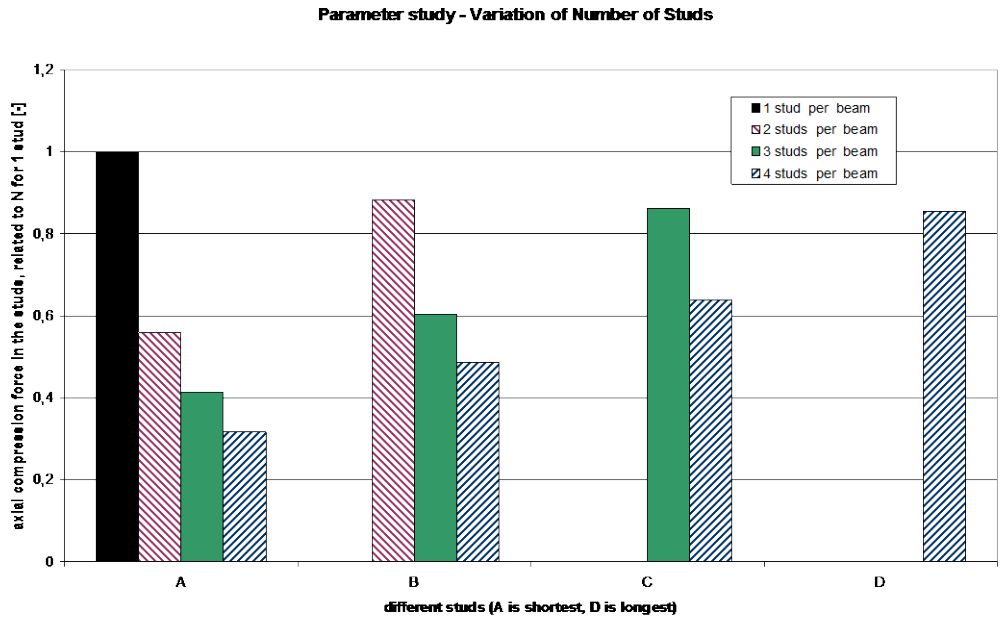

Figure 6-10: Axial compression force in the glulam studs for different number of studs per beam. The values are related to the axial compression force in the stud when only one stud is used per beam.

The bending moment in plane increases in the studs when more studs are introduced into the system, see Figure 6-11. Even if the relative increase in bending moment is high, the influence on the stud is low since the absolute bending moment values are low compared to the axial compression force. When designing the studs with consideration of axial compression force and bending moment as well as column buckling, the degree of utilisation does not exceed 51% (column buckling) for a cross-section of 290 mm x 290 mm. Even for one stud, the utilisation factors are low, but due to the kind of joint (T-joint), the stud has to have the same width as the beam. For other joint types, for example double beams with a stud fastened between them with dowel-type fasteners, the cross-section of the stud can be chosen with respect to its stresses, then being more cost-effective.

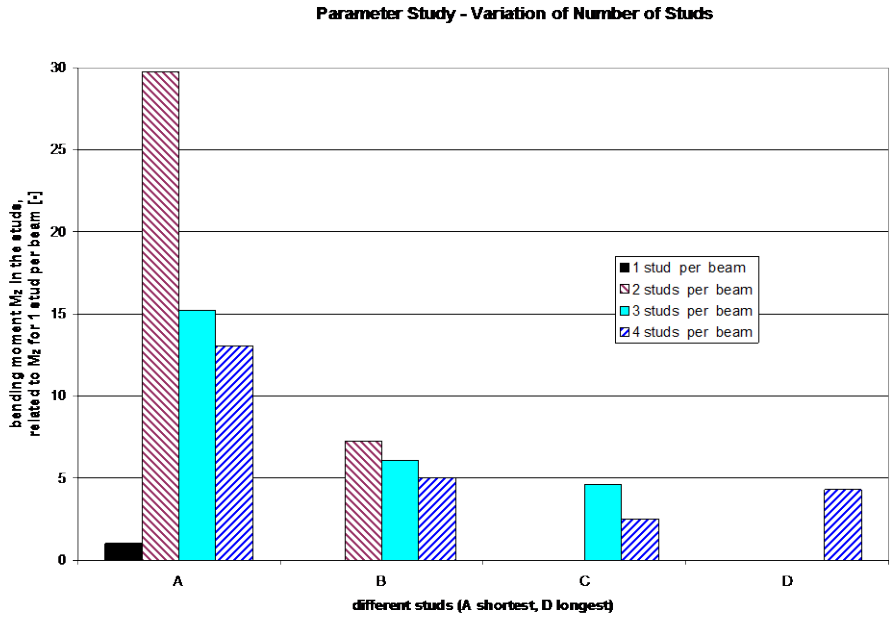

Figure 6-11: Maximum bending moment in the glulam studs for different number of studs per beam. The values are related to the bending moment in the stud when only one stud is used per beam.

The influence of the roof inclination on the section forces distribution and therefore on the required cross-sections was also investigated. The roof truss with a roof inclination of 14 degrees serves as a basis for the investigation. All trusses are loaded with the same vertical load. With decreasing roof inclination, the angle between the roof truss and the vertical load increases. This results in higher shear forces and lower axial compression forces in the beam, see Figure 6-12. Higher shear forces result in higher bending moments. To decrease the bay bending moment, the amount of prestressing of the tension rods has to be increased to reach the beams maximum utilisation of bending moment with $|M_{bay}| \cong |M_{\sup}|$. The increased tension force in the steel rods results in an increase in axial compression force in the beam. The increase in axial compression force due to the higher prestressing is larger than the decrease of axial compression in the beam due to decreased inclination. As the total increase in axial forces with decreasing roof inclination is not linear, the section forces have to be investigated for each roof inclination separately.
The roof inclination does not have a significant influence on the section forces of the studs. If the appearance of the truss shall be the same for all inclinations, with the prestressed tension rods being parallel to the horizontal tension rod between the heel joint and the joint between tension rod and stud, then the length of the stud has to be varied for various roof inclinations. This results in different utilisation factors in the stud due to the varying length. For increasing roof inclinations, the cross-section of the stud perhaps has to be increased. For the system investigated, the same width was necessary for both stud and beam because of the T-joint. Due to this, the utilisation factors for the stud (bending and axial compression as well as column buckling) are comparatively low, between 24 and 27% for the roof inclinations studied.

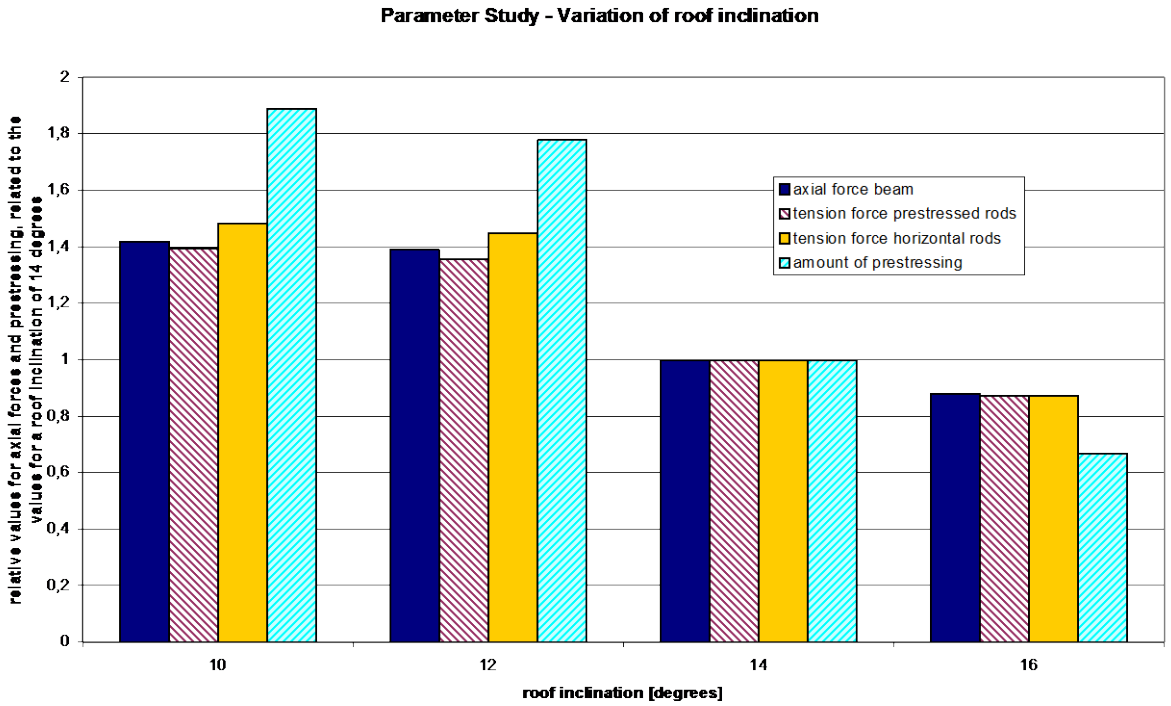

Figure 6-12: Axial compression forces and prestressing for different roof inclinations. The values are related to the ones for a roof inclination of 14 degrees.

The different structures shown in Figure 6-13 were investigated and compared to each other. Series A_1 to C_1 is a roof truss built up of two beam trusses with one stud each, series A_2 to C_2 a roof truss of trussed beams with 2 studs each. All the systems have a roof inclination of 14 degrees and a span of 60 m. The systems B and C have an angle of 16 degrees between the glulam beams and the inclined tension rods. To study the different effects of the horizontal tension rod, the rod was used between the supports in system B, whereas it was used only between the cantilevered ends of the studs in system C.

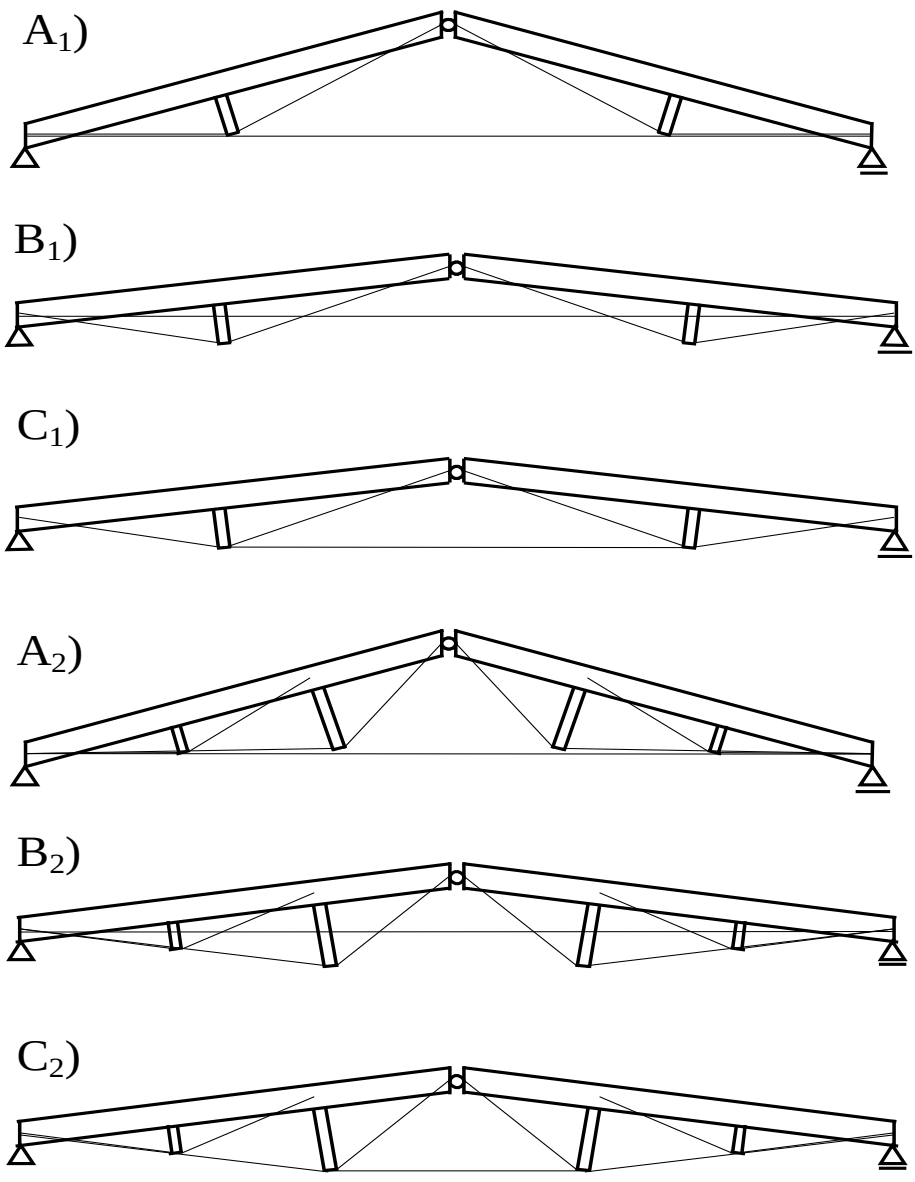

Figure 6-13: Different systems of roof trusses with trussed glulam beams. The roof inclinations is the same for all systems, whereas the angle between the glulam beam and the inclined tension rods was varied, as well as the number of studs per beam.

The prestressing in the inclined tension rods was chosen with respect to the bending moment in the beam. The condition $|M_{bay}| \cong |M_{\sup}|$ had to be fulfilled. To obtain this bending moment distribution, the highest prestressing is needed for system C and the lowest for system B. Therefore, the largest axial compression force in the beam as well as the largest tension force

in the inclined tension rods occur in system C, while the smallest values are obtained in system B. The bending moment in the stud is influenced by the choice of the system. The highest bending moment is achieved for system C, making it unfavourable. An additional problem in system C is the deflection of the stud. When the roof truss deflects vertically under load, the cantilevered end of the stud normally would deflect downwards and towards the supports, if the deflection was regarded as a stiff body motion. In system C, the horizontal tension rod between the stud ends prevents this deflection: The studs deflect downwards and towards the centre of the roof truss. This movement increases the bending moment in the stud and the stresses on the joint between stud and beam. The risk for in plane buckling of the stud is increased, compared to systems A and B.

Considering the design and production of the roof trusses details, systems A and C are advantageous. All tension rods that have to be fixed to the beam at the heel joint have the same inclination. If the tension rods lie on both sides of the glulam beam and are fastened in a steel plate that is fastened at the beam end, they can be fastened in the same plate providing that they have the same inclination. If the inclination of the tension rods is different as in system B, then two steel plates with different inclinations towards the beam would have to be used for this kind of joint. Otherwise, the tension rods could be fastened to slotted-in-steel plates. However, that kind of joint is only possible for a limited number of tension rods, or the beam width has to be increased. Additionally, there is a large risk for tension perpendicular to the grain as the load acts at an angle to the grain. Joints with slotted-in-steel plates can be a good choice for joints with a low number of tension rods, such as the joint at the ridge or at intermittent joints with the beam, which are needed if several studs are used on one beam.

With the systems B and C, the total height of the building can be reduced without reducing the angle between glulam beam and tension rods. However, a disadvantage is that the tension rods reduce the free height in the building.

Considering the effects of the different systems A, B and C on the section forces, the joint and overall design, system A can be assessed as the most favourable system to be used for roof trusses with trussed beams.

7 Conclusions

The purpose of this study was to assess the risk for instability in large-span glulam constructions with trussed beams. Both test results and calculations of the theoretical model showed that the steel tension rods have a high stabilising effect on the stud of the trussed beam and therefore on the whole system.

In regular design, the stud is considered as a cantilever with a buckling length of $\beta L = 2.0L$ (for a rigid joint). However, in this study, the buckling length of the stud was found to be nearly that of an ideal pin-ended Euler-strut with $\beta L = 1.0L$.
Additionally, the stiffness of the joint between stud and beam does not have an influence on the buckling length of the stud if a trussed beam is considered.
A high stabilising effect was also observed for large deflections at the beams midspan, which was thought to be unfavourable.

The stud has an influence on the stability of the beam: If the stud deflects out of plane to a high extent, then it causes a deformation in the beam that resembles a bow. As the beam is subjected to bending moments and axial compression forces, it fails in buckling and lateral buckling. For usual ratios of stud length to beam length, the stud faces a relatively high buckling load due to the short length. The normal failure mode in this case is lateral buckling in the beam. Therefore, the bracing of the beam itself (purlins, roof sheathing etc.) is most important for the stabilisation of the trussed beam. The stud end does not have to be braced as it is stabilised by the positive effect of the tension rods.

Trussed beam systems like for example three-hinged roof trusses should be calculated with second-order analysis to consider the deflections occurring in the system. The deflection of the ridge leads to an increase of axial compression force in the beams, which has a large influence on the stability of the system. A first-order analysis could be on the unsafe side if the system experiences large deformations.
Considering the results of this study, see sections 4 and 5, it is proposed to design the system with consideration of the buckling risk even if the section forces were obtained with a second-order analysis. The stud can be designed with a buckling length of $\beta L = 1.0L$.

8 References

Eurocode 5 / EN 1995-1-1. *Design of Timber Structures. Part 1.1: General rules and rules for buildings*. Final Draft 09.04.2001. European Committee for Standardization. Bruxelles, Belgium.

BKR1999. *Boverkets konstruktionsregler*. BFS 1993:58 med ändringar t o m BFS 1998:39. Boverket.1998. (Swedish)

EN408:1995. *Timber Structures – Structural timber and glued laminated timber – Determination of some physical and mechanical properties*. CEN. January 1995.

Bauen mit Holz. No. 5/98: *Unterspannte Träger*. (German)

Blom G.: *Sannolikhetsteori och statistikteori med tillämpningar*. Studentlitteratur Lund. 4th edition 1989. Lund. 1994. (Swedish)

Carling O., Johannesson B.: *Limträhandboken*. Third edition 1995. second release. Stockholm. 1998. (Swedish)

Curry, W.T, Fewell, A R: *The relations between the ultimate tension and the ultimate compression strength of timber and its modulus of elasticity*. Building Research Establishment / Princes Risborough Laboratory. Current Paper 22/77. Great Britain. 1977.

Degerman T.: *Dimensionering av betongkonstruktioner enligt sannolikhetsteoretiska metoder*. Institutionen för byggnadsteknik. Lunds Tekniska Högskolan. Report TVBK-1003. Lund 1981. table 5-10a. (Swedish)

Emilsson A. from Limträteknik Falun AB. personal information. 2001.

Grazer Holzbau-Fachtagung 1995. *Sortierung & Festigkeit. Entwicklung leistungsfähiger Holzleimbauteile durch den Einsatz von maschinell festigkeitssortiertem Holz.* Tagungsband zur Präsentation des FFF-Forschungsberichtes. Technische Universität Graz. 22. juni 1995. (German)

Gustafsson, P.J.: *Fracture Perpendicular to Grain – Structural Applications*. Course material for Advanced Timber Engineering 2000. Lund University. 2001.

Haller P.(editor): *Semi-rigid timber joints – structural behaviour, modelling and new technologies. Semi-rigid behaviour of civil engineering structural connections 1992 – 1999*. COST C1. final report of working group “Timber Joints”.

Hoffmeyer, P.: *Strength under Long-Term-Loading*. Course material for Advanced Timber Engineering 2000. Lund University. 2001.

Informationsdienst Holz: *Holzbauwerke, Bemessung und Baustoffe nach Eurocode 5 (STEP1)*. Duesseldorf. 1995. (German)

Isaksson, T.: *Structural Timber – Variability and Statistical Modelling*. Course material for Advanced Timber Engineering 2000. Lund University. 2001.

Jensen J.L.: *Forsög med excentrisk belastede sömforbindelser*. Ph.d-avhandling. SBI-Rapport 238. Statens Byggeforskningsinstitut. 1994. Hörsholm (Denmark). (Danish)

Jorissen A.: *The Stiffness of multiple bolted connections*. International Council for building research studies and documentation, Working Commission W8 – Timber Structures, CIB-W18/32-7-6. Paper presented at Meeting 32, Graz, Austria, August 1999.

Kessel, M.H.: *Zur seitlichen Stabilisierung des unterspannten Trägers.* In: Bauingenieur 63 (1988). (German)

Mårtensson, A.: *Short and long term deformations of timber structures*. Course material for Advanced Timber Engineering 2000. Lund University. 2001.

Mårtensson A. and Isaksson T.: *Tabell- och Formelsamling*. Avdelningen för Konstruktionsteknik. Lunds Tekniska Högskolan. Konstruktionsteknik AK 2000. third edition. (Swedish)

Natterer, Herzog, Volz: *Holzbau Atlas Zwei* (Studienausgabe). Arbeitsgemeinschaft Holz e.V. Duesseldorf. second edition. 1996. (German)

Nielsen, J.: *Trusses and Joints with Punched Metal Plate Fasteners*. Course material for Advanced Timber Engineering 2000. Lund University. 2001.

Norén B.: *Nailed Joints – Their Strength and Rigidity under Short-Term and Long-Term Loading*. Rapport 22/68 från Byggforskningen. Stockholm. 1968.

Pettersson, O.: *Ett icke-konservativt knäckningsproblem*. Festskrift till professor Carl Forssell. Stockholm 1956. In: Bygg, Handbok för hus-, väg- och vattenbyggnad. Huvuddel 1A. Allmänna grunder. AB Byggmästarens förlag. Stockholm. 1971. (Swedish)

Ranta-Maunus, A.: *Effects of climate and climate variations on strength*. Course material for Advanced Timber Engineering 2000. Lund University. 2001.

Serrano E.: *Mechanical Performance and modelling of glulam*. Course material for Advanced Timber Engineering 2000. Lund University. 2001.

Trahair, N.S., Bradford, M.A.: *The behaviour and design of steel structures*. Second edition 1988. Reprinted 1991. Chapman and Hall, London. Great Britain. 1991.

Whale L., Smith I., Hilson B.O.: *Behaviour of nailed and bolted joints under short-term lateral load – conclusions from some recent research*. International Council for building research studies and documentation, Working Commission W8 – Timber Structures. CIB-W18/19-7-1. Paper presented at Meeting 19, Florence, Italy, September 1986.

Yasumura, Sawata: *Determination of yield strength and ultimate strength of dowel-type timber joints*. International Council for building research studies and documentation, Working Commission W8 – Timber Structures. CIB-W18/33-7-1. Paper presented at Meeting 33, Delft, The Netherlands, August 2000.

9 Computer programmes

Microstran	V7.00.02b Engineering Systems (EEC) Limited.
Matlab	Version 6.0.0.88, Release 12. The MathWorks, Inc.
ABaS	Version 2000-09-05, Arbeitsbereich Massivbau TUHH.
Microsoft Word	Windows NT4.0
Microsoft Excel	Windows NT4.0